

ADSORPTION OF CHLORINATED GASES IN H₂
USING MODIFIED ZEOLITE NaY AND ACTIVATED CARBON

Mrs. Prapaporn Luekittisup



บทคัดย่อและแฟ้มข้อมูลฉบับเต็มของวิทยานิพนธ์ตั้งแต่ปีการศึกษา 2554 ที่ให้บริการในคลังปัญญาจุฬาฯ (CUIR)
เป็นแฟ้มข้อมูลของนิสิตเจ้าของวิทยานิพนธ์ ที่ส่งผ่านทางบัณฑิตวิทยาลัย

The abstract and full text of theses from the academic year 2011 in Chulalongkorn University Intellectual Repository (CUIR)
are the thesis authors' files submitted through the University Graduate School.

A Dissertation Submitted in Partial Fulfillment of the Requirements
for the Degree of Doctor of Philosophy Program in Environmental Management

(Interdisciplinary Program)

Graduate School

Chulalongkorn University

Academic Year 2014

Copyright of Chulalongkorn University

การดูดซับแก๊สคาร์บอนไดออกไซด์ในไฮโดรเจนโดยซีโอไลต์โซเดียมวอยและถ่านกัมมันต์ปรับสภาพ



วิทยานิพนธ์นี้เป็นส่วนหนึ่งของการศึกษาตามหลักสูตรปริญญาวิทยาศาสตรดุษฎีบัณฑิต
สาขาวิชาการจัดการสิ่งแวดล้อม (สหสาขาวิชา)
บัณฑิตวิทยาลัย จุฬาลงกรณ์มหาวิทยาลัย
ปีการศึกษา 2557
ลิขสิทธิ์ของจุฬาลงกรณ์มหาวิทยาลัย

ประภาพร ลือกิตติศัพท์ : การดูดซับแก๊สคลอไรด์ปนเปื้อนในไฮโดรเจนโดยซีโอไลต์ โขเดียมวายและถ่านกัมมันต์ปรับสภาพ (ADSORPTION OF CHLORINATED GASES IN H_2 USING MODIFIED ZEOLITE NaY AND ACTIVATED CARBON) อ.ที่ปรึกษาวิทยานิพนธ์หลัก: รศ. ดร. นุรักษ์ กฤษดานุรักษ์, 113 หน้า.

การปนเปื้อนของไฮโดรเจนคลอไรด์ (HCl) และไวนิลคลอไรด์โมโนเมอร์ (VCM) ในสายป้อนไฮโดรเจน (Feed H_2) ก่อให้เกิดผลกระทบต่อกระบวนการผลิตในอุตสาหกรรมปิโตรเคมี เนื่องจากไฮโดรเจนคลอไรด์ และไวนิลคลอไรด์โมโนเมอร์ (VCM) มีพฤติกรรมการถูกดูดซับที่แตกต่างกัน จึงทำการศึกษาเพื่อหาตัวดูดซับที่สามารถดูดซับสารปนเปื้อนทั้งสองชนิดได้ ในศึกษานี้ถ่านกัมมันต์ชนิดเม็ด (GAC) มีการปรับสภาพโดยการเติมโซเดียมในอัตราส่วนที่แตกต่างกัน และการปรับสภาพซีโอไลต์ที่ใช้แลกเปลี่ยนไอออนที่เป็นของเสียจากการเกษตรกรรมเป็นแหล่งของซิลิกา ในอัตราส่วนของซิลิกอนต่ออลูมิเนียม (5 ถึง 0.9) โดยเปรียบเทียบกับตัวดูดซับชนิดอื่นๆ ได้แก่ RH-SiO₂ RH-MCM-41 และ Al₂O₃ balls โดยทำการศึกษาเพื่อเปรียบเทียบประสิทธิภาพในการดูดซับ HCl และ VCM ที่ไหลผ่านหอดูดซับ การศึกษาจัดทำขึ้นที่ความเข้มข้นเริ่มต้นของ HCl และ VCM ที่ 600 และ 20 ppm ตามลำดับ

ด้วยอัตราการไหล 50 ml/min และตัวดูดซับ 6 g แสดงให้เห็นว่า M-NaY-RH-1.87 มีประสิทธิภาพในการดูดซับ HCl ได้ดีที่สุดที่ (1.444 g_{HCl}/g_{adsorbent}) ตามด้วย 6N-GAC Al₂O₃ balls GAC RH-MCM-41 และ RH-SiO₂ ตามลำดับ สำหรับการดูดซับ VCM พบว่า GAC มีประสิทธิภาพในการดูดซับสูง (0.0063 g_{VCM}/g_{adsorbent}) กว่าตัวดูดซับอื่น ๆ เรียงลำดับคือ 6N-GAC RH-SiO₂ และ Al₂O₃ balls ตามลำดับ โดย RH-MCM-41 และ M-NaY-RH-1.87 ไม่มีความสามารถดูดซับ VCM ดังนั้นจึงเลือกตัวดูดซับ GAC 6N-GAC และ M-NaY-RH-1.87 ซึ่งมีความสามารถในการดูดซับสูง เพื่อศึกษาผลกระทบของการสลับชั้นของตัวดูดซับทั้ง 3 ชนิด ในการดูดซับก๊าซไฮโดรเจนที่ปนเปื้อนด้วย HCl 600 ppm และ VCM 20 ppm จากผลการทดลองพบว่าอัตราส่วนชั้นที่เหมาะสมที่สุดคือ M-NaY-RH-1.87 / 6N-GAC / GAC ที่ 1/1/1 เมื่อสิ้นสุดการใช้งานตัวดูดซับที่ใช้งานแล้ว GAC ซึ่งมีคาร์บอนเป็นองค์ประกอบหลัก สามารถนำไปใช้เป็นเชื้อเพลิงทดแทน และ M-NaY ซึ่งมีซิลิกอนและอลูมิเนียมเป็นองค์ประกอบหลัก สามารถนำไปใช้เป็นวัตถุดิบทดแทนในการผลิตปูนซีเมนต์ได้

สาขาวิชา การจัดการสิ่งแวดล้อม

ลายมือชื่อนิติกร

ปีการศึกษา 2557

ลายมือชื่อ อ.ที่ปรึกษาหลัก

5287791720 : MAJOR ENVIRONMENTAL MANAGEMENT

KEYWORDS: GRANULAR ACTIVATED CARBON / ZEOLITE NaY / ADSORPTION / HYDROGEN CHLORIDE

PRAPAPORN LUEKITTISUP: ADSORPTION OF CHLORINATED GASES IN H₂ USING MODIFIED ZEOLITE NaY AND ACTIVATED CARBON. ADVISOR: ASSOC. PROF. DR. NURAK GRISDANURAK, 113 pp.

Contamination of hydrogen chloride (HCl) and chlorinated hydrocarbon compound (VCM) in H₂ feedstock causes adverse effects to the downstream petrochemical processes, even though in extremely low concentration. It is quite important to develop adsorbents which are able to uptake both chemicals. In this study, granular activated carbon (GAC) was modified by adding sodium with different concentrations, and zeolite NaY, using rice husk as a silica source, was synthesized and modified under different ratio of Si/Al (5 to 0.9). In addition, RH-SiO₂, RH-MCM-41, Al₂O₃ balls were also studied. All adsorbents have been tested for their adsorption efficiency on both HCl and VCM in a continuous fixed bed flow column. The tests were carried out with initial concentrations of HCl and VCM at 600 and 20 ppm, respectively.

Under the flow rate of 50 mL/min and bed of 6 g, for HCl adsorption, M-NaY-RH-1.87 showed the highest adsorption efficiency (1.444 g_{HCl}/g_{adsorbent}) followed by 6N-GAC, Al₂O₃ balls, GAC, RH-MCM-41, and RH-SiO₂ respectively. For VCM adsorption, GAC provided the highest adsorption efficiency (0.0063 g_{VCM}/g_{adsorbent}) followed by 6N-GAC, RH-SiO₂, and Al₂O₃ balls, respectively, while RH-MCM-41 and M-NaY-RH-1.87 were unable to capture VCM. For the mixed gases HCl and VCM, the mixture of GAC, 6N-GAC and M-NaY-RH-1.87 was found optimum with the ratio of 1/1/1 by weight, compared to a commercial one. Spent adsorbent contained some certain amount of sodium could be used for alternative fuel and alternative mixture in the cement kilns, for GAC and M-NaY, respectively. Co-processing in cement kilns will burns up the spent adsorbents.

Field of Study: Environmental
Management

Student's Signature

Advisor's Signature

Academic Year: 2014

ACKNOWLEDGEMENTS

I would like to express my sincere and deepest gratitude to my advisor, Assist. Prof. Dr. Nurak Grisdanurak, who always gives me a great supports, good opportunities, resounding helps, generous encouragements and all advice. He does not only educate me but also teaches me about life. Without his persistent push forward this dissertation would not have been possible. Besides, I would like to express my gratitude to my committee members, Assist. Prof. Dr. Chantra Tongcumpou, Assoc. Prof. Dr. Patipan Punyapalakul, Dr. Pichet Chaiwiwatworakul, Assist. Prof. Dr. Ratanawan (Wibulswas) Kiattikomol (PTT Public Company Limited), and Dr. Jitlada Chumee (Suan Sunandha Rajabhat) for valuable suggestions.

I feel very lucky to work in Catalyst laboratory at Thammasat University where is full of sympathy, help, and friendship. We share knowledge, tools, apparatus, food and stuff. I would like to thank Aoi who supports me in both academic and laboratory works including encourages me to pass through arduous periods of time. I would also like to thank you HCl & VCM team, Mai, O, First, Jew, and Mooh for their willingness to share and advise their knowledge and academic information. They are the important persons in my work. Furthermore, my thanks to all the notable persons in the Catalyst laboratory – Boy Yai, P Noi, Tu, Champ, Boy Lek, Puek, Job, Som-O, Fah, Pui, Mew, Eak, Rat, Tum, Pat, Eddy, A, New, Prai, Ying, M, Rute, Best, Jeejy, Gun, Toon, Mont, Plam, Kwan and everybody. My special thanks to my best friend, Nok, for your kindness and helpful assistances in everything more than 20 years since we first met. Moreover, I also would like to thank all my friends at International Program in Hazardous Substance and Environmental Management, Chulalongkorn University and my colleagues at Department of Industrial Works, Ministry of Industry for cheering me up.

Furthermore, I would like to express my sincere and deepest gratitude to my family for their supports which make me feel that they are always there for me through thick and thin. Without their encouragements, I would not even have a chance to get a doctoral degree. Special thanks to my lovely sisters, P Ying, P Ple, and Nong Yui who help me to take care of my son all the times and that allows me to step through all troubles and focus on finding solutions with worry-free. I am the luckiest woman in the world having the best husband – Sakchai Amornsakchai – who supports and helps me in everything I would like to do. Last but not least, I would like to thank my mum and dad who silently cheer me up but I hear their love loudly in my heart. Today I am ready to say that “Everything I do, I do it for you”.

CONTENTS

	Page
THAI ABSTRACT	iv
ENGLISH ABSTRACT.....	v
ACKNOWLEDGEMENTS	vi
CONTENTS.....	vii
LIST OF TABLES	x
LIST OF FIGURES	xi
CHAPTER 1 INTRODUCTION	1
1.1 Introduction.....	1
1.2 Objectives	3
1.3 Scopes of the study	3
CHAPTER 2 BACKGROUND AND LITERATURE REVIEWS	5
2.1 HCl and VCM.....	6
2.2 Adsorption	9
2.2.1 Literature review in HCl Adsorption.....	10
2.2.2 Literature review in VCM Adsorption	12
2.3 Adsorbents	13
2.3.1 Activated carbon.....	13
2.3.2 Zeolite NaY	15
2.3.3 RH-MCM-41	17
2.4 Modification of adsorbents	17
2.4.1 Modification of Activated Carbon	17
2.4.2 Modification of Zeolite NaY	18
2.5 Pelletization	20
CHAPTER 3 EXPERIMENTAL PROCEDURE.....	22
3.1 Material.....	23
3.1.1. Chemicals	23
3.1.2 Experimental gases.....	24
3.1.3 Instrument and apparatus.....	24

	Page
3.2 Material preparation and synthesis	25
3.2.1 Modified GAC.....	25
3.2.2 Preparation of RH-MCM-41	25
3.2.3 Preparation of RH-SiO ₂	26
3.2.4 Preparation of zeolite Meso-NaY	26
3.2.5 Material characterization	28
3.2.6 Pelletization of adsorbent	29
3.2.7 Adsorption	29
3.3 Flow behavior analysis	31
CHAPTER 4 RESULTS AND DISCUSSION.....	32
4.1 Preliminary results	32
4.2 HCl and VCM adsorption of commercial adsorbent	35
4.2.1 Effect of Si/Al	35
4.2.2 Characterizations of adsorbents.....	38
4.2.3 Spent adsorbent	42
4.3 HCl and VCM adsorption of Activated carbon	43
4.3.1 Effect of sodium content	43
4.3.2 Characterizations of Modified GAC	46
4.3.3 Effect of chemical impurity in the material synthesis	52
4.4 Alternate layer by layer	54
4.5 Cost estimation on using synthesized adsorbents for upscale	63
4.6 Waste Management	66
CHAPTER 5 MODELLING OF HCl AND VCM ADSORPTION IN PACKED BED COLUMN	68
5.1 Flow dispersion.....	68
5.2 Statistical Analysis on the breakthrough time	76
5.2.1 Quadratic regression model.....	78
5.2.2 Linear regression model	83
5.3 Model verification	86

	Page
CHAPTER 6 CONCLUSIONS AND RECOMMENDATIONS	87
6.1 Conclusions.....	87
6.2 Recommendations.....	88
REFERENCES	89
APPENDIX A Example of HCl Adsorption Calculation	94
APPENDIX B Example of Vinyl Chloride Monomer Adsorption Calculation ..	101
APPENDIX C Quantity of sodium on granular activated carbon	108
VITA.....	113



LIST OF TABLES

Table 2.1 HCl and VCM properties	8
Table 2.2 EN value of Silver (Ag), Nickel (Ni), Calcium (Ca), and Sodium (Na)	15
Table 2.3 NaOH properties	20
Table 3.1 Typical properties of GAC from Carbokarn Co., Ltd. Thailand.....	25
Table 4.1 HCl and VCM adsorption potentials.....	35
Table 4.2 BET-surface area of all adsorbents	41
Table 4.3 Elemental composition of NaY-RH-1.87 and M-NaY-RH-1.87	41
Table 4.4 Element composition of M-NaY-RH-1.87.....	42
Table 4.5 The adsorption capacity of HCl and VCM of adsorbents	46
Table 4.6 BET-surface area of all adsorbent.....	47
Table 4.7 Element composition of adsorbent from XRF	51
Table 4.8 The efficiency of HCl adsorption of M-NaY by using rice husk and commercial grade chemicals.....	53
Table 4.9 Packing arrangement for HCl guarding	54
Table 4.10 Adsorption capacities for each run.....	56
Table 4.11 Commercial adsorbent (used in industry)	64
Table 4.12 Experiment 3 M-NaY-RH-1.87 / 6N-GAC / GAC (1 / 1 / 1).....	64
Table 4.13 Cost of adsorbent.....	65
Table 4.14 NPV (Net Present value) Analysis	66
Table 5.1 Peclet number evaluation for the dispersion behavior for each run.....	71
Table 5.2 Breakthrough times for HCl adsorption over 6N-GAC in all studied parameters	76
Table 5.3 Comparison on several model fittings.....	78
Table 5.4 Variance analysis (Quadratic regression).....	81
Table 5.5 Variance analysis (Linear regression).....	85

LIST OF FIGURES

Figure 2.1 Effect of chloride in activity profiles of water-gas-shift over Cu/ZnO/Al ₂ O ₃ catalyst (Twiggs and Spencer, 2001).....	6
Figure 2.2 Moisture content of adsorbent on HCl adsorption efficiency. (Lee et al., 2003)	11
Figure 2.3 Chloride guard process (Twiggs and Spencer, 2001).	12
Figure 2.4 VCM adsorption by AC (Scamehorn, 1979).....	12
Figure 2.5 Zeolite NaY structure	16
Figure 2.6 Synthesis mechanism of RH-MCM-41 (Beck et al., 1992)	17
Figure 2.7 Silica: (a) crystalline silica; (b) amorphous silica (Grisdanurak and Wittayakun, 2004).....	18
Figure 2.8 Formation of mesopores in different Si/Al ratios (Realpe and Ramírez, 2010).	19
Figure 3.1 Schematic diagram of experiment	22
Figure 3.2 Synthesis of xN-GAC.....	26
Figure 3.3 Synthesis of RH-MCM-41.....	27
Figure 4.1 Breakthrough curves of (a) HCl and (b) VCM over several adsorbents.	34
Figure 4.2 Breakthrough curves of benchmark, modified rice husk and zeolite adsorbents for HCl adsorption	36
Figure 4.3 (a) Breakthrough curves of M-NaY-RH-xxx on HCl adsorption (b) Adsorption capacity based W_b and W_{sat} of M-NaY-RH of 3 ratios.	37
Figure 4.4 XRD spectra of M-NaY-RH-xxx.	38
Figure 4.5 FTIR spectrum of M-NaY-RH-1.87.....	39
Figure 4.6 N ₂ adsorption-desorption isotherm of M-NaY-RH-1.87.....	40
Figure 4.7 SEM images of (a) Zeolite NaY and (b) M-NaY-RH-1.87.....	40
Figure 4.8 XRD pattern of M-NaY-RH-1.87 after HCl adsorption.....	43
Figure 4.9 Breakthrough curves of (a) HCl (600 ppm) and (b) VCM (20 ppm) contaminated in H ₂	45
Figure 4.10 N ₂ adsorption-desorption isotherm of GAC and 6N-GAC.....	47

Figure 4.11 XRD pattern of 6N-GAC, GAC, RH-SiO ₂ and Al ₂ O ₃ balls	48
Figure 4.12 SEM images of GAC and 6N-GAC; (a) external surface and (b) cross-sectional surface	49
Figure 4.13 FTIR spectra of GAC and 6N-GAC	50
Figure 4.14 XRD pattern of GAC and 6N-GAC after HCl adsorption.....	51
Figure 4.15 Comparing XRD pattern of M-NaY-RH-1.87 laboratorial and commercial grade.....	52
Figure 4.16 Breakthrough curve of HCl Contaminated in H ₂	53
Figure 4.17 Flow diagram of fixed-bed flow reactor for alternate layer by layer.	55
Figure 4.18 Adsorption of HCl gas contaminated in H ₂ onto (a) GAC, (b) 6N-GAC, c) M-NaY-RH-1.87.	58
Figure 4.19 Adsorption of mixed gases of HCl and VCM contaminated in H ₂ onto	61
Figure 4.20 W _b between experiment and calculation	63
Figure 5.1 Control volume of molar flow rate of species I in an axially-dispersed PFR.	69
Figure 5.2 Effect of flow rate at L = 6 cm on breakthrough curves for HCl removal by 6N-GAC. Conditions: Particle diameter = 2.0 mm and column diameter = 20 mm. (To be continued)	73
Figure 5.3 Effect of flow bed length at a flow rate of 40 ml/min on breakthrough curves for HCl removal by 6N-GAC. Conditions: Particle diameter = 2.0 mm and column diameter = 20 mm.	74
Figure 5.4 Effect of particle diameter on breakthrough curves for HCl removal by 6N-GAC. Conditions: Particle diameter = 2.0 mm.	75
Figure 5.5 Normal probability plot of residuals.....	79
Figure 5.6 Residuals versus predicted plot	80
Figure 5.7 Parity plot of quadratic model (a) all factors.....	82
Figure 5.8 Normal probability plot of residuals (response is breakthrough point of HCl adsorption).	83
Figure 5.9 Residuals versus predicted plot (response is breakthrough point of HCl adsorption).....	84
Figure 5.10 Parity plot of linear model.	85

Figure 5.11 A comparison of breakthrough time to the prediction from two models..... 86

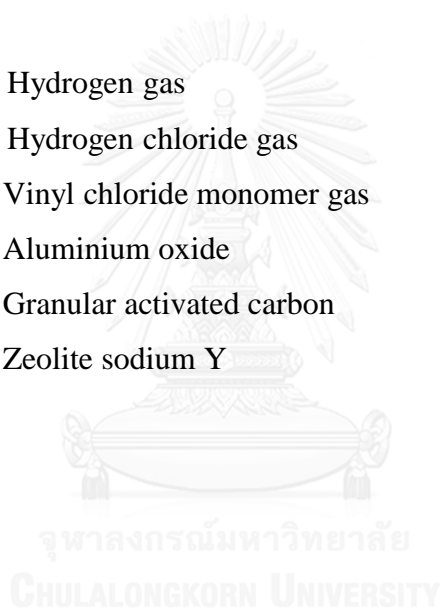


NOMENCLATURE

RH-SiO ₂	Silicon dioxide from rice husk
RH-MCM-41	MCM-41 from rice husk
M-NaY-RH-xxx	Mesoporous zeolite sodium Y from rice husk at silicon/aluminium ratio xxx
M-NaY-C-xxx	Mesoporous zeolite sodium Y from commercial grade chemicals at silicon/aluminium ratio xxx
xN-GAC	Granular activated carbon soaked in x normal sodium hydroxide

Abbreviation

H ₂	Hydrogen gas
HCl	Hydrogen chloride gas
VCM	Vinyl chloride monomer gas
Al ₂ O ₃ balls	Aluminium oxide
GAC	Granular activated carbon
NaY	Zeolite sodium Y



CHAPTER 1

INTRODUCTION

1.1 Introduction

A trace amount of chlorine and chlorinated hydrocarbon compounds contaminated in H₂ feed stock can be converted to hydrogen chloride (HCl) and vinyl chloride monomer (VCM) in severe conditions (Kameda et al., 2008). It has been noticed that HCl is a toxic gas, while VCM is an organochloride compound, with colorless, highly toxic, extremely flammable and carcinogenic properties. These contaminated gases could consequently corrode pipelines, poison catalysts and furthermore generate hazardous solid wastes. It has been reported by Twigg and Spencer (Twigg and Spencer, 2001) that reactivity of Cu/ZnO/Al₂O₃ on water gas shift reaction was reduced from 100 to 60% when feedstock was contaminated by HCl only 0.03% (by volume) in the feed stream. Even though a trace of VCM has shown no effect on the catalyst in downstream process, it still presents some serious concern as a hazardous release in working place. A chloride guard bed, furthermore, is placed previously to remove traces of chlorine and chlorinated hydrocarbons in feed stock. Commercial adsorbents usually used in this treatment are zeolites based.

Zeolite NaY is an alternative material for considering as an effective adsorbent. It is a micropore crystalline aluminosilicate which consists of SiO₄ and AlO₄ in faujasite family. It has high surface area and containing with sodium content (Yang, 2003; Gridanurak and Wittayakun, 2004). To enhance the adsorption efficiency, the zeolite NaY must possess mesopore material with positive charge in extra-frameworks. The Meso-NaY can be synthesized in various ways such as a chemical treatment method by leaching zeolite NaY with NaOH for creating mesopores (Abello et al., 2009). Referring to the charge, it should be effective to capture HCl, but not much on VCM capture. In order to overcome the capture of organochloride compound, high surface area adsorbent is required. Therefore, activated carbon is interested to investigate the adsorption performance of HCl and VCM.

Activated carbon is a general adsorbent used in technologies related to pollution treatment due to its highly porous, surface area and large adsorption capacity which also can be synthesized from solid waste-rice husk, coconut shell, palm shell, etc. It has been reported that activated carbon is effective applied to ozone, chlorofluorocarbons (CFCs), carbon dioxide (CO₂) and VCM removal (Scamehorn, 1979; Chatterjee et al., 2003; Walton et al., 2006). The adsorption ability of activated carbon is functional groups on its surface, surface area and pore structure. Normally, the functional groups on activated carbon are oxygen and carbon content on surface that can adsorb organic molecules with unpaired electrons (Rodríguez-reinoso, 1998). However, the application of activated carbon is limited for HCl removal because HCl is an active inorganic compound which completes with metals oxides (Na₂O, KO, CaO, MgO) (Hue, 1976; Park and Jin, 2005). Therefore, the activated carbon should be modified by adding cation metal on surface such as electroplating and soaking with metal solution to enhance the adsorption efficiency (Lee et al., 2003). Consequently, alkaline metal (sodium, Na) was considered due to cheap and nontoxic. NaOH was supported on activated carbon and used as adsorbent for HCl removal under steam in continuous fixed bed reactor, the results indicated the HCl treatment capacity of the NaOH on activated carbon increases with water and NaOH content increasing because of HCl gas reacted with water form to HCl aqueous and then reacted with NaOH to form salt (NaCl) (Lee et al., 2003).

In this study, adsorbents used to eliminate trace of HCl and VCM were developed. This work was to prepare modified activated carbon and zeolite by chemical treatments methods. The combination between sodium and porous materials that which have high surface area and optimize sodium content for the modified adsorption and its reliability for extremely low concentration of both HCl and VCM removal in a continuous fixed bed flow reactor and investigate its properties and also work on adsorption parameters which can be used to upscale the process.

1.2 Objectives

Main objective:

This study aims to develop adsorbent sodium modified to capture both inorganic and organic chlorinated gases contaminated in H₂ feed stock which are HCl and VCM, respectively.

Sub-objectives:

1. To evaluate the removal of HCl and VCM on several adsorbents.
2. To study effects of sodium content loaded on activated carbon on the inorganic and organic chlorinated gas adsorption.
3. To study effect of Silicon/Aluminium ratio of NaY on HCl adsorption
4. To simulate adsorption parameters for HCl and VCM adsorption.

1.3 Scopes of the study

1. Probes for inorganic and organic chlorinated gases are HCl and VCM, respectively.
2. There are 12 adsorbents for individual gas removal as follows;
 - GAC, 3N GAC, 6N-GAC and 12N GAC
 - RH-MCM-41
 - Alumina balls (Al₂O₃ balls) and silica (RH-SiO₂)
 - Zeolite Meso-NaY(Leaching) Si/Al ratios 5, 3.74, 1.87 and 0.93 by using rice husk as a silica source (M-NaY-RH-xxx).
 - Zeolite Meso-NaY(Leaching) Si/Al ratio which has high adsorption efficiency that synthesized from commercial grade (M-NaY-C-xxx).
3. 600 ppm of HCl and 20 ppm of VCM gas are used to study adsorption efficiency in a continuous fixed-bed flow reactor with 50 mL/min. of flow rate.
4. The HCl and VCM concentration is measured by using detector tube.

5. 6N-GAC which has high adsorption efficiency was selected to study hydrodynamic with different flow rate (40, 50 and 60 mL/min), particle size (0.50, 1.25 and 2.00 mm) and column diameter (1, 2 and 3 cm).
6. The mixed gas between HCl and VCM is used to study alternate layer by layer.
7. The study of flow behavior based axial flow dispersion was conducted with condition ranges: flow rate 40 and 60 mL/min, particle diameter 0.5 and 2.0 mm, and bed length 6, 10, 14 cm.
8. A prediction model for breakthrough time was evaluated under condition ranges: flow rate at 40, 50, and 60 mL/min, column diameter 10, 20, 30 mm, particle diameter 0.5, 1.25, and 2.0 mm.



CHAPTER 2

BACKGROUND AND LITERATURE REVIEWS

Natural gas received directly from wells contains a variety of hydrocarbons. Dienes are one of active hydrocarbons that can be reacted with chloride compounds to form chlorinated hydrocarbons (CHCs) under severe conditions (Kameda et al., 2008). Chlorinated hydrocarbons could be classified into both organic and inorganic forms, for examples; cyclobutane, benzene hexachloride and HCl respectively. They could be contaminated in the further feedstock. It has been known that, chlorinated compounds possibly cause the corrosion in pipelines and catalyst poisoning etc.

A classical example on catalyst poisoning in the presence of chlorinated compounds was described by Twigg and Spencer (Twigg and Spencer, 2001). They revealed the activity of Cu/ZnO/Al₂O₃ on water gas shift reaction was reduced from 100 to 60% within an hour of time on stream when H₂ feedstock was contaminated with an extremely low concentration of chlorinated hydrocarbons ca. 0.03 vol% as shown in Figure 2.1. In order to eliminate CHCs. from the feedstock, a chloride guarding process/unit should be added. According to its low concentration of the contamination (CHCs), a removal by adsorption would be a promising technique. Considering CHCs, it might be difficult to include every chlorinated hydrocarbons in the study. Probe chemicals representing inorganic CHCs. were HCl gas and VCM gas, respectively.

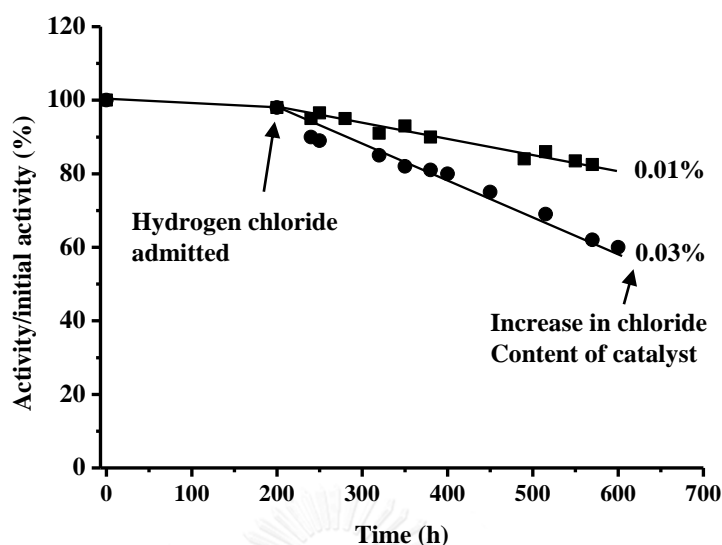


Figure 2.1 Effect of chloride in activity profiles of water-gas-shift over Cu/ZnO/Al₂O₃ catalyst (Twiggs and Spencer, 2001)

2.1 HCl and VCM

Hydrogen Chloride (HCl) is used in the production of various products, i.e. chlorides, fertilizers, dyes. It is also used in tanning leather, electroplating metals, and in the photographic, and rubber industries. HCl can be generated during the burning of many type of plastics. It is highly soluble, when contact with water, hydrochloric acid will be formed. Under normal conditions, HCl is a colorless to slightly yellow, corrosive, nonflammable gas with strong odor. In moist conditions, HCl gas reacts with moisture in the air, and give white clouds of Hydrochloric acid, which is corrosive and heavier than air.

EPA (Environmental Protection Agency) reported the health impact of HCl that *“HCl is corrosive to the eyes, skin, and mucous membranes. Acute (short-term) inhalation exposure may cause eye, nose, and respiratory tract irritation and inflammation and pulmonary edema in humans. Acute oral exposure may cause corrosion of the mucous membranes, esophagus, and stomach and dermal contact may produce severe burns, ulceration, and scarring in humans. Chronic (long-term)*

occupational exposure to hydrochloric acid has been reported to cause gastritis, chronic bronchitis, dermatitis, and photosensitization in workers. Prolonged exposure to low concentrations may also cause dental discoloration and erosion.”. EPA has not classified hydrochloric acid for carcinogenicity (EPA, 2000).

For environmental impacts of HCl, SEPA (Scottish Environmental Protection Agency) reported that *“Hydrogen chloride gas is highly corrosive and will damage metal structures and buildings or monuments made of limestone. If high levels of Hydrogen chloride gas dissolve in a water body, aquatic organisms will be harmed and even killed. This is only likely as a result of an accidental spill of much larger amounts of Hydrogen chloride than are typically released to the environment. The very high solubility of Hydrogen chloride gas means that releases to the atmosphere are quickly washed out by rain and moisture in the air. Some soils and lakes may be sensitive to this acid rain if amounts of it falling are above certain amounts defined as "critical loads". This makes Hydrogen chloride pollution a global as well as local environmental problem.*” (SEPA, 2015).

Vinyl chloride is a colorless gas with a mild, sweet odor. It is highly flammable, not stable at high temperatures. It is a manufactured product that does not occur naturally. It can be formed when other substances are broken down, i.e. trichloroethane, trichloroethylene, and tetrachloroethylene Vinyl chloride is used to make polyvinyl chloride (PVC), which is a raw material of various plastic products, i.e. pipes, wire and packaging materials. VCM is also known as chloroethylene, chloroethene, and ethylene monochloride.

For health impact, EPA (Environmental Protection Agency) reported that *“Exposure to vinyl chloride occurs mainly in the workplace. Breathing high levels of vinyl chloride for short periods of time can cause dizziness, sleepiness, unconsciousness, and at extremely high levels can cause death. Breathing vinyl chloride for long periods of time can result in permanent liver damage, immune reactions, nerve damage, and liver cancer.”*, (EPA, 2000)

Releases of both Hydrogen chloride and Chloroethene are regulated through the UK Pollution, Prevention and Control (PPC) Regulations.

In downstream industries, both HCl and VCM are considered as contaminant gases in their feed stock, since they are consequently corrode pipelines, poison catalysts

and generate hazardous solid wastes. Even though VCM has not been reported any effect to downstream process, it is eventually hazardous to working place. For that reasons, it have been concerned mainly to remove from industrial.

The HCl and VCM properties are shown in Table 2.1.

In practical, a chloride guard bed is applied industrially to remove the Cl species from the H₂ feedstock. The chloride guard bed works basically on the adsorption principle.

The adsorbents used in this study are activated carbon and zeolite based. They are effective for organic and inorganic CHCs.

Table 2.1 HCl and VCM properties

Properties	HCl	VCM
IUPAC name	Hydrogen chloride	Vinyl Chloride Monomer, Chloroethylene
Molecular formula	HCl	CH ₂ CHCl
Molecular weight	36.46 g/mol	62.5 g/mol
Density	1.477 g/l, gas	0.002.15 g/l, gas
Appearance	Colorless gas	Colorless gas
Flashpoint	Non-flammable	-77.8°C (extremely flammable)
Melting point	-114.2°C	-153.7°C
Boiling point	-85.1°C	-13.9°C
Solubility in water	72 g/100 mL (20°C)	1.1 g/l (25°C)
LD ₅₀	900 mg/kg (oral-rabbit)	500 mg/kg (oral-rat)

Properties	HCl	VCM
Hazards	<ul style="list-style-type: none"> - Poison, corrosive - In form of liquid and mist cause severe burns to all body tissue and may be fetal when swallowed or inhaled; lung damage 	<ul style="list-style-type: none"> - Extremely flammable, carcinogen - Inhalation: Headache, dizziness, narcosis, convulsions and death. Long-term exposure may cause impotence, blood disorders and liver problems.
Carcinogenicity (IARC)*	Group 3 (Not classifiable as to its carcinogenicity to humans)	Group 1 (Carcinogenic to humans)

* IARC: International Agency for Research on Cancer

2.2 Adsorption

The adsorption is an easy and uncomplicated method, which is preferred method to remove both HCl and VCM in this study. In general, the adsorption can be classified into 2 types, which are physisorption and chemisorption. The physisorption is a reaction that interact between dipole and dipole molecules by weakly force of intermolecular which is Van der Waals and/or force of dispersion. The chemisorption is a reaction between adsorbate molecule and surface of adsorbent molecule with strong force. In addition, the adsorptive separation can perform efficiency that depends on quality of adsorbent (Ruthven, 1984; Crittenden and Thomas, 1998; Grisdanurak and Wittayakun, 2004; Keller and Sraudt, 2005).

The most important factors affecting gas adsorption include

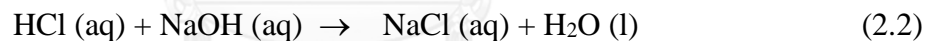
- Particle size of adsorbent: small particle size reduces internal diffusion and mass transfer limitation in term of the penetration of the adsorbate inside the adsorbent
- Surface area of adsorbent

- Flow rate: higher flow rate of adsorbate in gas phase passing through the adsorbent reducing the contact time
- Moisture content: moisture more than 50% reduces the efficiency of adsorption

An amount of cation metals in the adsorbent structure is a main factor of HCl removal, while pore size and surface area of adsorbent are minor factors of the removal. There are many types of adsorbents which have been used for HCl removal such as modified activated carbon using nickel and metal oxides (KO, CaO, MgO) (Hue, 1976; Park and Jin, 2005).

2.2.1 Literature review in HCl Adsorption

Lee et al (Lee et al., 2003), studied to modify GAC for HCl adsorption in reforming process by soaking GAC in 12N-GAC solution, to maximize NaOH adsorption on GAC. The modified GAC can adsorb 223,000 ppm HCl for 100 minutes. The chemical equations of the adsorption are as below;



In addition, an influence of moisture content of the adsorbent was studied over HCl adsorption efficiency. The study is conducted at 28°C, 1 atm, and varied percent moisture content (by weight) of the soaked GAC at (A) 29%, (B) 27%, (C) 25%, (D) 22%, (E) 17%, and (F) 9%, and found that the soaked GAC with 27 percent moisture content (by weight) has highest adsorption efficiency as shown in Figure 2.2.

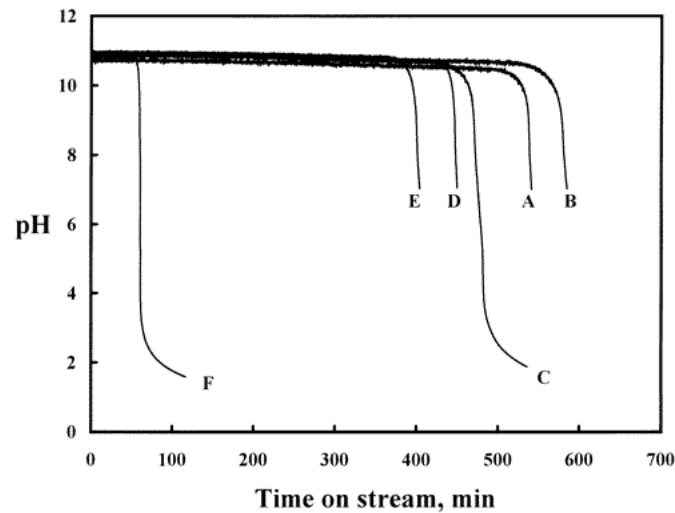
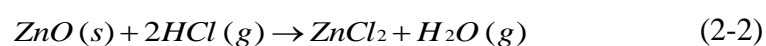
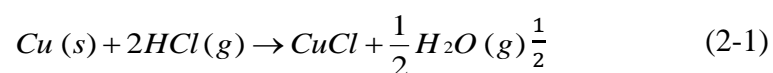


Figure 2.2 Moisture content of adsorbent on HCl adsorption efficiency.
(Lee et al., 2003)

Park and Jin studied by adding Silver (Ag) and Nickel (Ni) on activated carbon fiber (ACF) to increase HCl adsorption efficiency (Park and Jin, 2005). The study found that the ACF that formed as a sheet within 3 minutes for Silver, and 2 minutes for Ni, have highest HCl adsorption efficiency. The output concentration can be detected at 6.1, and 6.5 hours, respectively.

Silver and nickel are expensive. Through-put guarding unit might not be adequate. The unit requires frequent maintenances. To overcome those stated problems, two systems were together installed, hydro-treatment unit and chloride guard beds shown in Figure 2.3. It is also believe that sulfur is one of contaminated chemical causing several problems downstream, for example chloride compounds. HCl which is convert from hydrogen gas in the reactor is adsorbed on Cu or ZnO acting as chloride guards as shown in equation 2-1 to 2-2 (Twigg and Spencer, 2001).



In addition, Kim et al (Kim et al., 2008) studied by adding Silver (Ag), and Nickel (Ni) on ACF using Ag/Ni Bimetallic system, and found that at 22 wt%, and

5.2 wt% for Ag, and Ni, respectively, the ACF can adsorb HCl 21%, which were better than the single metal (14%).

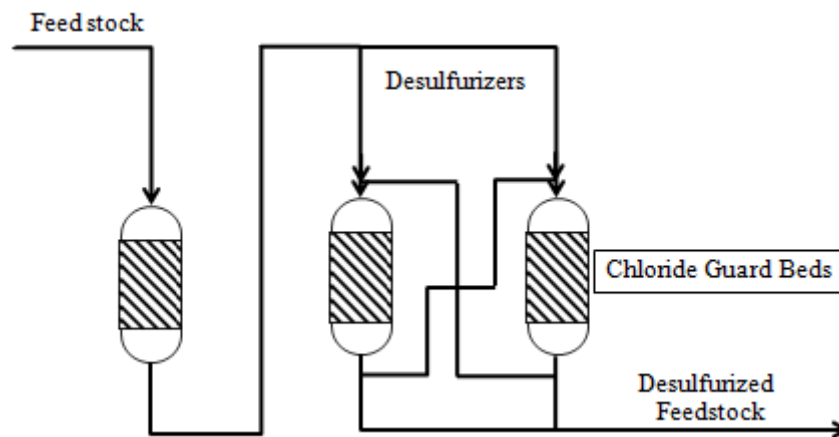


Figure 2.3 Chloride guard process (Twig and Spencer, 2001).

2.2.2 Literature review in VCM Adsorption

Scamehorn (Scamehorn, 1979) studied an adsorption of VCM using AC with surface area of 1150-1250 m²/g, and Iodine number 1200 mg/g, and found that it can adsorb VCM at a good level (Figure 2.4). Therefore, GAC is an interesting adsorbent for VCM adsorption.

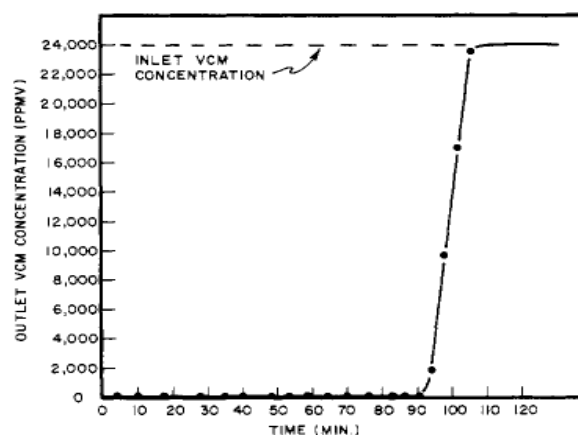


Figure 2.4 VCM adsorption by AC (Scamehorn, 1979)

2.3 Adsorbents

Commercial adsorbents usually used in industry are activated carbon, zeolite, silica (SiO_2) and alumina balls (Al_2O_3 balls). In this work focus on the adsorbents that have high surface area, pore size and sodium content that relates to adsorption performance of VCM and HCl removal. Consequently, activated carbon, zeolite NaY and RH-MCM-41 were selected to study.

2.3.1 Activated carbon

Activated carbon is a general adsorbent that is used in technologies related to pollution treatment due to its highly porous, surface area and large adsorption capacity. It has been reported that activated carbon is effective applied to any organic vapor substance removal (Scamehorn, 1979; Chatterjee et al., 2003; Walton et al., 2006). The adsorption ability of activated carbon depends on the functional groups cooperated on its surface, surface area and pore structure. Normally, the functional groups on activated carbon are associated with high concentration of unpaired electrons in imperfect sections of graphite that can react with molecular oxygen to form carbon-oxygen surface complexes such as carboxyl, lactone, phenol, carbonyl, ether, pyrone and chromene. These surface groups present an acid-base character of activated carbon that can adsorb organic compounds. (Rodríguez-reinoso, 1998).

To improve the inorganic gas adsorption onto activated carbon, it should be modified by adding a positive charge of the metal on surface such as by electroplating or soaking with metal solution to enhance the adsorption efficiency (Lee et al., 2003). Ag and Ni nanoparticles were electroplated on the surface of activated carbons fibers (ACFs). When HCl was adsorbed on the surface, it formed AgCl and NiCl_2 more effective for HCl removal than untreated ACFs (Park and Jin, 2005; Kim et al., 2008). Nevertheless electroplating and transition metals are high-cost operations. Consequently, alkaline metal, like Na, has been considered due to cheap and nontoxic. A few studies of HCl adsorption by active carbon modified Na have been done. The tests were carried out in HCl concentration of about 1,000 ppm under humid condition. Activated carbon modified Na showed an effective performance and was reused

repeatedly (Lee et al., 2003). However, the removal of VCM through adsorption has not been publicly reported.

There are various types of Activated Carbon, with different property and characteristics, as followings;

1) Powder Activated Carbon (PAC)

PAC is an activated carbon that has particle size less than 1 mm, with average diameter in a range of 0.15-0.25 mm. PAC has very high ratio of surface area per volume, and short distance for diffusion.

2) Granular Activated Carbon (GAC):

GAC has larger particle size, with smaller outside surface area than PAC. Therefore diffusion efficiency of adsorbent is a key factor for GAC. Suitable sizes of GAC for absorption are 8x20, 20x40 or 8x30 inch for liquid, and 4x6, 4x8, or 4x10 inch for gas, respectively.

3) Extruded Activated Carbon (EAC)

EAC is a formation of PAC with binder, with a rod shape, size of 0.8-130 mm. EAC is mainly used for gas absorption, due to less pressure drop, high strength, and less dust.

4) Impregnation carbon

Impregnation carbon is a carbon that impregnated with inorganic materials, i.e. Iodine (I), Silver (Ag), Aluminum (Al), Manganese (Mn), Zinc (Zn), Iron (Fe), Lithium (Li) and Calcium (Ca).

5) Polymer coated carbon

Polymer coated carbon is a product of coating process of porous carbon with a biocompatible polymer to provide a smooth and permeable coat without blocking the pores, which enhance a diffusion efficiency of the carbon. The polymer coated carbon has been used for medical treatment in order to remove toxic substances from blood of victim.

The goal of this work was to develop high efficiency adsorbent for both HCl and VCM removal. Activated carbon has high efficiency to adsorb both of them,

however, to develop higher adsorption efficiency, modified activated carbon is synthesized for this purpose.

Although, Silver and Nickel are transition metals that are expensive, and electroplating method are high cost. For economic reason, sodium (Na), which is commonly use, cheap, and has low electronegativity (EN) as show in Table 2.2, which chloride likes to react with, is interested to use (The University of Sheffield and WebElements Ltd, 2015).

Table 2.2 EN value of Silver (Ag), Nickel (Ni), Calcium (Ca), and Sodium (Na).

Element	EN
Ag	1.9
Ni	1.8
Ca	1.0
Na	0.9

Activated carbon and modified activated carbon performed high adsorption efficiency although they had no active metal and low surface area, respectively. To enhance the adsorption efficiency, the adsorbent must be composed of the both active metal and high surface area (Yang, 2003). Zeolite is one of material which contains both functions.

2.3.2 Zeolite NaY

Zeolite NaY is a micropore crystalline aluminosilicate which consists of SiO_4 and AlO_4 sharing a same oxygen atom. When Si^{4+} is replaced with Al^{3+} , an anion will be created on atoms, then cation in extra-framework of Na^+ will be balance in structure. It is an alternative material for considering as an effective adsorbent by reason of high surface area and containing with sodium content in molar ratio $\text{Na}_{56}[\text{Al}_{56}\text{Si}_{136}\text{O}_{384}]:250\text{H}_2\text{O}$. It consists of linking of 6 sodalite units as show in Figure 2.5 (Yang, 2003; Grisdanurak and Wittayakun, 2004). Zeolite NaY is an adsorbent effective to adsorb carbon dioxide (CO_2), ozone, and chlorofluorocarbons (CFC)

(Chatterjee et al., 2003; Walton et al., 2006). However, the application of zeolite is limited due to the microporous property cause mass transfer problem. Therefore, the microporous zeolite is modified to mesoporous zeolite that increased the accessibility to the internal surface and active sites. The Mesoporous zeolite NaY (Meso-NaY) can be synthesized in various ways such as a chemical treatment method by leaching zeolite NaY with sodium hydroxide (NaOH) and hydrochloric acid (Abello et al., 2009; Realpe and Ramírez, 2010). The other method is an addition of organic template such as cetyltrimethyl ammonium bromide (CTAB) and polydiallyldimethylammonium chloride (PDADMAC) (García et al., 2005; Liu et al., 2008).

From Yangyaim (Yangyaim, 2010), the Meso-NaY which synthesized by leaching with NaOH is effective to HCl, but not much to VCM.

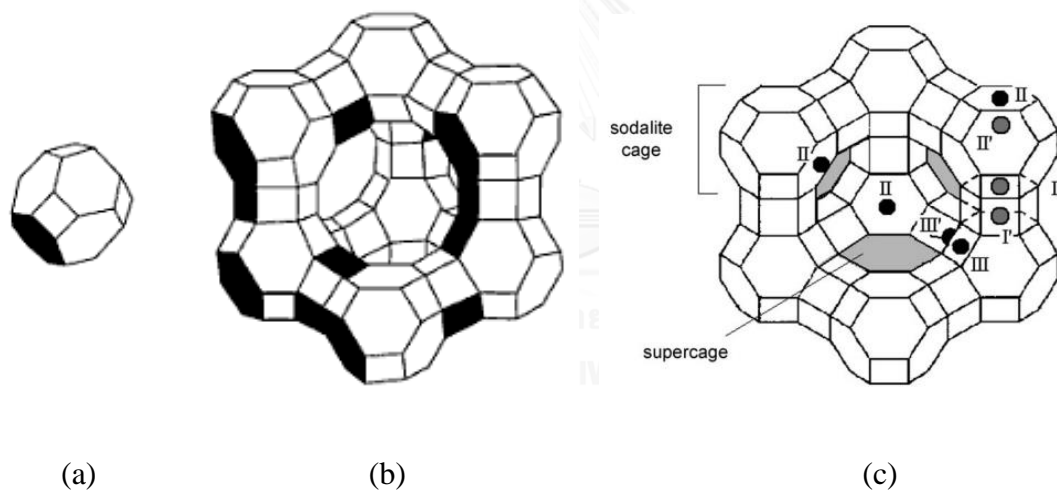


Figure 2.5 Zeolite NaY structure

(a) sodalite cage or truncated octahedron or beta cage

(b) faujasite or unit cell of zeolite NaY

(c) cation site in type Y locate at site I, I', II and II' (Yang, 2003)

2.3.3 RH-MCM-41

The RH-MCM-41 is an amorphous silica with a regular pore system consisting of an array of unidimensional, hexagonally shaped mesopores, pore size range of 2-50 nm and high surface area around 700-1,500 m²/g . The pore size of the RH-MCM-41 can be controlled by use of appropriate surfactants with various chain lengths as templates. Because of its uniform size and shape of mesopores as well as thermal stability, RH-MCM-41 is interesting as a model substance for gas adsorption, catalyst support. RH-MCM-41 was synthesized in ambient condition (Figure 2.6) and utilized as adsorbent for chlorinated volatile organics and has been continuously studied by modification with silane functional group on surface. However, the structure might be destroyed due to the thin pore wall. Therefore, it has been developed for synthesis of RH-MCM-41 by hydrothermal technique, using thermal and pressing conditions to improve stronger structure.

In this work, the RH-MCM-41 is considered to compare the adsorption efficiency with activated carbon; both of them have high surface area.

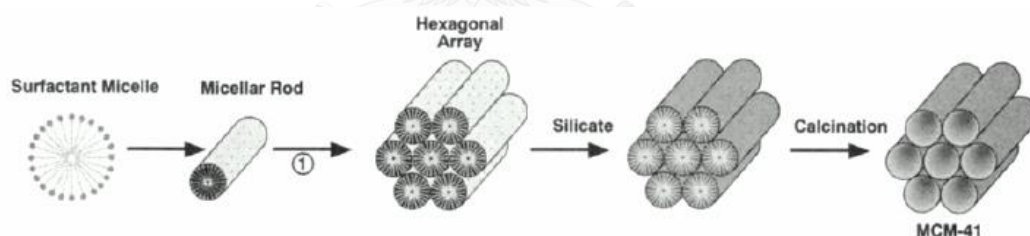


Figure 2.6 Synthesis mechanism of RH-MCM-41 (Beck et al., 1992)

2.4 Modification of adsorbents

2.4.1 Modification of Activated Carbon

There are various studies about surface modification of Activated Carbon to enhance its adsorption efficiency for different contaminant in both gaseous and aqueous conditions. In 2010, (Shafeeyan et al., 2010) reviewed the influence of surface modification of activated carbon on adsorption properties toward carbon

dioxide (CO_2), and summarized that “It was apparent from the literature survey that the surface chemistry of activated carbon strongly affects the adsorption capacity.”

2.4.2 Modification of Zeolite NaY

1) Rice husk silica

Rice husk is agricultural waste in Thailand which can utilize as fuel source in power plant. Moreover, it is widely use as silica source due to constituents of SiO_2 more than 90% in amorphous phase (Rahman et al., 2009). Silica is one of main constituents in zeolite NaY. Silica is not toxic and inert substance. There are two major types of silica; natural and synthesized silica. Generally, natural silica is divided into classes:

- Crystalline silica: This form depends on crystalline temperature. The structure would be formed in high crystallinity when temperature is increased. The main crystalline silica includes quartz, tridymite and cristobalite. The crystalline silica is showed in Figure 2.4 (a).
- Amorphous silica; It has higher reactivity and porosity such as silica gel which prepared from sodium silicate. The amorphous silica structure is incompletely arrangement due to fast crystallization during the ageing as shown in Figure 2.4 (b).

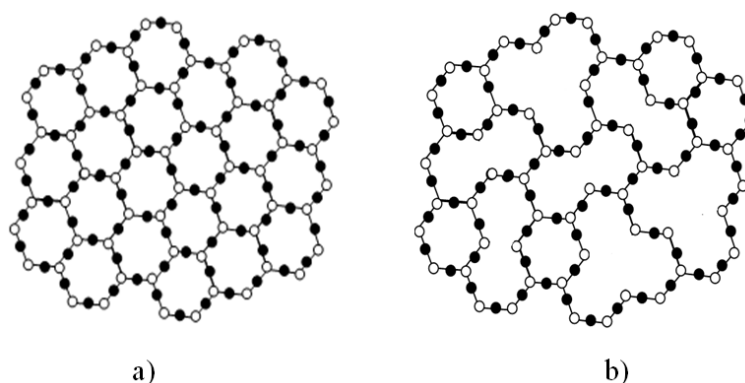


Figure 2.7 Silica: (a) crystalline silica; (b) amorphous silica
(Grisdanurak and Wittayakun, 2004).

2) To enhance the adsorption efficiency of zeolite, by modifying its surface to have mesopores is one possible technique, which enhance the adsorption of larger kinetic-size chemical. There are two techniques that can be used to enlarge the micropore to mesopore, which are adding template and chemical treatments. For this study, NaOH leaching was used as a chemical treatment. Detail of each technique can be described in the following sections.

- Adding template

Hexadecyltrimethylammonium bromide (CTAB) and polydiallyldimethylammonium chloride (PDADMAC) as organic template can be applied into the adsorbents. Adding template into zeolite NaY to create the mesopore of its structure. Therefore, the template in form of micelle is catches with silica and alumina around the micelle and form to particle. After calcinations, the mesopore particle is achieved (García et al., 2005; Liu et al., 2008).

- NaOH leaching is a chemical treatment technique that can be done using NaOH or hydrochloric acid. The slipping out of zeolite material texture under base condition can be showed in Figure 2.7. The texture of original Si/Al material was slipped out higher than that of low Si/Al material (Abello et al., 2009; Realpe and Ramírez, 2010). NaOH properties are shown in Table 2.3.

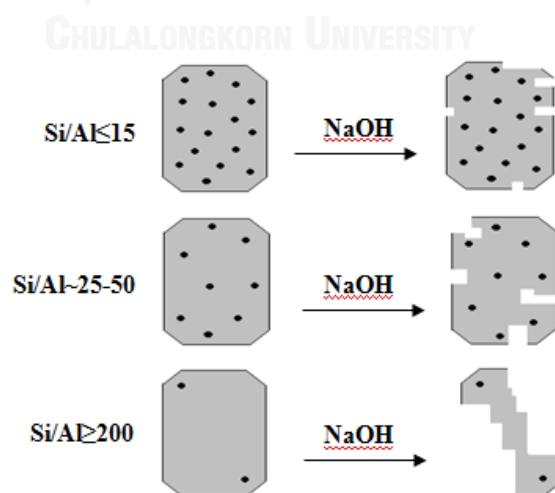


Figure 2.8 Formation of mesopores in different Si/Al ratios
(Realpe and Ramírez, 2010).

Table 2.3 NaOH properties

IUPAC name	Sodium hydroxide
Molecular formula	NaOH
Molar mass	256.41 g/mol
Appearance	White crystalline solid
Density	2.3 g/cm ³ (anhydrous)
Melting point	681°C (lit)
Boiling point	145°C
pH	14
Solubility in water	125 g/100 mL
Electronegativity	0.9

2.5 Pelletization

The adsorbent is synthesized in powder form. Due to pressure drop is increase during the use. The pellet form might be better form and considered. The pelletization has three methods including pressing, mechanical coating, and extrusion (McWilliams, 1988; Rahman et al., 1994; Yoshida et al., 2009).

1) Pressing is the adsorbent compaction method involving uniaxial pressure applied to the powder placed in a die between two rigid punches (Rahman et al., 1994).

2) Extrusion is the adsorbent force passing through a die, resulting in a long product (rods, bars, long plates, pipes) of regular cross-section, which may be cut into pieces of required length (McWilliams, 1988).

3) Mechanical coating is the adsorbent impact with mechanic force from ball mill and coat on the ball (Yoshida et al., 2009).

Yangyaim (Yangyaim, 2010), revealed that the pelletization of Meso-zeolite was used pressing method by pressurized pelletizer under condition 3 bar for 2 min, it shows high surface area and adsorption performance for HCl removal.

The method for pelletization of adsorbent can be used different via. The pressing is one method for pelletization. Rahman and co-workers used Urea Ammonium Sulphate (UAS) fertilizer by hydraulic pressure machine. The process was done under a condition of 500 kg/cm^2 (49.5 bar) for 2 min followed by pounding in small particles and drying (Rahman et al., 1994). The pelletization is used pressing by pressurized pellelizer under condition 3 bar for 2 min of zeolite Meso-NaY (Leaching) to study HCl and VCM adsorption potential, it shows higher than mechanical coating and extrusion methods (Yangyaim, 2010). Because of the result of BET of zeolite Meso-NaY (Leaching) by pressing method is highest.



CHAPTER 3

EXPERIMENTAL PROCEDURE

The adsorption study was tested over our synthesized material. Therefore, in this chapter, the detail of material preparation characterizations and column setup will be described. An upscale adsorption based simulation being in the management part is also covered. The experiment scheme is shown in Figure 3.1.

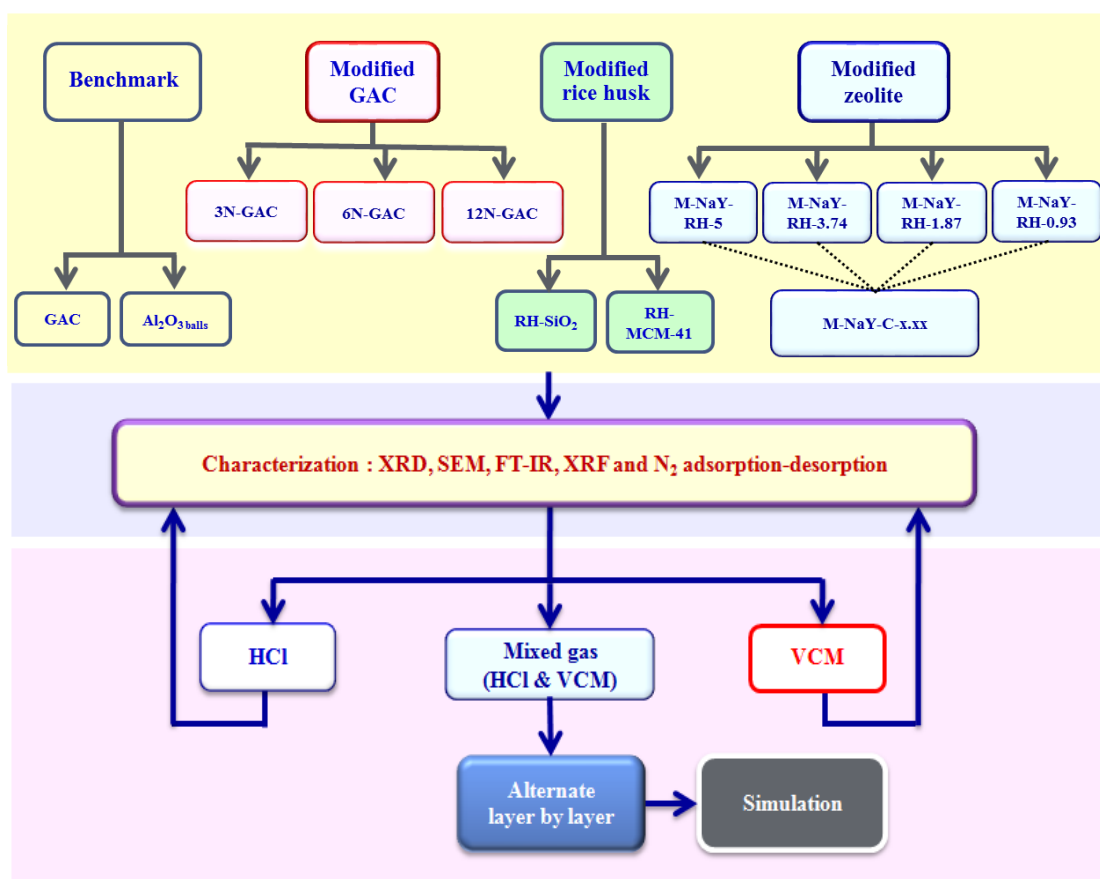


Figure 3.1 Schematic diagram of experiment

The experiment of this study is divided into three parts which are adsorbent synthesis, characterization, and HCl / VCM adsorption testing, respectively.

The first part, adsorbent synthesis, focuses on removal both HCl and VCM through four groups of adsorbents - benchmark adsorbents, modified from rice husk,

modified GAC, and zeolite Meso-NaY(Leaching). There are 12 adsorbents for individual gas removal as follows;

Group 1 : Benchmark adsorbents

- Alumina balls (Al_2O_3 balls)
- Granular activated carbon (GAC)

Group 2 : Modified rice husk

- RH-MCM-41 from rice husk
- RH-SiO₂ from rice husk

Group 3 : Modified GAC using NaOH

- 3N-GAC
- 6N-GAC
- 12N-GAC

Group 4 : Modified zeolite

- M-NaY-RH Si/Al ratio 5, 3.74, 1.87 and 0.93 by using rice husk as a silica source.
- M-NaY-C Si/Al ratio was selected by using sodium hydroxide and sodium silicate in commercial grade.

The second part, characterization, both fresh and spent adsorbents were characterized for their physical and chemical properties.

The last part, HCl and VCM adsorption testing, adsorption performances of studied adsorbents in form of bead were carried out in a continuous fixed-bed flow reactor.

3.1 Material

3.1.1. Chemicals

- Sodium hydroxide, pellets 99% (NaOH, MERK)
- Sodium aluminate anhydrous (NaAlO_2 , Sigma-Aldrich)
- Hydrochloric acid 37% (CARLO ERBA Reagents S.A.S)
- Sodium hydroxide, commercial grade 98% (AGC Chemicals (Thailand) Co., Ltd)

- Sodium silicate, commercial grade (Union Chemical 1986 Co., Ltd.)
- Aluminium Oxide, 99.637% commercial grade (Al_2O_3 , Union Chemical 1986 Co., Ltd.)
- Cetyltrimethylammonium bromide (CTAB, Fluka)
- Alumina balls (Al_2O_3 balls, Pingxiang Huihua Packing Co, Ltd, China)
- Phenolphthalein ($\text{C}_{20}\text{H}_{14}\text{O}_4$, Ajax Chemical)

3.1.2 Experimental gases

- Hydrogen gas 99.99% (H_2 , Praxair Co., Ltd)
- Hydrogen chloride gas 1,000 ppm Balance Hydrogen (HCl , Thai Industrial Gas Public Company Limited)
- Vinyl chloride gas 20 ppm. Balance Hydrogen ($\text{C}_2\text{H}_3\text{Cl}$, Thai Industrial Gas Public Company Limited)
- Mixed gas between 600 ppm. of HCl and 20 ppm. of VCM (Praxair Co., Ltd)

3.1.3 Instrument and apparatus

- Parafilm
- Filter-paper (Whatman no. 1)
- pH tester-paper
- Polypropylene bottle
- Filter-funnel
- Teflon-line autoclave
- Vacuum pump
- Magnetic stirrer and stirrer
- Furnace with temperature controller, with operating temperature up to 800°C
- Basin with temperature controller for the reflux set
- Detector tubes number (GASTEC Corporation)
 - 14L (0-76 ppm) and 14M (0-1,000 ppm) for HCl
 - 131La (0-20 ppm) for VCM

3.2 Material preparation and synthesis

3.2.1 Modified GAC

Activated carbon was obtained in granular form. The properties of GAC are presented in Table 3.1. The modified activated carbon was prepared by soaking in 3N, 6N and 12N solution for 3 h. Afterwards, it was filtered and dried at 80°C overnight. The obtained material was noted as 3N-GAC, 6N-GAC and 12N-GAC. Sodium content composed on the xN/GAC was determined by a titration technique.

Table 3.1 Typical properties of GAC from Carbokarn Co., Ltd. Thailand.

Source	Coconut shell	
Iodine number (mg/g)	1,254.0	
CTC adsorption (%)	57.2	
Particle size distribution	+8	7.4
	8×16	90.0
	-16	2.6
Moisture content (%)	5.3	
Corrected bulk density (g/mL)	0.5	

3.2.2 Preparation of RH-MCM-41

RH-MCM-41 was synthesized from a gel having a molar composition $4\text{SiO}_2:1\text{Na}_2\text{O}:1\text{CTAB}:0.29\text{H}_2\text{SO}_4:400\text{H}_2\text{O}$ (Chumee et al., 2009). Solution “A” was prepared by 4.5 g of CTAB in 90 mL of distilled water, while solution “B” was that rice husk silica 3 g dissolved in a solution containing NaOH 6 g in distilled water. Two solutions were mixed gradually until a clear solution was obtained. The pH of the gel mixture was adjusted to 11 with H_2SO_4 then the gel mixture was stirred for 2 h and finally the mixture was transferred into a teflon-lined autoclave and kept at 100°C for 3 days. The solid product was washed several times until pH=7 and dried at 100°C overnight. Finally the resulting material was calcined at 550°C for 6 h, with a heating

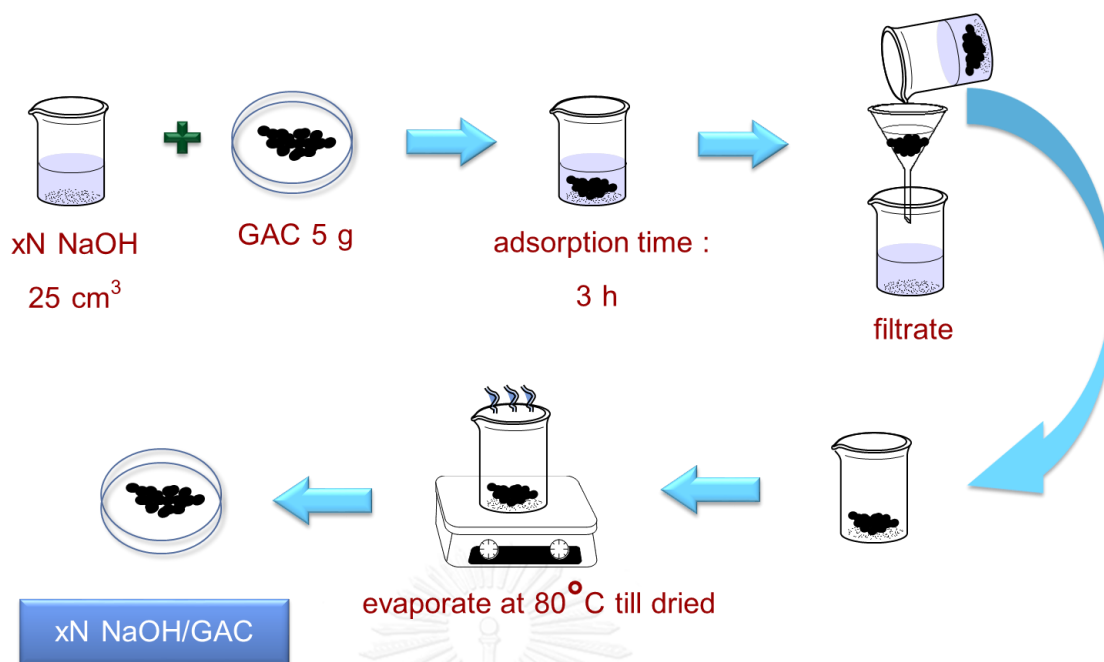


Figure 3.2 Synthesis of xN-GAC

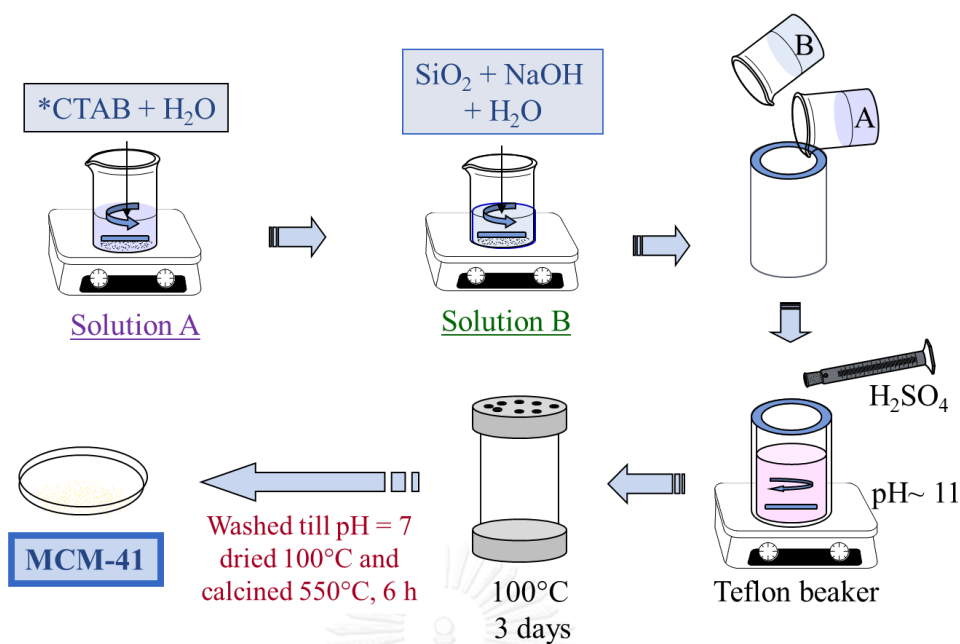
ramp of 5°C /min. The obtained material was named as RH-MCM-41. The synthesis RH-MCM-41 diagram is shown in Figure 3.3.

3.2.3 Preparation of RH-SiO₂

Rice husk was washed thoroughly with water to remove the adhering soil and dust and dried at 100°C overnight. The dried rice husk then was refluxed in 3M HCl solution for 6 h, filtered and washed repeatedly with water until the filtrate was neutral and dried in an oven at 100°C overnight. Finally, the refluxed rice husk was pyrolyzed in a hot air furnace muffle (Carbolite, CWF1200) at 550°C for 3 h to remove the organic contents to obtain the white RHS (Wittayakun et al., 2008).

3.2.4 Preparation of zeolite Meso-NaY

Zeolite NaY was synthesized first by hydrothermal method, where rice husk silica was used as a silica source in form of sodium silicate. The technique initially requires a seed gel and a feedstock gel (Wittayakun et al., 2008). For zeolite was



*CTAB: Cetyl trimethyl ammonium bromide

Figure 3.3 Synthesis of RH-MCM-41

intended to synthesize for Si/Al ratio of 3.74, which was able to compare to The International Zeolite Association (IZA).

The seed gel was prepared by NaOH, NaAlO₂, and Na₂SiO₃. The recipe in molar composition was set at 4.30Na₂O:Al₂O₃:10SiO₂:180H₂O. In this case 4.09 g of NaOH and 2.09 g of NaAlO₂ are dissolved in 20 mL of deionized water before adding of 22.72 g of Na₂SiO₃ solution. The mixture was aged at room temperature for 1 day.

The feedstock gel was prepared by NaOH, NaAlO₂, and Na₂SiO₃. The procedure in molar composition of 10.67Na₂O:Al₂O₃:10SiO₂:180H₂O. In this case 0.14 g of NaOH and 13.09 g of NaAlO₂ are dissolved in 130 mL of deionized water before addition of 142.43 g of Na₂SiO₃ solution but without aging.

Afterward, both gels were mixed, and crystallized for overnight at 90°C. The filtrated solid product was washed many times until pH was below 10. The solid product was further dried at 100°C.

Zeolite NaY in different ratios was synthesized. The variation of Si/Al ratio was set at 5, 3.74, 1.87 and 0.93. In this synthesis part, silica source was obtained from rice husk extraction and named as NaY.

Zeolite NaY was further modified using a leaching technique. NaOH solution was used. One gram of zeolite NaY and 0.2 N NaOH 60°C was mixed for 30 min. Material was washed until pH=10 and dried at 90°C for overnight (Abello et al., 2009). Material was named as M-NaY-RH-xxx.

Under the similar procedure, Meso-NaY was synthesized using sodium silicate as a silica source. The material obtained by this procedure was called as M-NaY-C-xxx. This was to investigate the effect of silica source on zeolite NaY.

3.2.5 Material characterization

Both fresh and spent adsorbents were characterized for their physical and chemical properties by X-ray diffraction (XRD, Bruker-AXS D8 A25 Advance), nitrogen adsorption-desorption isotherms (Quantachrome-Autosorb-1 BL model), Scanning electron microscopy (SEM, JEOL-5410), Fourier transform infrared (FTIR, Bruker-Tensor27), and X-ray Fluorescence (XRF, Philips-PW 2400).

The XRD spectrometer was used to measure crystallinity structures of adsorbent using CuK α source of 40kV, 40 mA. The scanning is performed at 2 θ radiation in regular range from 15° to 80° and 5° to 50° for modified GAC and for all zeolite adsorbents, respectively. The mean crystallite sizes of samples (D) will be calculated by the Scherer equation (3-1):

$$D = \frac{k\lambda}{\beta \cos\theta} \quad (3.1)$$

Where $k = 0.9$, $\lambda = 1.54$ corresponding to irradiation wavelength

β = the full width at half maximum of strongest line

θ = the Bragg angle of the most intense peak at a specific phase

The adsorbent were measured its isotherm at -196°C in relative pressure (P/P_0) range of 0.01-0.99 using nitrogen adsorption-desorption isotherms with a Quantachrome-Autosorb-1 BL model. The Brunauer-Emmet-Teller (BET) equation was used to determine the surface areas, while, the Barret-Joyner-Halenda (BJH) method was used to calculate pore size distribution and pore volume.

SEM was used to examine the surface morphology of samples at 15 kV. Powder samples were uniformly spread over an adhesive tape and coated with gold using sputter coater, before feeding into the microscope.

Hundred mg of KBr was mixed with 1 mg of sample and powdered. BRUKER-TENSOR27 GX FTIR was used to determine the functional groups of adsorbent. Pelletization of adsorbent was performed by pressing the sample at 10 N/m^2 . The wave number was scanned in the region of 1200 to 400 and 4000 to 3000 cm^{-1} .

The chloride quantities in fresh and spent adsorbents was determined by X-ray Fluorescence Spectrometer.

3.2.6 Pelletization of adsorbent

The modified GAC in this experiment, 90% of particle size of GAC is 2 mm. In the part of hydrodynamic is varied particle size (0.50, 1.25 and 2.00 mm) for good result in alternate layer by layer.

For RH-MCM-41 and M-NaY is synthesized in powder form. Due to pressure drop is increase during the use. The pellet form might be better form and considered. The pelletization methods is used pressing by pressurized pellelizator under condition 3 bar for 2 min. (Yangyaim, 2010).

3.2.7 Adsorption

Adsorption performances of studied adsorbents in form of bead were carried out in a continuous fixed-bed flow reactor. The column of 1 cm diameter was constructed with glass. Each layer was packed in 2 cm high of studied adsorbent was packed in 3 layers. Either 600 ppm HCl or 20 ppm VCM in feed gas with major component of H_2 was flowed into the column with feed rate of 50 mL/min (Figure 3.4(a)). The adsorption column is packed by glass wool, glass bead and NaOH/GAC,

with a fixed sequence as shown in Figure 3.4(b). The distance from air inlet to an adsorbent has to be more than 0.001 meter in order to create turbulence for more adsorption efficiency. Effluent from the adsorption column was monitored using special gas detector tubes No. 14L-14M for HCl and 131La for VCM. Detection limits for gas detector tubes No. 14L, 14M and 131La are 0.05, 2.5 and 0.25 ppm., respectively. The height and weight of adsorbent are used to calculate bed capacity of HCl and VCM adsorption by equation (3-2) to (3-4). The HCl and VCM removal tests were also investigated against RH-SiO₂ and commercial Al₂O₃ balls.

$$W_{\text{sat}} = \frac{F_A \times \text{Area above the breakthrough curve graph}}{\text{Mass of adsorbent per unit cross section area of bed}} \quad (3.2)$$

$$W_b = \frac{F_A \times \text{Area above the breakthrough curve graph at breakpoint}}{\text{Mass of adsorbent per unit cross section area of bed}} \quad (3.3)$$

$$\text{Bed capacity} = \frac{W_b}{W_{\text{sat}}} \quad (3.4)$$

where W_{sat} is adsorption potential (g_{HCl}/g)

W_b is adsorption potential when C/C_0 is the concentration in fluid relative to that in feed (Breakpoint: $C/C_0 = 0.05^*$)

F_A is the feed rate of solution (g·(cm²/h)).

* Breakpoint: $C/C_0 = 0.05$ is relative concentration at breakpoint.

3.3 Flow behavior analysis

Guarding of HCl is important part. The selected adsorbent was used to work on this part. The experiments was carried out based on the experimental design using Box-Benkhen model. There were three parameters for the analysis. These included flow rate (40-60 mL/min), column diameter (10, 20, 30 mm) and particle diameter of adsorbent (0.5, 1.25 and 2.0 mm)

* Since VCM contaminated in H₂ is in extremely low concentration, longer period of uptake has been required compared to HCl.



CHAPTER 4

RESULTS AND DISCUSSION

Adsorption performances of studied adsorbents were carried out in a continuous fixed-bed flow reactor. Studied adsorbent was packed in 3 layers. Each layer was packed in 2 cm high. To prevent the flow blockage, material was packed alternated with quartz wool. Feed gas with major component of H₂ contaminated with either 600 ppm HCl or 20 ppm VCM was flown into the column with a feed rate of 50 mL/min. Effluent from the adsorption column was monitored. Overall of this chapter is to describe about 1) preliminary results 2) HCl and VCM removal under different modified adsorbents. All work was compared the results with Al₂O₃ balls, commercial basis.

4.1 Preliminary results

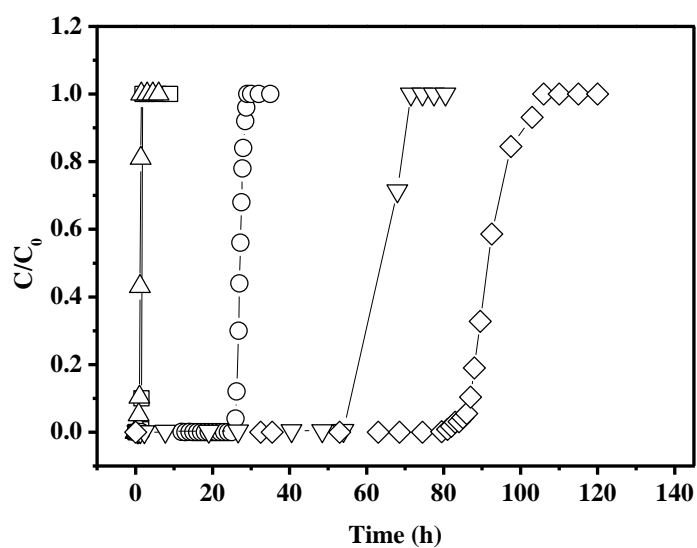
According to the literature review, five kinds of adsorbents materials have been interested. They included RH-SiO₂, RH-MCM-41, Al₂O₃ balls, GAC and M-NaY-RH-xxx. In this study, all materials were grinded to the same size of 2 mm. Initially, material which was leached by NaOH, was fixed its Si/Al ratio at 5. The results from a continuous flow provided in breakthrough curves. Figure 4.1 shows breakthrough curves of captured gases (a) HCl and (b) VCM, respectively) over all studied materials. Considering breakthrough curves of HCl, it was found that all curves were risen steeply after the breakthrough. This pattern implied that adsorption sites had been used uniformly. It was collaborated with no slugging flow occurring during the experiment, which confirmed the experiment was set properly.

Comparing the breakthrough time of all materials, it could be ranked as follows; M-NaY-RH-5 >> Al₂O₃ balls >> GAC >> RH-SiO₂ ~ RH-MCM-41. M-NaY-RH-5 shows the longest breakthrough time at 132.5 h, while material based silica, like RH-SiO₂ and RH-MCM-41, present the shortest breakthrough time at 50 and 92.73 min, respectively, shown in Figure 4.1(a).

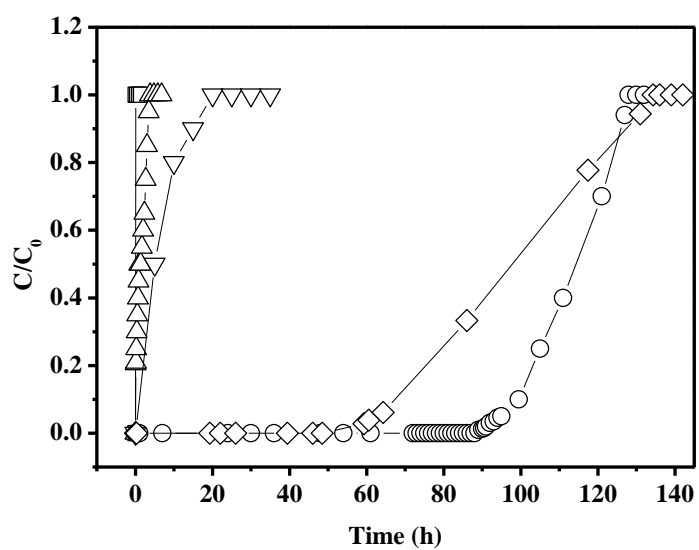
In term of numerical results, the dynamic adsorptions on each adsorbent are determined, and tabulated in Table 4.1. The area above breakthrough curve represented W_{sat} while the rectangular area in the region upto its breakthrough point represented W_{b} . The adsorption of HCl over M-NaY-RH-5 was found approximately 4, 5, 60, and 100 times compared to that over Al_2O_3 balls, GAC, RH-MCM-41 and RH-SiO₂, respectively.

Overall, M-NaY-RH-5 showed high potential in capture HCl, and it would be one of selective adsorbents for the further study.

NaY is a zeolite material composed of alumina and silica in the lattice. The ratio of Si/Al can be varied from 1.5 to 5. Na is a key component of lattice, which has surface area of 621 m²/g (described in section 4.2.2). Both factors could be taken into account for HCl adsorption efficiency over NaY. Considering the breakthrough curves of VCM (Figure 4.1(b)), all curves present in similar trend of rising up, except GAC. Comparing the breakthrough time of all studied materials, the rank from high to low could be listed as GAC >> RH-SiO₂ ~ Al_2O_3 balls ~ M-NaY-RH-5 ~ RH-MCM-41. GAC provided the longest breakthrough time of 99.5 h, while the adsorption took very little over RH-SiO₂, Al_2O_3 balls, RH-MCM-41 and M-NaY-RH-5, as shown in Figure 4.1(b). The dynamic adsorption of VCM over GAC is of 0.0063 g_{VCM}/g (Table 4.1). The capacity was not high, but it was considerably high compared to those of RH-SiO₂ and Al_2O_3 balls. Therefore, under this screening experiments, GAC was selected for further study in the case of chlorinated organic hydrocarbons. High capture of chlorinated hydrocarbon of GAC might be due to high surface area which is one of main factors as mentioned in section 4.3.2.



(a)



(b)

RH-MCM-41 (\square), RH-SiO₂ (Δ), GAC (\circ), Al₂O₃ balls (∇), and M-NaY-RH-5 (\diamond)

Figure 4.1 Breakthrough curves of (a) HCl and (b) VCM over several adsorbents.

Table 4.1 HCl and VCM adsorption potentials

Adsorbent	W_b		W_{sat}		Bed Capacity	
	gHCl/g	gVCM/g	gHCl/g	gVCM/g	gHCl/g	gVCM/g
M-NaY-RH-5	0.1295	-	0.1326	-	0.9769	-
Al ₂ O ₃ balls	0.0301	2.28x10 ⁻⁷	0.0356	4.01x10 ⁻⁶	0.8448	0.0569
GAC	0.0259	0.0063	0.0274	0.0078	0.9453	0.8134
RH-MCM-41	0.0021	-	0.0023	-	0.9228	-
RH-SiO ₂	0.0011	1.57x10 ⁻⁶	0.0015	0.0001	0.7333	0.0123

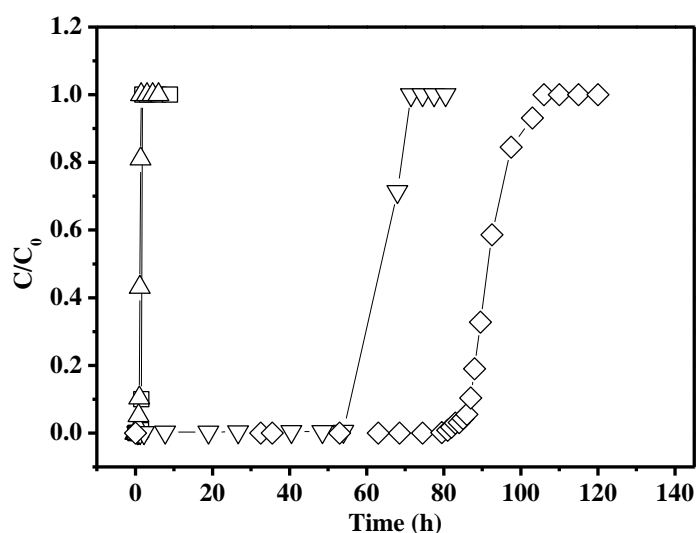
It was interesting that porous modified zeolite NaY had no adsorption potential on VCM. Similar to Figure 4.1 (b), breakthrough curve of VCM on RH-SiO₂ reached by 5 minutes time on stream.

4.2 HCl and VCM adsorption of commercial adsorbent

4.2.1 Effect of Si/Al

A chemical treatment method by leaching zeolite NaY with sodium hydroxide (Abello et al., 2009; Realpe and Ramírez, 2010) was chosen to modify microporous structure of zeolite to mesoporous structure. The method increased the accessibility to the internal surface and active sites. Previously, Yangyaim (Yangyaim, 2010) disclosed that mesoporous zeolite NaY with Si/Al ratio of 3.74 was effective to capture HCl gas. To investigate of mesoporous effect with Si/Al ratio, M-NaY-RH ratio 5, 3.74, 1.87 and 0.93 were synthesized and studied on HCl adsorption efficiency in fixed-bed flow reactor. The VCM adsorption study over M-NaY-RH-5 was not carried out, as mention in 4.1. Figure 4.2 presents breakthrough curve of HCl contaminated in H₂ feedstock by using four kinds of zeolite adsorbents including RH-SiO₂, RH-MCM-41, Al₂O₃ balls and M-NaY-RH-5. The results showed that M-NaY-RH-5

had higher adsorption efficiency of HCl than Al_2O_3 balls, RH-MCM-41 and RH-SiO₂. The evaluations of breakthrough adsorption capacity (W_b) were determined of 0.1295, 0.0301, 0.0021 and 0.0011 $\text{g}_{\text{HCl}}/\text{g}$ for M-NaY-RH-5, Al_2O_3 balls RH-MCM-41 and RH-SiO₂, respectively as shown in Table 4.1.

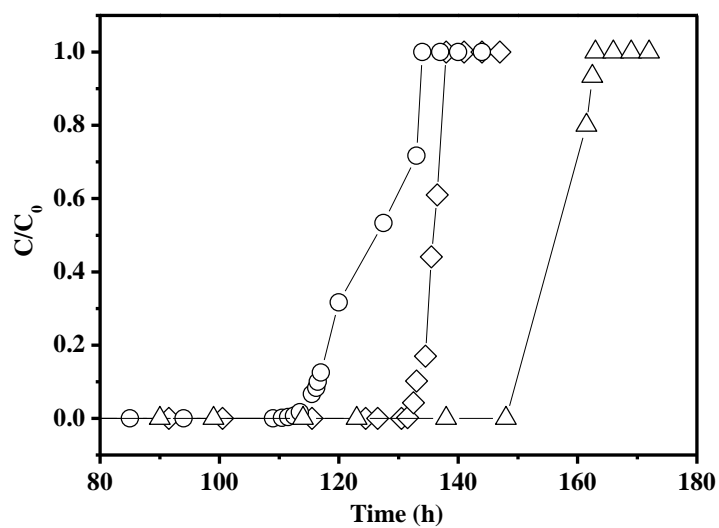


RH-MCM-41 (□), RH-SiO₂ (Δ), Al_2O_3 balls (∇), and M-NaY-RH-5 (◇)

Figure 4.2 Breakthrough curves of benchmark, modified rice husk and zeolite adsorbents for HCl adsorption

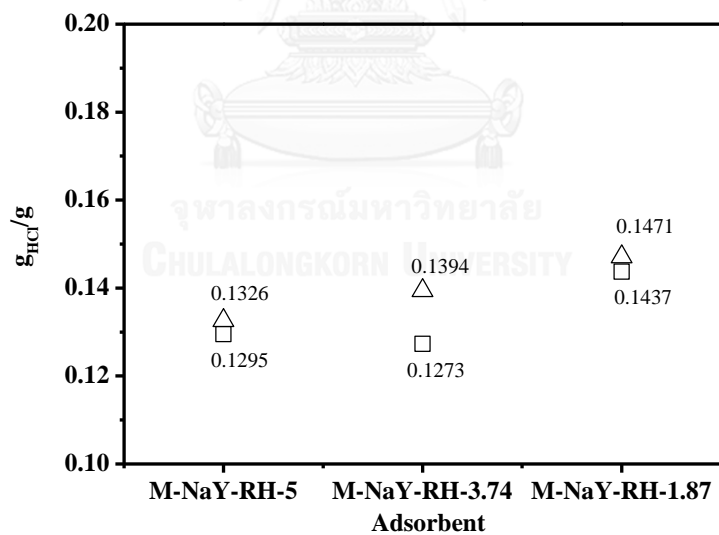
The breakthrough curves of M-NaY-RH-5, 3.74, 1.87 and 0.93 on HCl adsorption are considered, as shown in Figure 4.3(a). The breakthrough time could be ranked from high to low as follows; M-NaY-RH-1.87 > M-NaY-RH-5 ~ M-NaY-RH-3.74 respectively. As seen, the order was not in a descending order. However, the adsorption capacity based W_b and W_{sat} on mass basis of M-NaY-RH-5 and M-NaY-RH-3.74 was not different from each other much, shown in Figure 4.3(b). Their values lie on the same range which are 0.127-0.129 $\text{g}_{\text{HCl}}/\text{g}$. Therefore M-NaY-RH-1.87 was selective adsorbents for the further study.

Breakthrough curve of M-NaY-RH-0.93 was out of scope of consideration and the ranking. It could be due to its missing structure of NaY zeolite.



M-NaY-RH-5 (\diamond), M-NaY-RH-3.74 (\circ), and M-NaY-RH-1.87 (\triangle)

(a)



W_b (\square) and W_{sat} (\triangle)

(b)

Figure 4.3 (a) Breakthrough curves of M-NaY-RH-xxx on HCl adsorption
 (b) Adsorption capacity based W_b and W_{sat} of M-NaY-RH of 3 ratios.

4.2.2 Characterizations of adsorbents

XRD patterns of M-NaY-RH with different ratios are shown in Figure 4.4. Three samples with high ratio of Si/Al exhibited the NaY characteristic peaks compared with that of the parent zeolite. There were three-strong peaks of 2θ at 6.5° , 15.6° , and 23.7° , which showed the same positions as those of zeolite NaY reported in JCPDS file no.38-238 (Rayalu et al., 2000).

However, the pattern of XRD of M-NaY-RH-0.93 differed from the NaY original XRD pattern. The strong peak was shifted to higher angle 2θ . The structure of zeolite NaY was no longer be existed at lower the Si/Al ratio. Our result was correspond to the results presented by Berger (2005), which disclosed that the loss of NaY zeolite could be observed when the dealumination was carried out to make Si/Al ratio less than 1.8 (Berger et al., 2005).

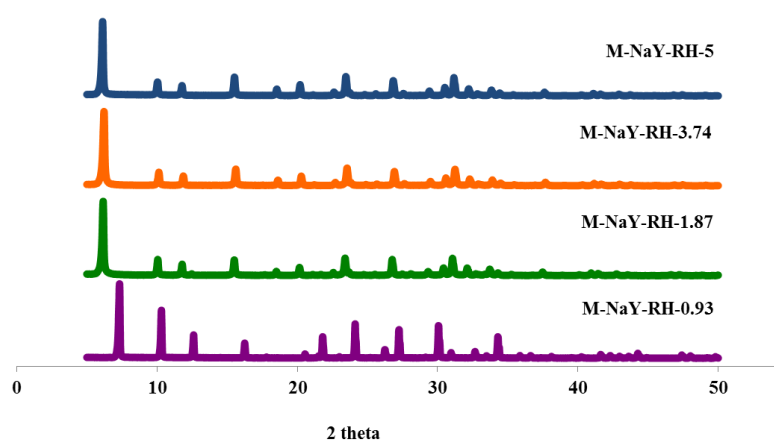


Figure 4.4 XRD spectra of M-NaY-RH-xxx.

FTIR analysis was also evaluated. The spectrum of M-NaY-RH-1.87 shows peaks at 3450 cm^{-1} , 1025 cm^{-1} , 578 cm^{-1} and 456 cm^{-1} , as shown in Figure. 4.5. The peak at 3435 cm^{-1} is corresponded to the O-H stretching vibration mode of hydroxyl functional groups. The appearance peaks at 1025 cm^{-1} and 456 cm^{-1} could be assigned for tetrahedral vibration. Moreover, the double ring external linkage peak at the band around 578 cm^{-1} is associated with FAU structure (Sang et al., 2006; Rahman et al., 2009).

FTIR spectra of M-NaY-RH-3.74 and M-NaY-RH-5 were similar to that with the M-NaY-RH-1.87, as described previously.

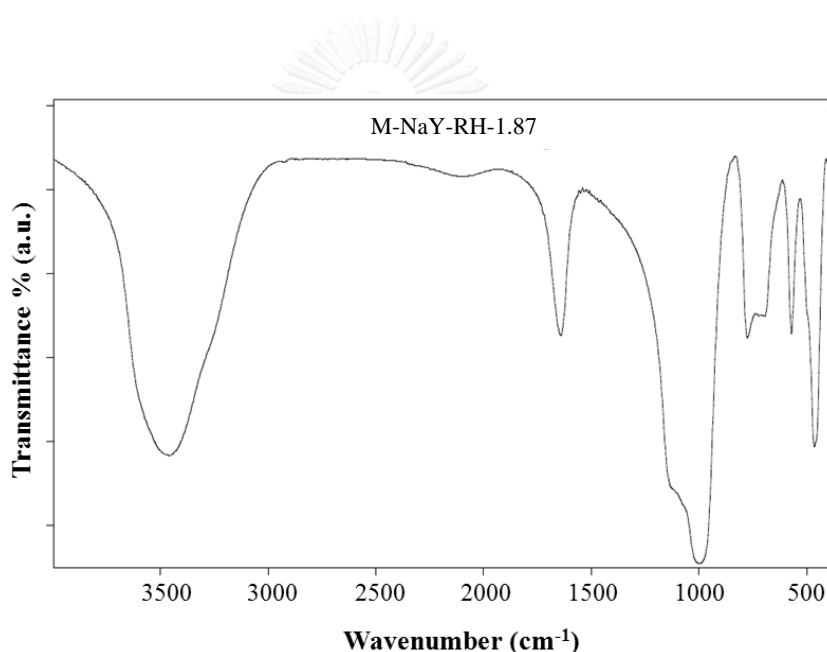


Figure 4.5 FTIR spectrum of M-NaY-RH-1.87.

The specific surface of M-NaY-RH-1.87 was measured. The N_2 adsorption-desorption isotherms of NaY-RH-1.87 are shown in Figure 4.6. The isotherm presented in type IV typical according to the IUPAC classification for mesoporous material. The hysteresis loop was occurred at relative pressure indicating that the mesopore were generated. This result confirmed that M-NaY-RH possess both micropores and mesopores.

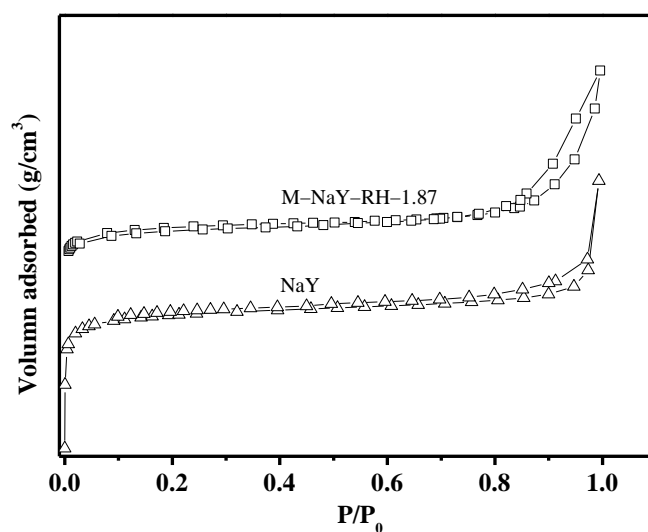


Figure 4.6 N₂ adsorption-desorption isotherm of M-NaY-RH-1.87

The morphology with a magnification of 10,000 of synthesized Zeolite NaY and M-NaY-RH-1.87 by SEM technique show in Figure 4.7. Particle shape of zeolite NaY in octahedral and twinned could be observed, while most of particle shape of M-NaY-RH-1.87 was twinned.

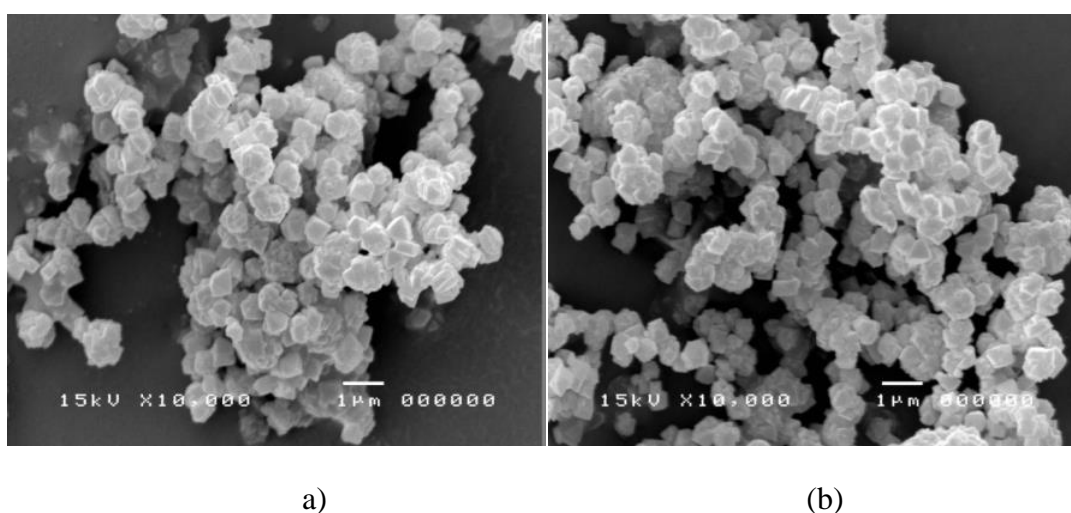


Figure 4.7 SEM images of (a) Zeolite NaY and (b) M-NaY-RH-1.87.

Measurement of BET P/P_0 at 0.01-0.03 as shown in Table 4.2 reports that RH-MCM has higher surface area (1,102 m^2/g) than M-NaY-RH-1.87, Al_2O_3 balls and RH-SiO₂, which are 621, 307, and 85 m^2/g , respectively. However, M-NaY-RH-1.87 has the highest HCl adsorption efficiency compare to other, as described previously in section 4.2.1. It was to confirm that HCl adsorption efficiency was not only depend on high surface area but also an optimal sodium content.

Table 4.2 BET-surface area of all adsorbents

Adsorbent	Surface area (m^2/g)
RH-SiO ₂	85
Al_2O_3 balls	307
M-NaY-RH-1.87	621
RH-MCM-41	1,102

As seen, sodium content in the structure should be one of main factors providing higher availabilities of adsorptive sites to HCl species. To clarify that hypothesis, elemental analysis was approximately analyzed by XRF. A composition of NaY and modified NaY are investigated by XRF, as tabulated those oxides of elements in Table 4.3. Material with an initial state detected no chloride species. This confirms that the leaching process could not destroyed chemical structure and composition of NaY, only expanded pore structure of NaY larger.

Table 4.3 Elemental composition of NaY-RH-1.87 and M-NaY-RH-1.87

Adsorbent	Na ₂ O (%)	Al ₂ O ₃ (%)	SiO ₂ (%)	Cl (%)
NaY-RH-1.87	8.23	25.69	65.93	-
M-NaY-RH-1.87	7.83	26.56	65.28	-

Remark : * Other : K₂O, CaO, TiO₂, CuO, Fe₂O₃, ZnO

4.2.3 Spent adsorbent

To prove that sodium is an adsorptive site, the elemental analysis of spent M-NaY-RH-1.87 are characterized and it was found that portion of sodium is decreased, while the portion of chloride is increased. The characterizations on each layer: (top, middle, and bottom) are shown in Table 4.4.

Table 4.4 Element composition of M-NaY-RH-1.87

Adsorbent	Na ₂ O	Al ₂ O ₃	SiO ₂	Cl	Other*
M-NaY-RH-1.87 adsorbed HCl-Top	4.71	14.15	30.09	50.64	0.40
M-NaY-RH-1.87 adsorbed HCl-Middle	4.55	14.35	31.20	49.58	0.33
M-NaY-RH-1.87 adsorbed HCl- Bottom	4.64	14.59	31.50	48.97	0.31

Remark : * Other : K₂O, CaO, TiO₂, CuO, Fe₂O₃, ZnO

Crystallinity of NaCl is characterized by XRD, referring to the hypothesis that Na is an active site for Cl atom.

The XRD patterns of M-NaY-RH-1.87 after HCl removal is shown in Figure 4.8. A sharp and strong peak at 32° and small peak at 46° were observed. The pattern was corresponded to NaCl crystalline pattern, reported by (Lee et al., 2003). Consequently, the forming of NaCl was occurred by chemisorption reaction between HCl and sodium content in M-NaY-RH-1.87 structure.

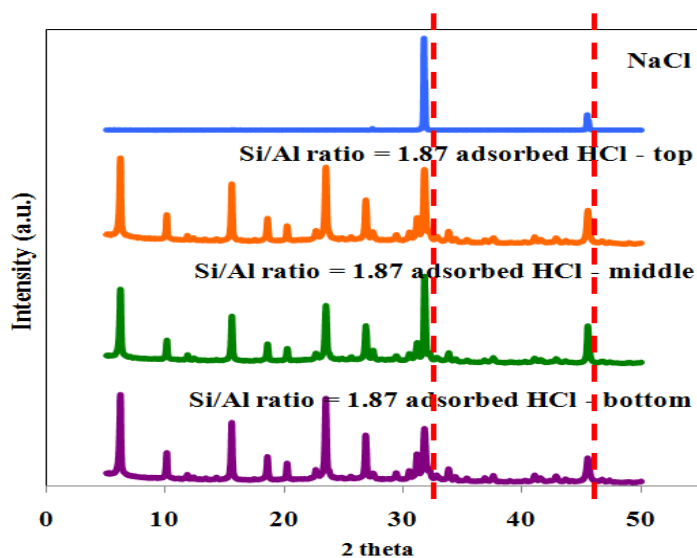


Figure 4.8 XRD pattern of M-NaY-RH-1.87 after HCl adsorption

4.3 HCl and VCM adsorption of Activated carbon

From preliminary results in section 4.1 it indicated that GAC showed the highest efficiency on VCM adsorption, and sodium can support HCl adsorption. In this section, the effect of sodium on GAC should be investigated.

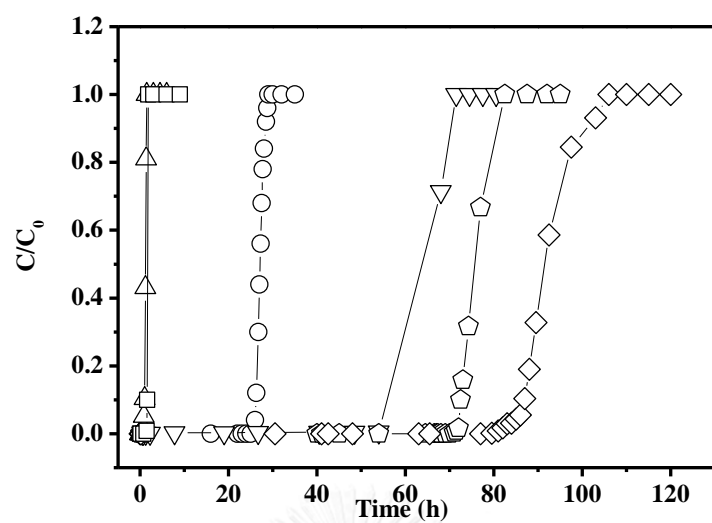
4.3.1 Effect of sodium content

The adsorption ability of activated carbon is probably in functions of specific surface area and pore structure. Normally, the functional groups on activated carbon are oxygen and carbon content on surface that can adsorb organic molecules with unpaired electrons (Rodríguez-reinoso, 1998). However, the application of activated carbon was limited for HCl removal because HCl is an active inorganic compound. A little adsorption capacity of HCl can be observed on GAC as previously confirmed in Figure 4.1(a). Metal oxides like Na_2O , KO, CaO, and MgO was found to adsorb HCl completely (Hue, 1976; Park and Jin, 2005). Therefore, a modification on active carbon should be studied. Lee (Lee et al., 2003) explained the addition of cation ion metal on surface by soaking with metal solution could enhance the adsorption efficiency. GAC were modified to investigate the optimal sodium content by soaking in 3-12N of NaOH.

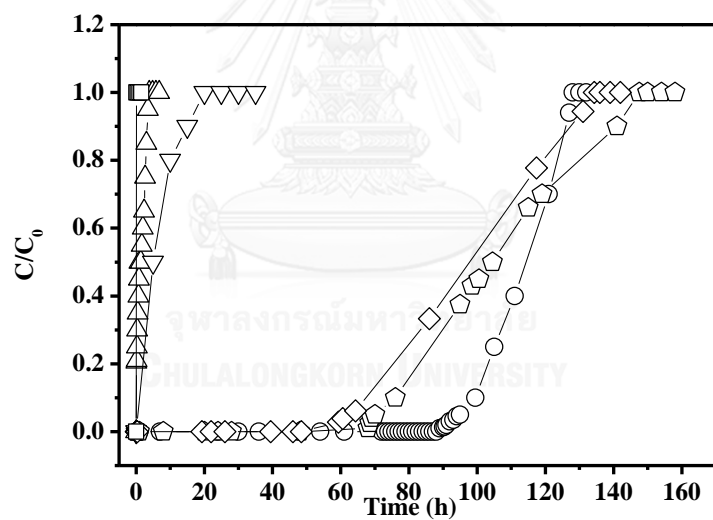
In the preparation, the physical investigation of material after doping NaOH at high concentration of 9N and 12N was observed some sodium white powder remaining on the surface of GAC. This would be possible due to the precipitation of Na salts. Moreover, the presence of sodium in water content could react violently with water during the drying. The reaction was exothermic which the heat release may cause the loss of crystallinity. Therefore, only 3N and 6N of NaOH doping onto GAC were used to test the adsorption.

Figure 4.9 shows breakthrough curves of HCl and VCM over 3N-GAC and 6N-GAC compared to GAC and Al₂O₃ balls as benchmark adsorbents. The breakthrough time of HCl could be ranked as 6N-GAC, 3N-GAC, Al₂O₃ balls, GAC, RH-MCM-41 and RH-SiO₂ sequentially as shown in figure 4.9(a). Table 4.5 shows adsorption potential (W_b) at 0.0681, 0.0592, 0.0301, 0.0259, 0.0021 and 0.0011 g_{HCl}/g over 6N-GAC, 3N-GAC, Al₂O₃ balls, GAC, RH-MCM-41 and RH-SiO₂ respectively.

For VCM adsorption, GAC has higher adsorption efficiency of VCM than 3N-GAC, 6N-GAC, RH-SiO₂, and Al₂O₃ balls with adsorption potential (W_b) at 0.0063, 0.0033, 0.0026, 1.57×10^{-6} , and 2.28×10^{-7} g_{VCM}/g respectively. RH-MCM-41 has no VCM adsorption capacity. This study focuses on adsorption of HCl which is a major contaminant in feed gas, and the results demonstrated that the 6N-GAC was optimum sodium content for HCl and VCM adsorption, therefore 6N-GAC will be selected for further study.



(a)



(b)

RH-MCM-41 (□), RH-SiO₂ (Δ), GAC (○), Al₂O₃ balls (∇),
3N-GAC (◡), and 6N-GAC (◊)

Figure 4.9 Breakthrough curves of (a) HCl (600 ppm)
and (b) VCM (20 ppm) contaminated in H₂

Table 4.5 The adsorption capacity of HCl and VCM of adsorbents

Adsorbent	W_b		W_{sat}		Bed Capacity	
	(gHCl/g)	(gVCM/g)	(gHCl/g)	(gVCM/g)	HCl	VCM
6N-GAC	0.0681	0.0026	0.0727	0.0041	0.9364	0.6341
3N-GAC	0.0592	0.0033	0.0625	0.0049	0.9478	0.6613
Al ₂ O ₃ balls	0.0301	2.28×10^{-7}	0.0356	4.01×10^{-6}	0.8448	0.0569
GAC	0.0259	0.0063	0.0274	0.0078	0.9453	0.8134
RH-MCM-41	0.0021	-	0.0023	-	0.9228	-
RH-SiO ₂	0.0011	1.57×10^{-6}	0.0015	1.27×10^{-4}	0.7333	0.0123

4.3.2 Characterizations of Modified GAC

Similar to zeolite NaY, GAC and modified GAC were characterized for their surface area, FTIR, SEM characteristics. Starting with specific surface area, N₂ adsorption-desorption isotherms in the relative pressure (P/P_0) ranges of 0.01-0.03 are shown in Figure 4.10. Both isotherms were of type I according to the IUPAC classification which are characteristic of the microporous structure. The adsorbed amount of NaOH/GAC was lower than GAC indicating that its surface areas decreased after NaOH adding (see Table 4.6). It was possible that the surface area decreased because the pores of GAC might be blocked by NaOH particles. The hysteresis on each isotherm were also observed. This would indicate some mesopores existing in the structure of GAC. Table 4.6 summarizes GAC surface area compared to those of benchmark adsorbents. GAC originally was found in higher surface area than 3N, 6N, 12N-GAC, RH-SiO₂ and Al₂O₃ balls which at 995, 902, 846, 412, 258, 307, and 85 m²/g, respectively. As shown the surface area of 12N-GAC at was less than an original GAC approximately 3 times.

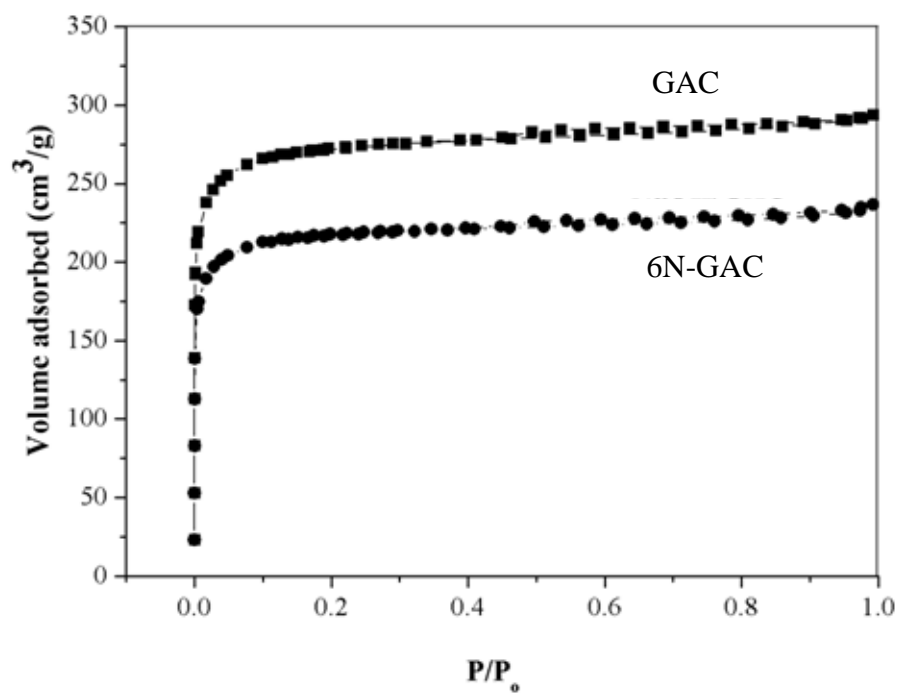


Figure 4.10 N₂ adsorption-desorption isotherm of GAC and 6N-GAC

Table 4.6 BET-surface area of all adsorbent

Adsorbent	Surface area (m ² /g)
GAC	995
3N-GAC	902
6N-GAC	846
9N-GAC	412
12N-GAC	258
Al ₂ O ₃ balls	307
RH-SiO ₂	85

NaOH/GAC was characterized by XRD to confirm the structure. The 6N-GAC XRD spectrum shows similar characteristic peaks of GAC structure as shown in Figure 4.11. Therefore this method is successful synthesized NaOH/GAC. XRD patterns of GAC and NaOH/GAC showed two broad peaks around 23° and 43° , which could be attributed to the presence of carbon and graphite (Bouchelta et al., 2008). After soaking in NaOH solution, the XRD pattern of NaOH/GAC shows sharp peaks at 30° and small peaks around $32-50^\circ$ correspond to crystalline of NaOH that contained on granular activated carbon surface. Moreover, the XRD pattern of silica and alumina balls present its characteristic peaks in amorphous phase of benchmark adsorbents.

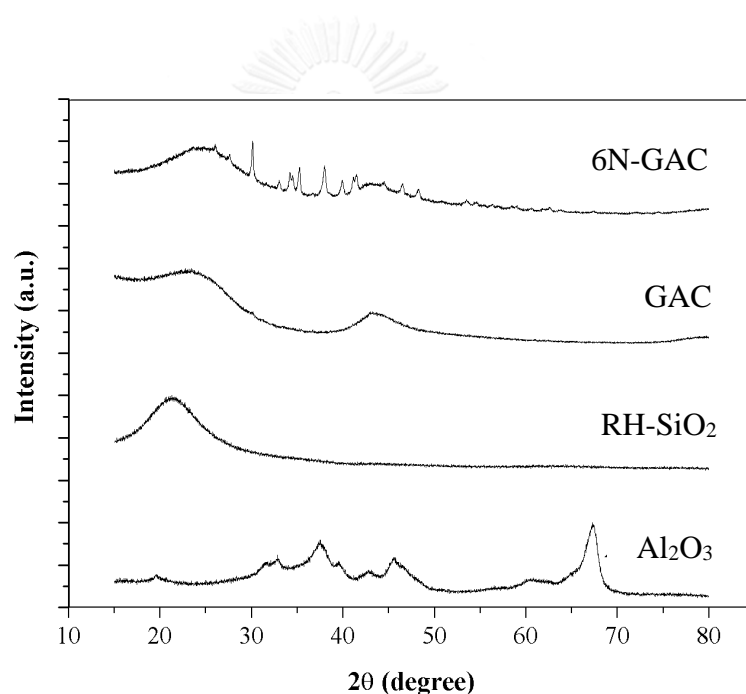


Figure 4.11 XRD pattern of 6N-GAC, GAC, RH-SiO₂ and Al₂O₃ balls

SEM images of GAC and 6N-GAC are shown in Figure 4.12. The structure and morphological characteristics of microcrystalline cellulose (Pettersson and Oksman, 2006) and lignin (Gani and Naruse, 2007) was observed. The external surfaces of GAC were presented smooth open pores of different sizes. The large pores in GAC are contained multiple smaller pore like sponge as shows in cross-section image (Figure 4.12 (b)). It was observed mostly micropores with nearly uniform dimensions. In other hand, the external surfaces of 6N-GAC were presented decomposing of micro crystalline cellulose and blocked pore due to high concentration of NaOH solution. The cross-section images show the small pore inside large pore also block by NaOH particles that correspond with BET surface area and XRD results.

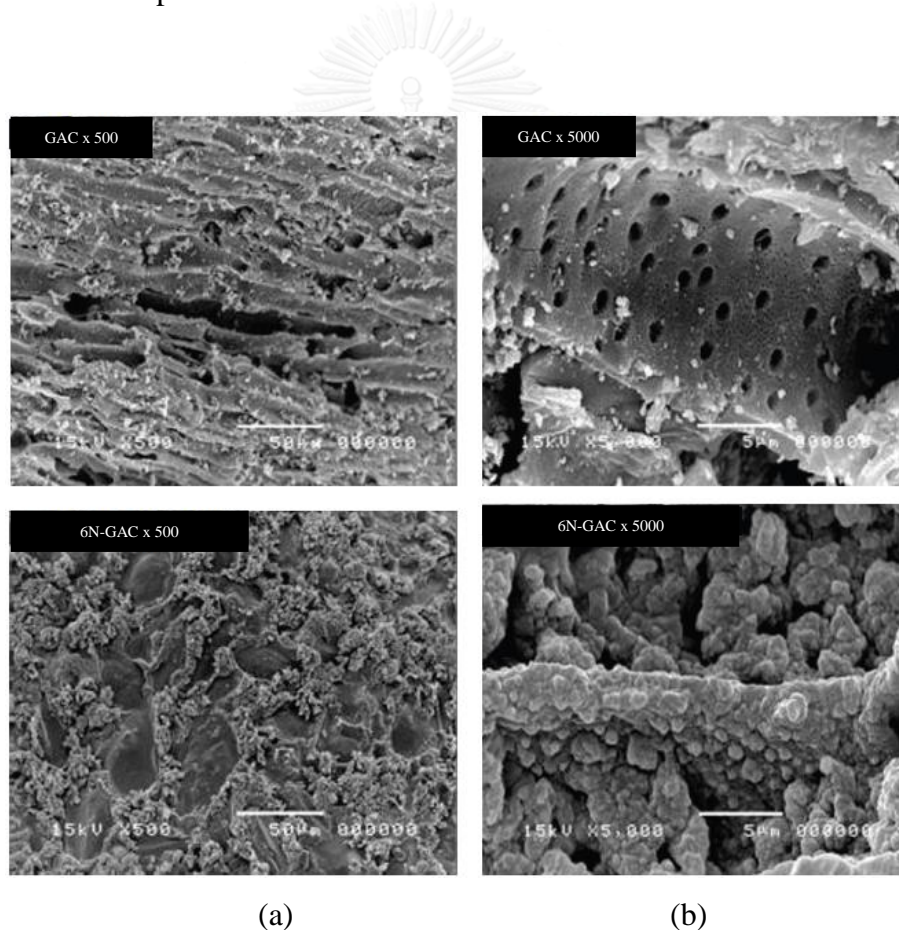


Figure 4.12 SEM images of GAC and 6N-GAC;
(a) external surface and (b) cross-sectional surface

FTIR spectra of GAC and 6N-GAC (Figure 4.13) presented peaks at 3435 cm^{-1} , 2950 cm^{-1} , 2850 cm^{-1} , 1650 cm^{-1} , 1384 cm^{-1} , 1450 cm^{-1} , 1110 cm^{-1} and 675 cm^{-1} . According to the peaks that appeared at 3435 cm^{-1} were assigned to the O-H stretching vibration mode of hydroxyl functional groups including H bonding, at 2950 cm^{-1} and 2850 cm^{-1} presented aliphatic C-H stretching, at 1650 cm^{-1} indicates stretching of conjugated C=C or C-O in aromatic. The bands between 1384 cm^{-1} and 1450 cm^{-1} are assigned to -OH bending vibration that present strong peak when NaOH adding. The band around 1100 cm^{-1} is assigned to in-plane bending of aromatic ring C-H bond. Finally, a small peak appeared at around 675 cm^{-1} for C-C out of plane ring deformation. From those groups, the main ones appeared on acidic and basic surface are activated carbon (El-Sheikh et al., 2004; Namasivayam and Kavitha, 2006; Bouchelta et al., 2008).

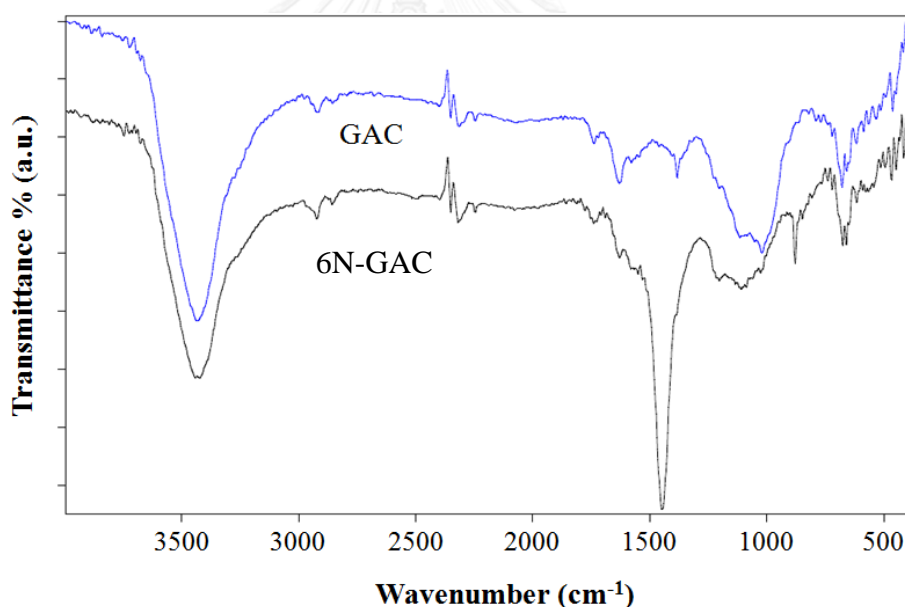


Figure 4.13 FTIR spectra of GAC and 6N-GAC

The HCl adsorption potential (W_b) of 6N-GAC at $0.0681\text{ g}_{\text{HCl}}/\text{g}$ showed higher adsorption efficiency than GAC because of the sodium content in GAC structure reacted with HCl to form salt (NaCl) crystalline as show in XRD result of adsorbent after adsorb HCl (Figure 4.14). Moreover, the GAC also adsorb HCl because of the unpaired electrons of oxygen and carbon in graphite surface can react with HCl as show

beam XRD pattern. After spent of 6N-GAC were characterized with XRF to find the amount of Cl residues, the result shows in Table 4.7. The amount of Cl residues in each layer were different indicate that the packing of adsorbent should be improve. In other hand, the VCM adsorption potential (W_b) of GAC was 0.063 g_{VCM}/g , which higher than 6N-GAC because surface area of 6N-GAC was decreased after NaOH incorporate thus the active functional group also decreased corresponding with BET result.

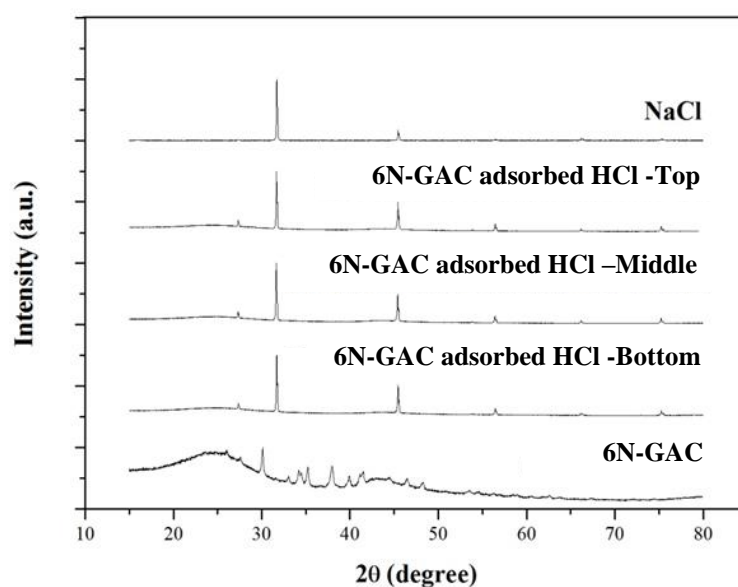


Figure 4.14 XRD pattern of GAC and 6N-GAC after HCl adsorption

Table 4.7 Element composition of adsorbent from XRF

Adsorbent	Na ₂ O	Al ₂ O ₃	SiO ₂	Cl
GAC	0.01	<0.01	0.04	0.05
6N-GAC	5.49	<0.01	0.25	0.17
6N-GAC adsorbed HCl-Top	0.16	<0.01	0.01	1.68
6N-GAC adsorbed HCl-Middle	0.37	<0.01	0.01	3.89
6N-GAC adsorbed HCl-Bottom	0.47	<0.01	0.01	4.59

4.3.3 Effect of chemical impurity in the material synthesis

It is an intention of using this material (M-NaY-RH-1.87) in the process. In order to produce in a large quantity the price of all chemicals would be a big concern. In this study caustic soda, and sodium silicate solution in commercial grade should be considered compared to rice husk. The synthesis of M-NaY-C-1.87 using commercial grade and laboratory grade was done and then tested on HCl adsorption.

M-NaY-RH-1.87 synthesized by rice husk as silica source was characterized its crystallinity with XRD, as shown in Fig.4.15. M-NaY-C-1.87 synthesized by commercial grade chemicals provided an XRD pattern corresponding to that synthesized by M-NaY-RH-1.87. This could be concluded that impurities (Ca, Mg, etc.) in commercial grade chemicals did not affect to the structure of M-NaY. All peaks representing zeolite NaY are shown in both spectra, in Figure 4.15.

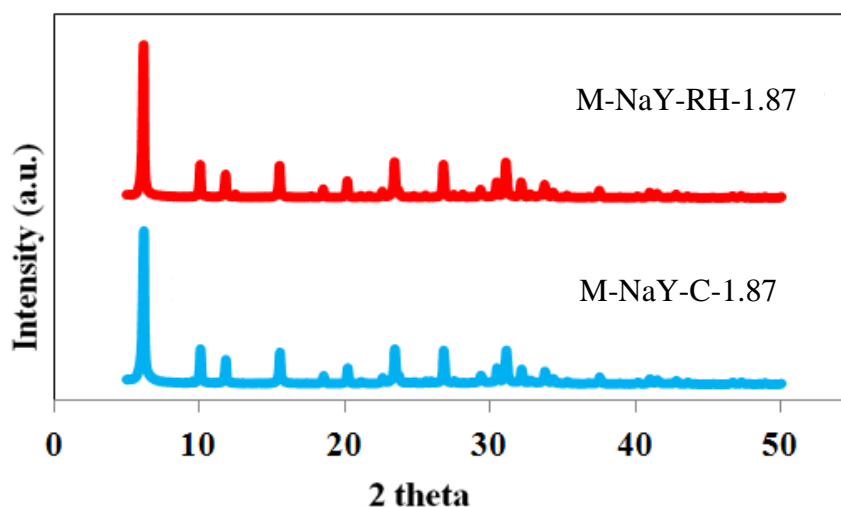
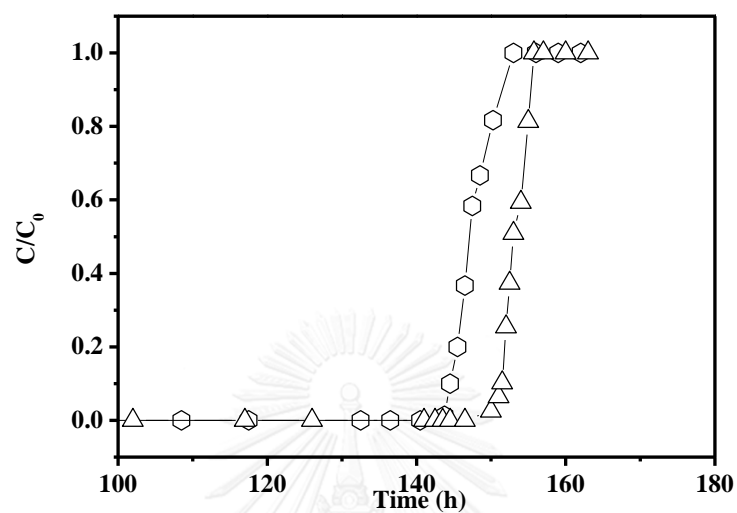


Figure 4.15 Comparing XRD pattern of M-NaY-RH-1.87 laboratorial and commercial grade

The breakthrough curve results of M-NaY-xx-1.87 synthesized by either rice husk or commercial grade chemicals tested over HCl adsorption are shown in Figure 4.16 which found that the efficiency of HCl removal was not significantly different. It provided similar potential adsorption, M-NaY-RH-1.87 ($W_b=0.1444$ g_{HCl}/g) and M-NaY-C-1.87 ($W_b=0.1437$ g_{HCl}/g) as shown in Table 4.8. Therefore, the

following experiment will use M-NaY-RH-1.87 as adsorbent to adsorb main HCl, GAC and 6N-GAC to remove both HCl and VCM.



M-NaY-C-1.87 (\circ) and M-NaY-RH-1.87 (Δ)

Figure 4.16 Breakthrough curve of HCl Contaminated in H₂

Table 4.8 The efficiency of HCl adsorption of M-NaY by using rice husk and commercial grade chemicals.

Adsorbate	Adsorbent	W_b (gHCl/g)	W_{sat} (gHCl/g)	Bed Capacity
HCl	M-NaY-RH-1.87	0.1444	0.1469	0.9832
	M-NaY-C-1.87	0.1437	0.1471	0.9765

4.4 Alternate layer by layer

GAC has been noticed for capturing VCM (a representative for chlorinated organic compound), while M-NaY-RH-1.87 showed, on the other hand, higher capture of HCl (a representative for chlorinated inorganic compound). Moreover, modified GAC with NaOH could improve the ability on HCl adsorbing. In order to increase the adsorptive performance of both chlorinated compounds, all three materials should be utilized in the adsorption packing arrangement study. M-NaY-RH-1.87/6N-GAC/GAC were mixed in different ratios, including the ratio of 1/1/1, 1/1/2, and 1/1/8. All these materials were tested over the mixed gases. The objective of doing this was to test whether the mixing rule could be applied to predict the adsorption capacity for other adsorbent mixing conditions. Nine experiments shown in Table 4.9 were carried out.

Table 4.9 Packing arrangement for HCl guarding

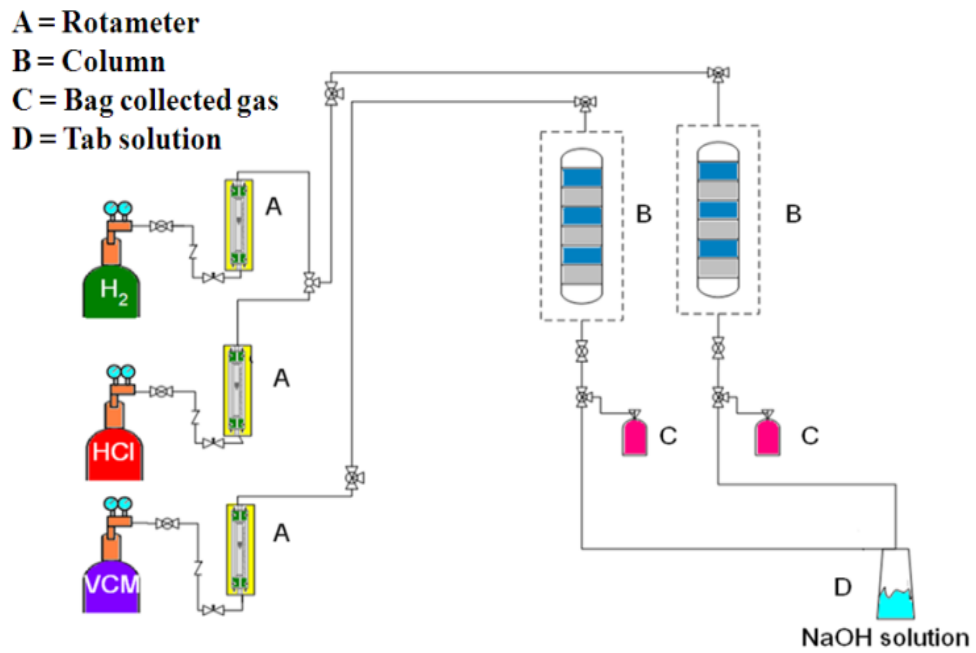
Run #	Condition of flow gas	Adsorbent arrangement
1	Individual flow*	GAC
2	Mixed gas flow**	GAC
3	Individual flow	6N-GAC
4	Mixed gas flow	6N-GAC
5	Individual flow	M-NaY-RH-1.87
6	Mixed gas flow	M-NaY-RH-1.87
7	Mixed gas flow	M-NaY-RH-1.87/6N-GAC/GAC in the ratio of 1/1/1
8	Mixed gas flow	M-NaY-RH-1.87/6N-GAC/GAC in the ratio of 1/1/2
9	Mixed gas flow	M-NaY-RH-1.87/6N-GAC/GAC in the ratio of 1/1/8

* Individual flow: HCl gas

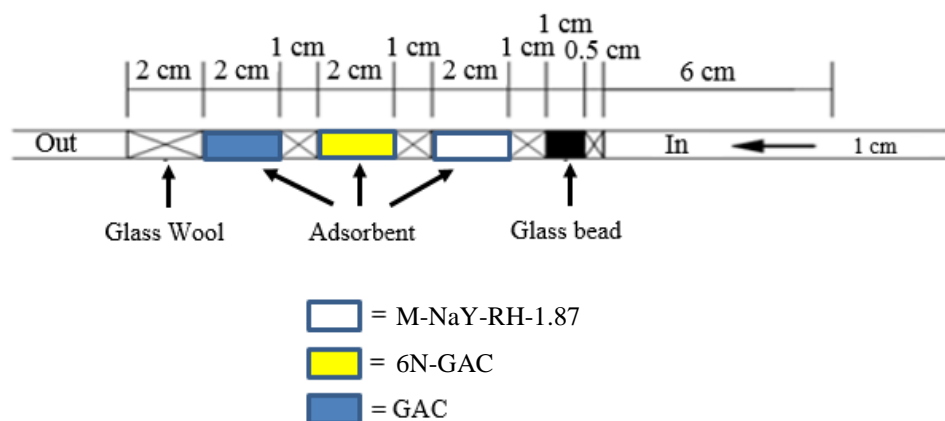
** Mixed gas flow: HCl gas and VCM gas

GAC, 6N-GAC and M-NaY-RH-1.87 which has high adsorption efficiency was selected to study alternate layer by layer with mixed gas between HCl and VCM concentration at flow rate 50 mL/min, particle size 2.00 mm and column

diameter 1 cm. as shown in Table 4.9. Flow diagram of fixed-bed flow reactor and column packing for alternate layer by layer with mixed gas as shows in Figure 4.17 (a) and (b) respectively.



(a) Adsorption testing for mixed gas



(b) Column packing for alternate layer by layer

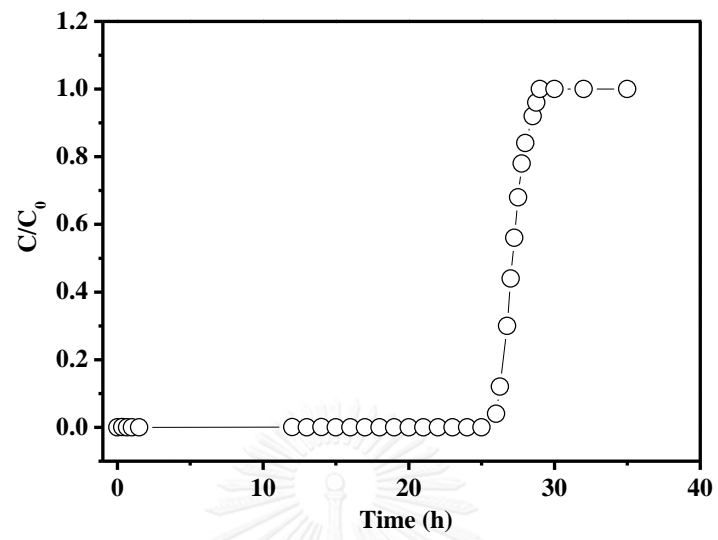
Figure 4.17 Flow diagram of fixed-bed flow reactor for alternate layer by layer.

To investigate the interference of two gases in the adsorption and the mixed adsorbent ratio, simple three individual tests on each gas and each adsorbent were tested. Moreover, six runs of the mixed gases adsorption performance over alternate layer by layer of adsorbents were performed. The results of those runs are shown in Figure 4.18 – 4.19.

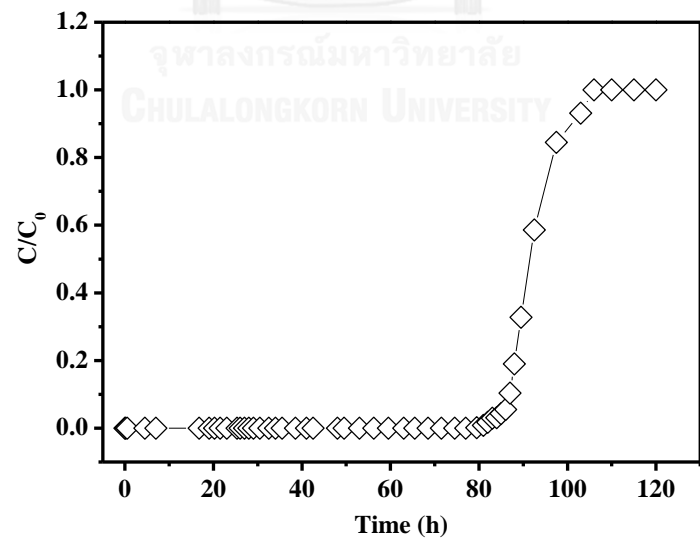
The adsorption capacities for each run were determined and tabulated in Table 4.10.

Table 4.10 Adsorption capacities for each run

Inlet gas	Adsorbent	W_b (g _{HCl} /g)	W_b (g _{VCM} /g)
Single gas	GAC	0.0259	0.0063
	6N-GAC	0.0681	0.0026
	M-NaY-RH-1.87	0.1444	-
Mixed gas	GAC	0.0336	0.0031
	6N-GAC	0.0512	0.0030
	M-NaY-RH-1.87	0.1444	-
	M-NaY-RH-1.87/6N-GAC/GAC in the ratio of 1/1/1	0.0747	0.0012
	M-NaY-RH-1.87/6N-GAC/GAC in the ratio of 1/1/2	0.0705	0.0015
	M-NaY-RH-1.87/6N-GAC/GAC in the ratio of 1/1/8	0.0443	0.0019



(a)



(b)

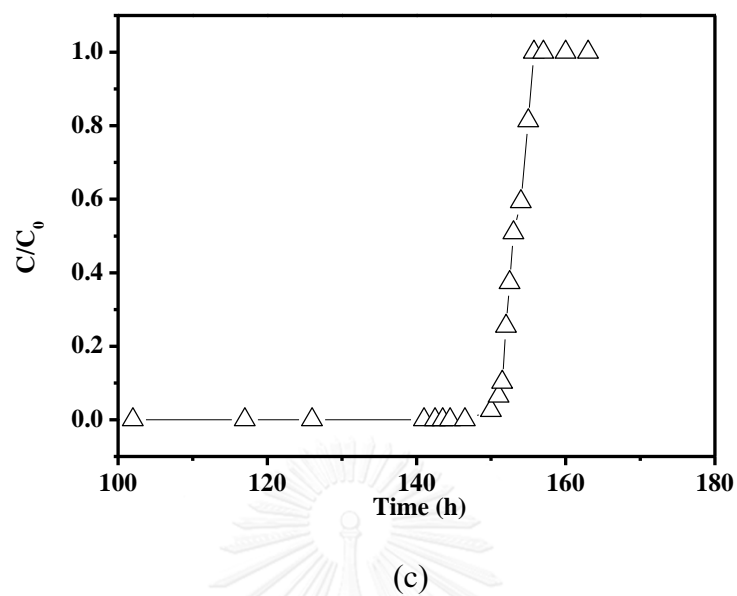
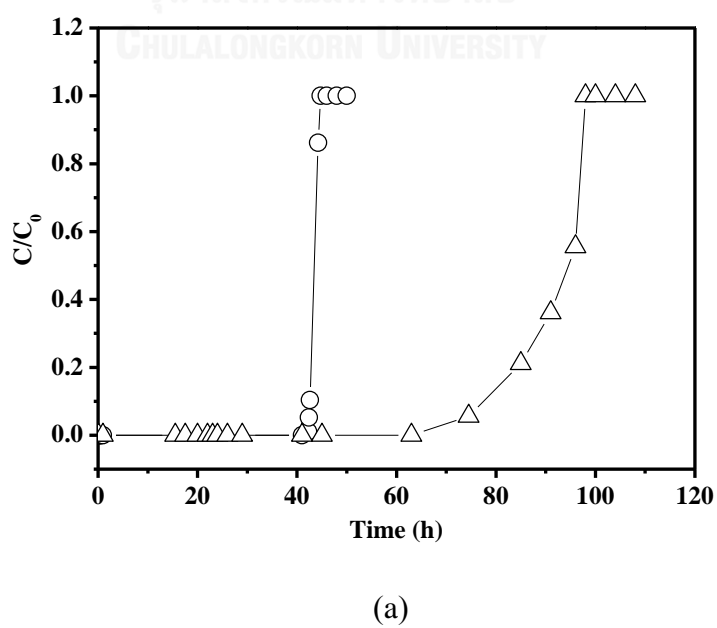
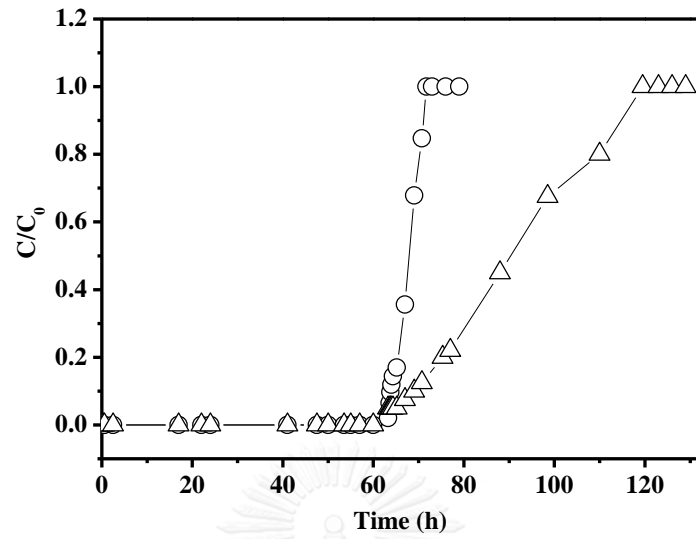


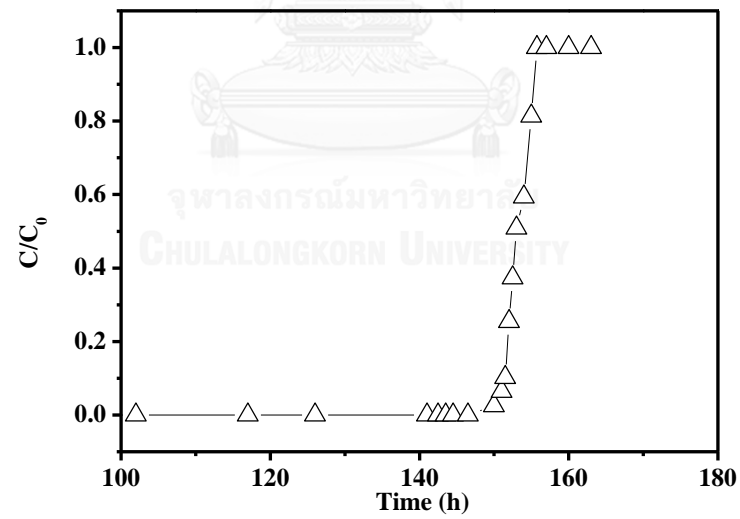
Figure 4.18 Adsorption of HCl gas contaminated in H₂ onto
(a) GAC, (b) 6N-GAC, c) M-NaY-RH-1.87.

Conditions: flow rate 50 mL/min, inlet concentration of HCl = 600 ppm,
column diameter 1 cm. and particle size 2 mm

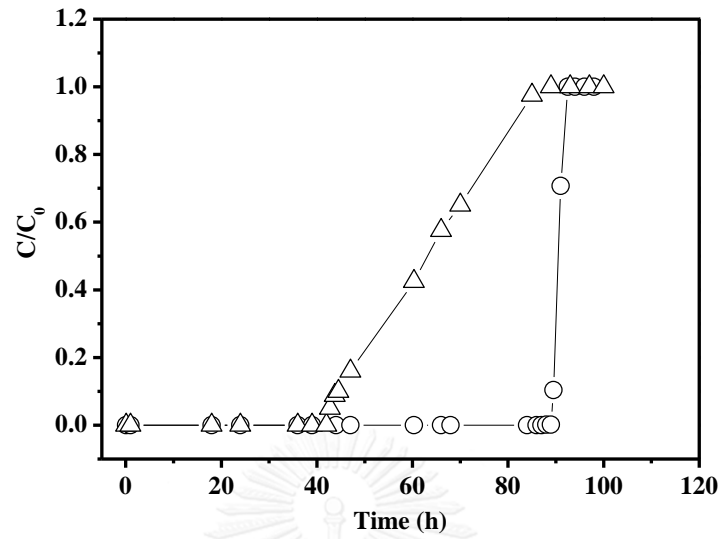




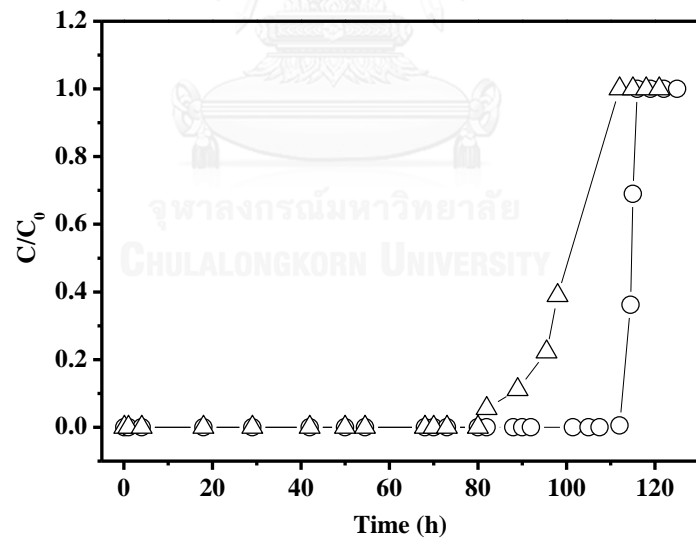
(b)



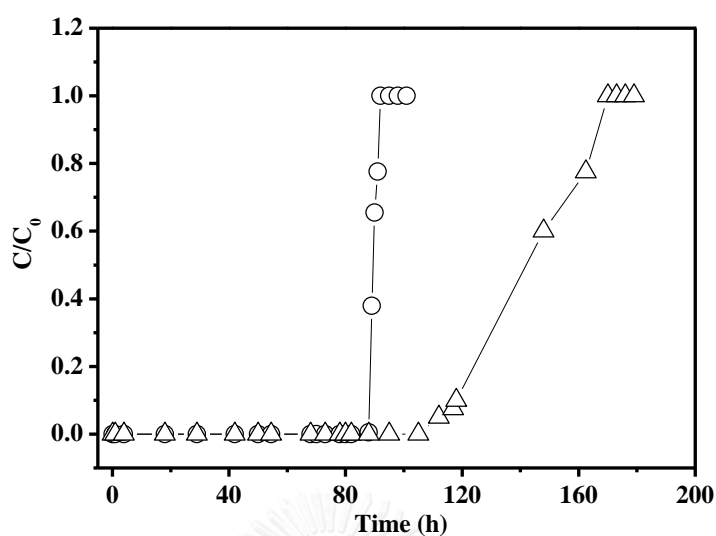
(c)



(d)



(e)



(f)

Figure 4.19 Adsorption of mixed gases of HCl and VCM contaminated in H₂ onto (a) GAC, (b) 6N-GAC, (c) M-NaY-RH-1.87, (d) M-NaY-RH-1.87/6N-GAC/GAC in the ratio of 1/1/1, (e) M-NaY-RH-1.87/6N-GAC/GAC in the ratio of 1/1/2, (f) M-NaY-RH-1.87/6N-GAC/GAC in the ratio of 1/1/8.

Conditions: flow rate 50 mL/min, inlet concentration of HCl = 600 ppm and VCM = 20 ppm, column diameter 1 cm. and particle size 2 mm

Once again, GAC could be able to adsorb both HCl and VCM. However, the adsorption capacity for HCl could be increased by 6N-GAC. When M-NaY-RH-1.87 was added HCl adsorption efficiency is significantly increase, while VCM is slightly less adsorbed due to amount of 6N-GAC and GAC is lesser, as observed in M-NaY-RH-1.87/6N/GAC ratio 1/1/1. The study with higher GAC amount for this set of adsorbents (M-NaY-RH-1.87/6N/GAC ratio 1/1/2), VCM adsorption efficiency was significantly increased, as well as HCl. The higher amount of GAC portion, which was added to 1/1/8, VCM adsorption efficiency was high, nevertheless HCl adsorption efficiency was decreased.

A comparison between $W_{b,exp}$ and $W_{b,cal}$ from alternate layer by layer was evaluated. $W_{b,exp}$ in all cases were compared with $W_{b,cal}$ as follows;

M-NaY-RH-1.87/6N-GAC/GAC ratio of 1/1/1:

$$\begin{aligned} \text{HCl : individual flow :Average} &= \frac{0.1444+0.0681+0.0259}{3} = 0.0794 \quad \text{gHCl/g} \\ \text{mixed flow :Average} &= \frac{0.1444+0.0512+0.0336}{3} = 0.0764 \quad \text{gHCl/g} \\ \text{experimental simultaneous} &= 0.0747 \quad \text{gHCl/g} \end{aligned}$$

$$\begin{aligned} \text{VCM : individual flow :Average} &= \frac{0.0+0.0026+0.0063}{3} = 0.0029 \quad \text{gVCM/g} \\ \text{mixed flow :Average} &= \frac{0.0+0.0031+0.003}{3} = 0.0020 \quad \text{gVCM/g} \\ \text{experimental simultaneous} &= 0.0012 \quad \text{gVCM/g} \end{aligned}$$

M-NaY-RH-1.87/6N-GAC/GAC ratio of 1/1/2:

$$\begin{aligned} \text{HCl : individual flow :Average} &= \frac{0.1444+0.0681+(0.0259 \times 2)}{4} = 0.0661 \quad \text{gHCl/g} \\ \text{mixed flow : Average} &= \frac{0.1444+0.0512+(0.0336 \times 2)}{4} = 0.0657 \quad \text{gHCl/g} \\ \text{experimental simultaneous} &= 0.0705 \quad \text{gHCl/g} \end{aligned}$$

$$\begin{aligned} \text{VCM : individual flow : Average} &= \frac{0.0+0.0026+(0.0063 \times 2)}{4} = 0.0038 \quad \text{gVCM/g} \\ \text{mixed flow : Average} &= \frac{0.0+0.0031+(0.003 \times 2)}{4} = 0.0023 \quad \text{gVCM/g} \\ \text{experimental simultaneous} &= 0.0015 \quad \text{gVCM/g} \end{aligned}$$

M-NaY-RH-1.87/6N-GAC/GAC ratio of 1/1/8:

$$\begin{aligned} \text{HCl : individual flow : Average} &= \frac{0.1444 \times 0.5 + 0.0681 \times 0.5 + (0.0259 \times 4)}{5} = 0.0420 \quad \text{gHCl/g} \\ \text{mixed flow : Average} &= \frac{0.1444 \times 0.5 + 0.0512 \times 0.5 + (0.0336 \times 4)}{5} = 0.0464 \quad \text{gHCl/g} \\ \text{experimental simultaneous} &= 0.0443 \quad \text{gHCl/g} \end{aligned}$$

$$\begin{aligned} \text{VCM : individual flow : Average} &= \frac{(0.0 \times 0.5) + (0.0026 \times 0.5) + (0.0063 \times 4)}{5} = 0.0053 \quad \text{gVCM/g} \\ \text{mixed flow : Average} &= \frac{(0.0 \times 0.5) + (0.0031 \times 0.5) + (0.003 \times 4)}{5} = 0.0027 \quad \text{gVCM/g} \\ \text{experimental simultaneous} &= 0.0018 \quad \text{gVCM/g} \end{aligned}$$

From above calculation, experimented W_b and calculated W_b were plotted as shown in Figure 4.19. There are no significant different between the experimented W_b and calculated W_b .

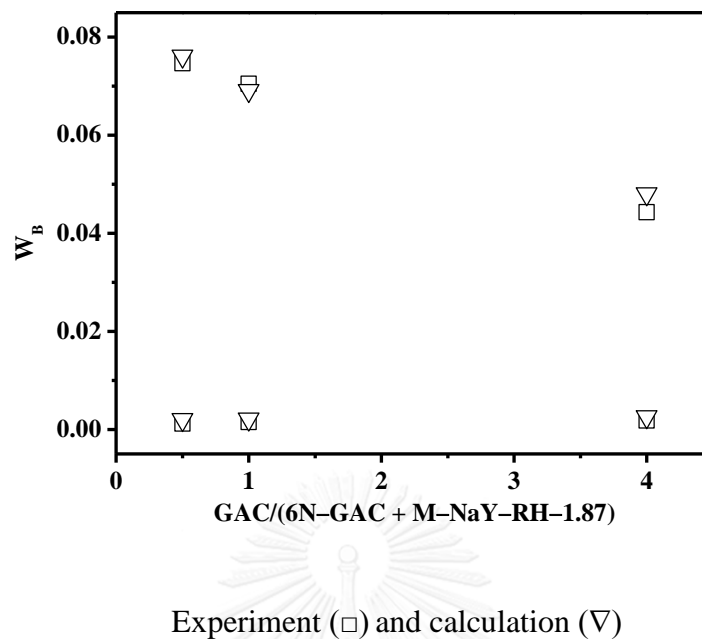


Figure 4.20 W_b between experiment and calculation

4.5 Cost estimation on using synthesized adsorbents for upscale

From the mass balance and adsorption capacity obtained from the previous calculation, it was found that the life spans of M-NaY-RH-1.87/6N-GAC/GAC ratio 1/1/1, 1/1/2, and 1/1/8, were estimated of 6.32, 5.97, and 3.75 months based on industrial condition. A combination of M-NaY-RH-1.87/6N-GAC/GAC, with a ratio of 1/1/1, and 1/1/2 was selected for the cost estimation. Price of zeolite and GAC were relied on the global price in China, and local company in the country, respectively. The estimation of the synthesized adsorbent was shown in Table 4.11 commercial adsorbent (used in industry), Table 4.12, Table 4.13 M-NaY-RH-1.87 / 6N-GAC / GAC ratio 1/1/1, and 1/1/2, respectively. Information of adsorbents show in Table 4.14. The example for calculation is shown as follows.

Table 4.11 Commercial adsorbent (used in industry)

HCl amount			Adsorption capacity (Base on industrial condition)
1 h	450,000	mg	1,296 kg uptake
	450	g	27,410 kg adsorbent
4 months	1,296,000	g	
	1,296	kg	0.0472 kg HCl / kg adsorbent

Table 4.12 M-NaY-RH-1.87 / 6N-GAC / GAC ratio 1 / 1 / 1

HCl amount			Adsorption capacity (Base on industrial condition)
1 h	450,000	mg	2,047.5 kg uptake
	450	g	27,410.0 kg adsorbent
6.3 months	2,047,500	g	
	2,047.5	kg	0.0747 kg HCl / kg adsorbent

Table 4.13 M-NaY-RH-1.87 / 6N-GAC / GAC ratio 1 / 1 / 2

HCl amount			Adsorption capacity (Base on industrial condition)
1 h	450,000	mg	1,932.4 kg uptake
	450	g	27,410.0 kg adsorbent
5.97 months	1,932,400	g	
	1,932.4	kg	0.0705 kg HCl / kg adsorbent

Table 4.14 Cost of adsorbent

Commercial adsorbent	Combination adsorbents
<p>Adsorbent cost: \$US4/kg or 120 Baht/kg</p> <p>Amount of usage: 27,410 kg/column</p>	<p>Selected Adsorbent: Meso-NaY / 6N-GAC / GAC ratio 1/1/1 and 1/1/2</p> <p>Adsorbent cost: Pellet Meso-NaY (from China): 103-230 Baht/kg 6N-GAC: 85 Baht/kg GAC: 80 Baht/kg</p> <p>Average adsorbent cost for ratio 1/1/1: 130 Baht/kg</p> <p>Average adsorbent cost for ratio 1/1/2: 120 Baht/kg</p> <p>Amount of usage: 27,410 kg/column</p>

A comparison of the basic inorganic chemical cost considering 10 year period (between 2002 and 2012) was found no significant difference <http://data.bls.gov/pdq/SurveyOutputServlet>. To determine the NPV of the project, 8% Interest Rate will be used as a basis for economic calculation (MOR/MLR/MRR = 7.956/7.601/8.622 Source: Bank of Thailand, August 31, 2012).

Table 4.15 shows Net Present value (NPV) analysis using commercial adsorbent, a mixed-adsorbent of Meso-NaY / 6N-GAC / GAC ratio of 1/1/1, and 1/1/2. Adsorbents, like commercial adsorbent, Meso-NaY / 6N-GAC / GAC ratio 1/1/1, and 1/1/2 have their life spans of 4, 5, and 6 months, respectively. Considering only one year period, it was indicated that life span of adsorbent was a key factor to reduce the material cost. NPV of the project using those adsorbents are approximately 11, 7.9, and 8.4 million baht, respectively. It is confirmed that Meso-NaY / 6N-GAC / GAC with a ratio of 1/1/1 is the most attractive option in term of both replacement time (6 months)

and cost (7.9 million baht). However, this analysis excluded the cost adsorbent modification processes. Therefore, if an investment for adsorbent modification processes is less than 3 million baht, the proposed new practice 1/1/1 will be practically applied, and the payback period is estimated within the first year of the project.

Table 4.15 Net Present value (NPV) analysis using different adsorbents

	Commercial adsorbent (use in industry)	Meso-NaY / 6N-GAC / GAC ratio 1/1/1	Meso-NaY / 6N-GAC / GAC ratio 1/1/2
Material cost (Baht)	9,867,600	7,126,600	7,894,080
Operation. Cost (Baht)	300,000	200,000	240,000
Disposal cost (Baht)	822,300	548,200	657,840
Present value index	0.926	0.926	0.926
Replacement time (month)	4	6	5
Cumulative cost (Baht)	11,055,684	7,918,656	8,393,259

Conditions:

- Annual purchasing of Adsorbent
- Fix Disposal at 10,000 Baht/ton
- Operation cost at 100,000 Baht/time
- Interest Rate 8%

4.6 Waste Management

After replacing adsorbents (both GAC and Zeolite NaY), the spent adsorbents which are classified as waste code 15 02 xx (absorbents, filter materials, wiping cloths and protective clothing) per Appendix 1 of The Notification of Ministry of Industry Re:

Industrial Waste Disposal B.E. 2548 (MOI, 2005), are needed to be properly managed to prevent environmental and health impact. Spent adsorbents could be classified as;

1. Spent GAC can be used as alternative fuel in the cement kilns. This is due to high heating value referring to high carbon content.
2. Spent M-NaY, which contains SiO_2 and Al_2O_3 as main components, can be used as raw material as alternative material in the cement kilns. Co-processing in cement kilns will burn up the spent adsorbents.



CHAPTER 5

MODELLING OF HCl AND VCM ADSORPTION IN PACKED BED COLUMN

A flow of mixed gas passing through beds composed of stationary granular particles is a similar pattern in the chemical industry and therefore some involved factors are needed to concern. Examples are pressure drop across beds, chemical dispersion, and breakthrough time prediction. In our study, the experiment was carried out in gas-solid condition. Particles in small size were screened out to avoid the pressure drop generating through the column. Moreover, a high voidage of packing material (glass wool in our case) was packed to higher flow distribution, consequently to reduce the resistance caused by the presence of the particles.

5.1 Flow dispersion

Two dispersion models have been described in the phenomena of fluid flow through the column. They are axial dispersion or axially-dispersed plug flow model, and radial dispersion model. The adsorption rate depends on temperature. For our case the study was carried out in ambient condition without any introduced heat. If the heat accumulation took place, it would be very small. And, the temperature would be considered be the same at different radial positions in the bed. Moreover, there was no mass which was removed at the wall. As the discussion, there would be no mechanism to create concentration variations in the radial direction, provided the concentration was uniform upstream. In that case, a radial dispersion model should not be considered (Charles G. Hill, 1977; Fogler, 1999). Only axially-dispersed plug flow model was achieved.

Considering (shown in Figure 5.1) the effluent of the flow in the column in control-volume, the total flow rate can be written as:

$$F_i = \underbrace{uA_c C_i}_{\text{(convection)}} - \underbrace{A_c |D_a \frac{dC_i}{dz}}_{\text{(dispersion)}} \quad (5.1)$$

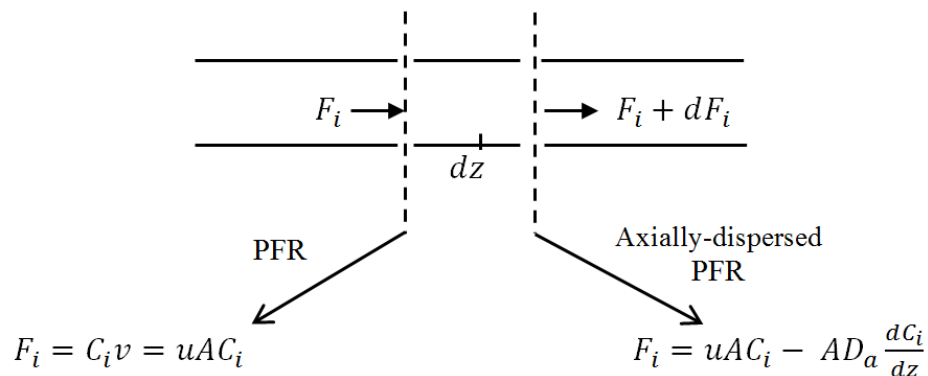


Figure 5.1 Control volume of molar flow rate of species I
in an axially-dispersed PFR.

The total flow are included the dispersion or diffusion term superimposed on the convective flow in the axial direction, where D_a is assigned as *axial-dispersion coefficient*, and that the dispersion term of the molar flow rate is analogized to molecular diffusion, described by Fick's First Law.

The flux of species A is expressed, according to the Fick's First Law, as

$$N_A = -D_{AB} \frac{dC_A}{dz} + uC_A \quad (5.2)$$

This expression is for a binary mixture, where D_{AB} is molecular diffusion coefficient. It is obvious that in laminar flow, the axial dispersion processes will occur by molecular diffusion. On the other word, both equations are identical. Therefore $D_a = D_{AB}$. When the flow velocity is in the turbulent region, the processes are different and D_a will be not identical to D_{AB} . The correlations might be require for the computing of the value.

In general, the transient material balance for flow model is described by the differential mass balance equation given below (Charles G. Hill, 1977; Fogler, 1999):

$$v \frac{\partial(C)}{\partial z} - D_L \frac{\partial^2 C}{\partial z^2} + \frac{\partial C}{\partial t} = 0 \quad (5.3)$$

where v is the interstitial velocity of the carrier fluid, C and q the HCl and VCM concentration in the mobile and stationary phase, respectively, z the distance from the inlet of the column, ε the void fraction of the bed and t is the operating time.

The above expression, once again, was written based on the assumptions as follows;

1. constant temperature
2. constant flow rate with position inside the column,
3. no chemical reactions occur in the column;
4. only mass transfer by convection is important and negligible radial dispersion.
5. For a long fixed bed, initially free of solute and with a constant inlet concentration, C_0 ,

Considering the dimensionless solving technique, equation 5.3 can be rewritten with

$$\frac{\partial c_i}{\partial \theta} + \frac{\partial c_i}{\partial Z} = \frac{1}{Pe_a} \frac{\partial^2 c_i}{\partial Z^2} \quad (5.4)$$

Where $\theta = tu/L$

Pe (axial Peclet number) = $(Lv)/Da$

$Z = z/L$

the solution of equation (5.3) is

$$\frac{c}{c_0} = \frac{1}{2} \left\{ 1 + \operatorname{erf} \left[\frac{Pe}{4\theta} \frac{V - V_{min}}{(VV_{min})^{\frac{1}{2}}} \right] \right\} \quad (5.5)$$

According to the term of axial Peclet number (Pe), the value is a ratio of column length and the diffusion coefficient. Therefore, Pe was used to determine the estimated dispersion coefficient D_a . On the other word, Pe can be used to determine whether the flow is influenced with the dispersion. To consider whether the mass transfer affecting to the flow, axial Peclet number has to be set. Eagleton (1979) disclosed that the Pe number of 0-2 is considered as axial dispersive flow in case of flowing gas.

For examples:

1. If $Pe_{ax} > \alpha$ means that the flow is free of dispersion.
2. If $Pe_{ax} > 0$ means that the flow is in the region of maximum mixing, or under high dispersion effect.

The dimensionless group Pe is a ratio of convective to dispersive flow:

$$Pe_a = \frac{L_v}{D_a} = \frac{\text{convective flow}}{\text{dispersive flow}} \text{ in the axial direction} \quad (5.6)$$

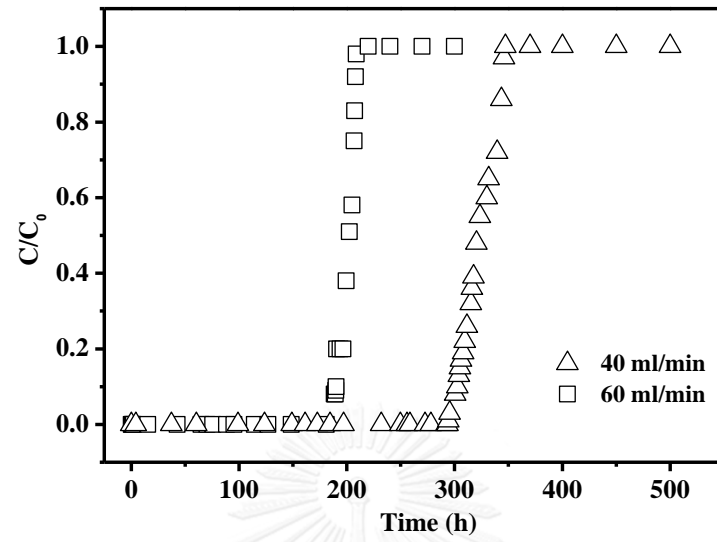
The simulation was done to achieve the correlation coefficient, R^2 , close to 0.95. It could use to indicate that equation 5.5 can be used to describe the breakthrough data with good accuracy. Under this circumstance, the higher flow rate caused the higher Peclet number shown in Table 5.1. It means that lower dispersion of the axial flow. Figure 5.2 and 5.3 show the effect of bed length and the particle size.

a) Effect of the flow rate:

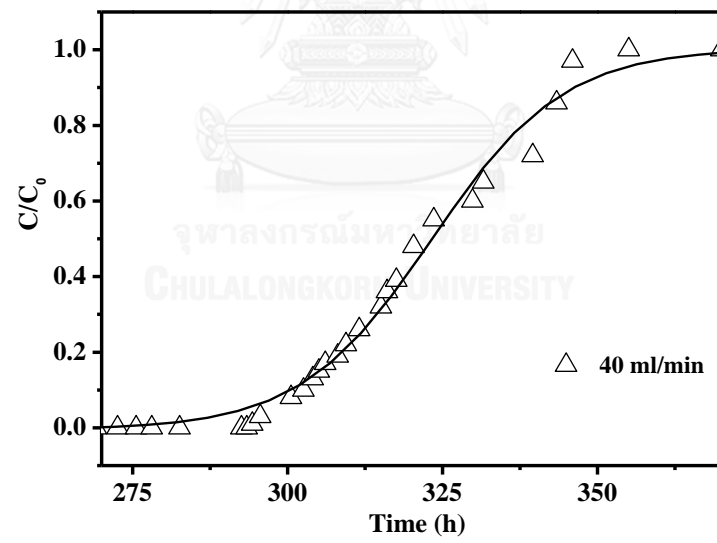
Under the same size of 2 mm diameter of adsorbent and column diameter of 20 mm, concentration profiles in normalized values from the experimental breakthrough data in the effect of different flow rates (40 and 60 mL/min) are plotted in Figure 5.2, shown in symbol patterns. The data was fitted with the analytical solution of equation 5.5, shown in line patterns. Parameter of Pe is estimated and presented in Table 5.1.

Table 5.1 Peclet number evaluation for the dispersion behavior for each run

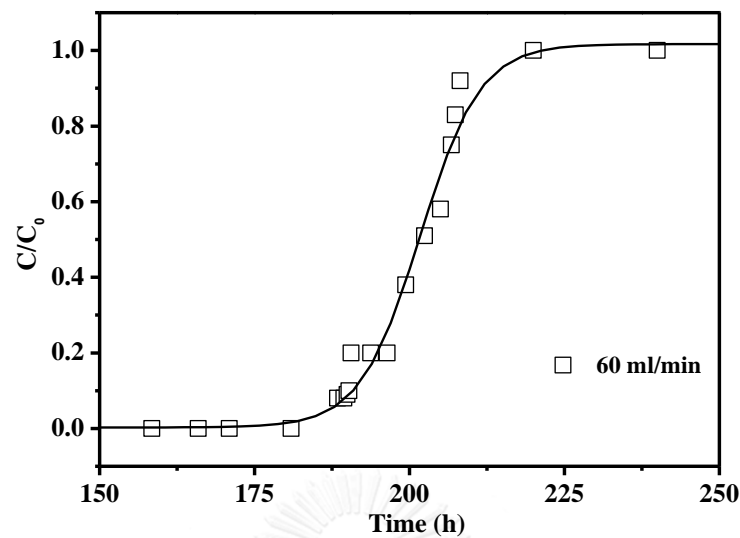
Conditions				Peclet number
Flow rate, ml/min	L, cm	d _p , mm	D _c , cm	
40	6	2	20	0.57
		0.5		5.71
	10	2	3.46	
		14	2.33	
60	6	2	1.62	
		0.5	4.15	



(a)



(b)



c)

Figure 5.2 Effect of flow rate at $L = 6$ cm on breakthrough curves for HCl removal by 6N-GAC. Conditions: Particle diameter = 2.0 mm and column diameter = 20 mm. (To be continued)

b) Effect of the bed length:

When the bed length was longer, it was obvious that the breakthrough time was drawn to longer time. As seen in Figure 5.3 that the bed length of 6 cm provided the breakthrough time around 280 hr., while the bed length of 14 cm provided the breakthrough time around 370 hr. Pe value was still high when the bed length was longer. This might be due to at high operating times it is plausible to say that most of the GAC particles are saturated with the adsorbate and the access to the smallest pores closer to the center of the particle becomes slower and thus pore diffusion becomes the controlling mechanism.

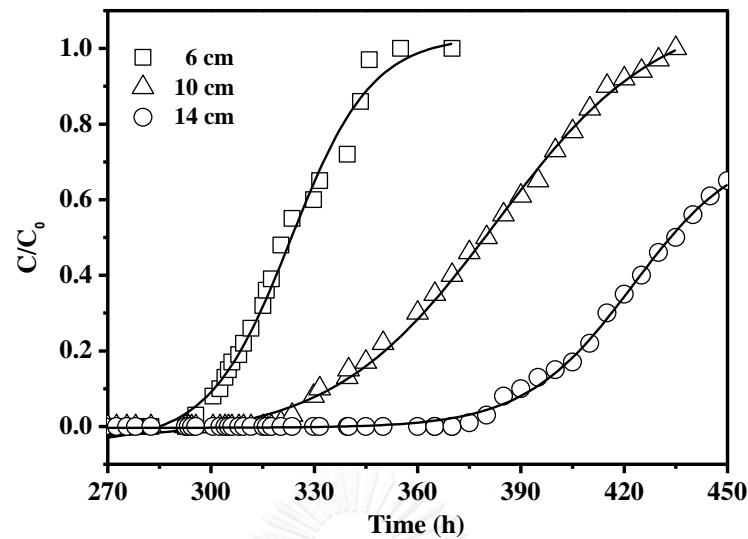


Figure 5.3 Effect of flow bed length at a flow rate of 40 ml/min on breakthrough curves for HCl removal by 6N-GAC.

Conditions: Particle diameter = 2.0 mm and column diameter = 20 mm.

c) Effect of particle diameter:

On the other hand, the study on different particle sizes shows that a smaller particle size make the normalized concentration profiles declining, as seen in Figure 5.4 (a) for 40 ml/min and (b) for 60 ml/min). It was found that Pe value increased from 0.57 for particle diameter was 2 mm to 3.71 when the particle diameter was 0.5 mm. This was implied that particle diameter decreases the flow behavior in packed bed column could be approach to plug flow phenomena due to lower dispersion. However, it is an essential to understand that small particles provide better usage of the bed, but it may not be in practice because of the high accumulation of pressure drop in the packed bed.

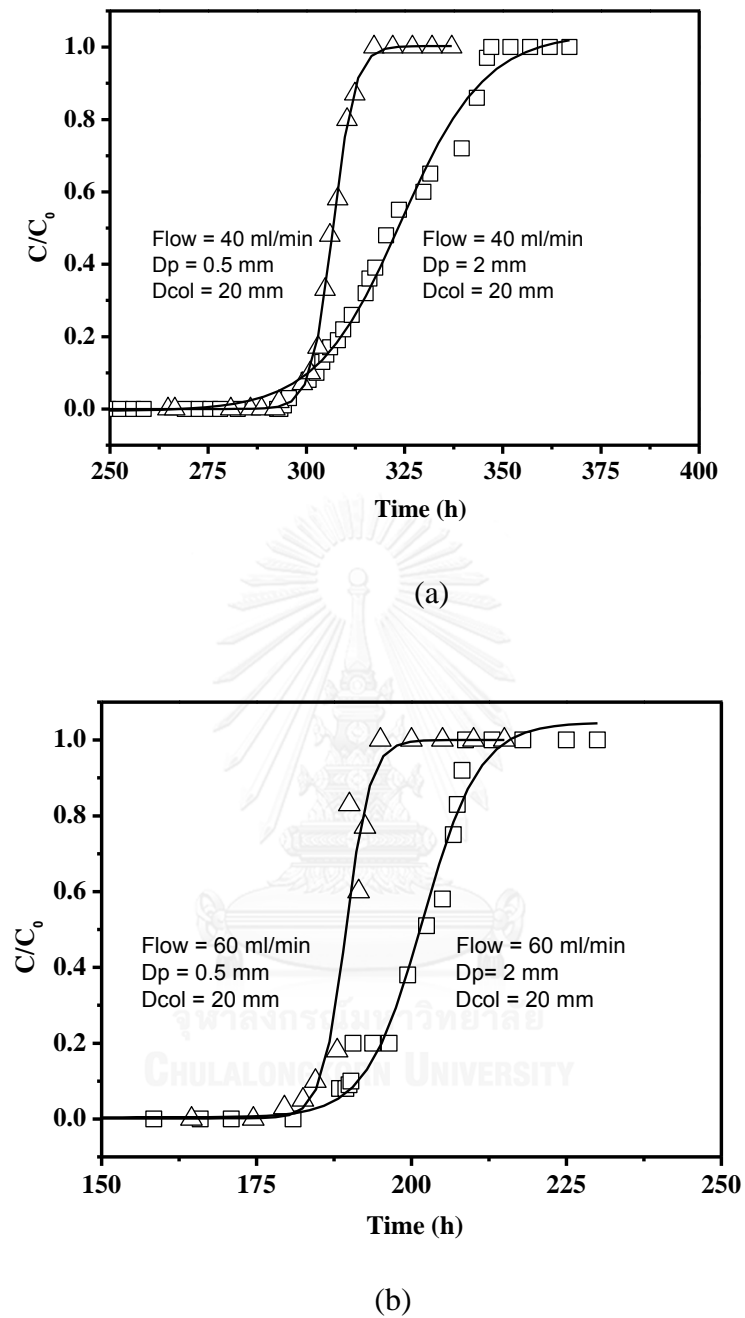


Figure 5.4 Effect of particle diameter on breakthrough curves for HCl removal by 6N-GAC. Conditions: Particle diameter = 2.0 mm.

5.2 Statistical Analysis on the breakthrough time

From those three studied parameters (flow rate, particle diameter, and column diameter) with the respect to breakthrough time, it should be understand whether those all factors whether were significant for the further study. To systematically evaluate the effects of studied parameters studied, a statistical analysis was applied. The statistical analysis which was used in this work was ANOVA, based Design expert version 8.

Experimental runs were referred to Box-Benkhen experimental design. Only HCl adsorption was carried out because inorganic chlorinated hydrocarbons (We used HCl as a probe chemical) caused serious problem compared to VCM contaminated. The results is now tabulated in Table 5.2.

Table 5.2 Breakthrough times for HCl adsorption over 6N-GAC in all studied parameters

Exp. No.	Flow rate (ml/min)	Column Diameter (mm)	Particle size (mm)	Breakthrough times for HCl adsorption (h)
1	50	10	2.00	73.49
2	60	20	2.00	185.61
3	40	20	2.00	297.58
4	50	10	0.50	76.33
5	60	20	0.50	182.50
6	40	20	0.50	296.60
7	50	20	1.25	190.67
8	60	10	1.25	72.96
9	40	10	1.25	79.43
10	50	30	2.00	254.13
11	50	30	0.50	251.00
12	50	20	1.25	185.41
13	50	20	1.25	187.30
14	60	30	1.25	207.40
15	40	30	1.25	331.70

There are four types of fitting models to be considered as follows;

1. Linear: The response is the function of first order with respect to each parameter.
2. 2FI: The response is the function of two-factor interaction with respect to each parameter.
3. Quadratic: The response included 2FI model and term with the function of second order with respect to each parameter.
4. Cubic: The response included quadratic model and term with the function of two-factor interaction and third order with respect to each parameter.

Regression model fitting was performed to correlate the breakthrough time with the specified operating conditions for the HCl adsorption over 6N-NaOH-GAC. All four model fittings were used in the analysis. Among several models tested, the linear and quadratic models were found superior for predicting the breakthrough time. Considering the p-value of linear fitting, the value of 4.55×10^{-5} (shown in Table 5.3) which is lower than 0.05. As well as the sequential p-value be added to 2FI model could improve the model to the acceptable one. And, the model of quadratic fit gave p-value (0.0004; shown in Table 5.3) < 0.05 . However, when the quadratic model was added more terms of cubic correlations, the revised model had been not improved much. The cubic correlation therefore, should not be mentioned.

The evaluations for the lack of fit of both models are 0.000126 and 0.003933 of p-value (shown in Table 5.3) for linear and quadratic model, respectively. If the values is smaller than 0.05, meaning that the model shows insignificant lack-of-fit. Therefore, the model can be used for the prediction. In our case, both two values are smaller than 0.05, so the fits are alright to predict.

The statistical analysis showed that the models are acceptable for prediction with the adjusted determination coefficient (R^2 adj.) of 77 and 97% (shown in Table 5.3), with respect to linear and quadratic model, respectively.

Table 5.3 Comparison on several model fittings

Source	Sequential p-value	Lack of Fit p-value	Adjusted R-Squared	Predicted R-Squared	
Linear	4.55×10^{-5}	0.000126	0.774241	0.617522	
2FI	0.548931	9.18E-05	0.760181	0.236091	
Quadratic	0.000402	0.003933	0.970899	0.804776	Suggested
Cubic	0.003933		0.997649		Insignificant improved

5.2.1 Quadratic regression model

To systematically evaluate the effects of parameters studied, a statistical analysis was applied. Figure 5.5 shows the plot of residual of breakthrough time collected from all experiments to verify the assumption of ANOVA. The data lies mostly on a reference diagonal line. It means that the result obtained from the experiment was in normal distribution.

To clarify the distribution of residuals, the analysis of ANOVA residual on the predicted values should be analyzed in Figure 5.6. The data was somewhat scattering in the same range from zero. It was no specific distribution pattern of residuals. On the other word, the variance of residuals was constant. For this reason, it can be inferred ANOVA could be used for our full factorial experiments.

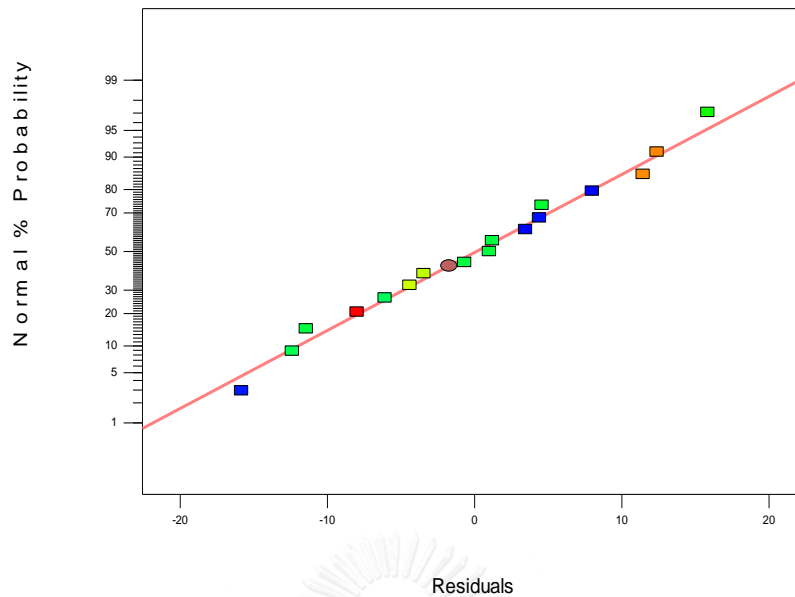


Figure 5.5 Normal probability plot of residuals
(Response is breakthrough point of HCl adsorption).

In this research, the significance level of 95% was used throughout the analysis of variance. By testing the following assumptions, the main and interaction effects on the breakthrough time obtained from the adsorption of HCl in a column were specified.

- (i) H_0 : all parameters did not affect the breakthrough time.
- (ii) H_1 : at least one of parameters affected the breakthrough time.

The effect of parameters on breakthrough time could be specified by p-value. As understood, an effect could be counted for significant effect only if the p-value is less than 0.05. In the other word, it could not be considered significant if the value is greater than 0.05.

The analysis of variance for breakthrough time under quadratic model is summarized in Table 5.4. p-values of particle size (B), two factor-interaction of flow rate with particle size (A-B) and column size with particle size (B-C) are 0.91, 0.94, and 0.83 found higher than 0.05. Therefore, these three effects were considered insignificant. For the main effects, the p-values of A, and B were of 3.74×10^{-5} and 2.69×10^{-7} , respectively. Consequently, the null hypothesis (H_0) was rejected

supporting that some main effects were significant. The analysis of variance for breakthrough time is summarized in Table 5.4.

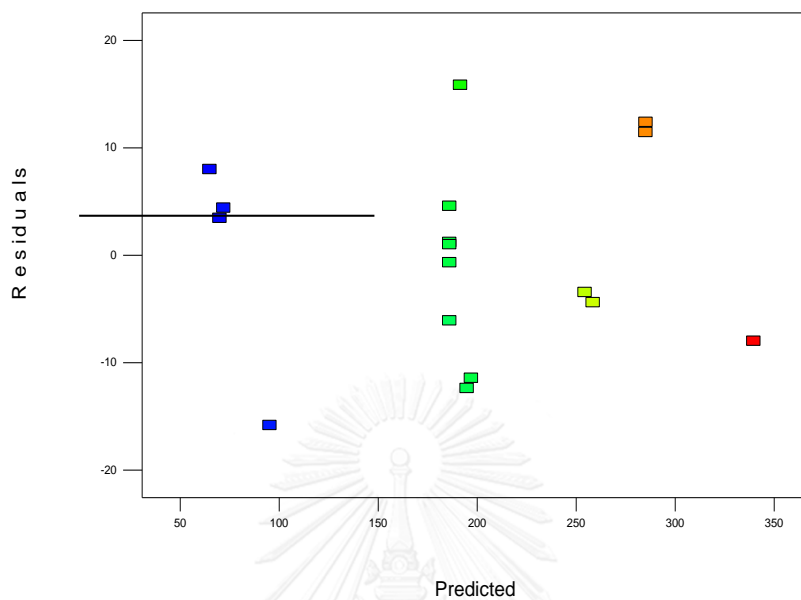


Figure 5.6 Residuals versus predicted plot
(Response is breakthrough point of HCl adsorption)

Table 5.4 Variance analysis (Quadratic regression).

Source	Degree of freedom	Sum of squares	Mean square	F-value	Prob>F (p-value)
Flow rate, (A)	1	15916.85	15916.85	84.32	3.74E-05
Column diameter, (B)	1	68824.21	68824.21	364.62	2.69E-07
Particles diameter, (C)	1	2.40	2.40	0.01	0.91
A*B	1	3470.98	3470.98	18.39	0.004
A*C	1	1.13	1.13	0.01	0.94
B*C	1	8.91	8.91	0.05	0.83
A ²	1	4259.66	4259.66	22.57	0.002
B ²	1	8537.02	8537.02	45.23	0.00027
C ²	1	2164.24	2164.24	11.46	0.012
Residual	7	1321.30	188.76		
Lack of fit	3	1260.31	420.10	27.55	0.004
Pure error	4	60.99	15.25		
Correlation total	16	103779.70			

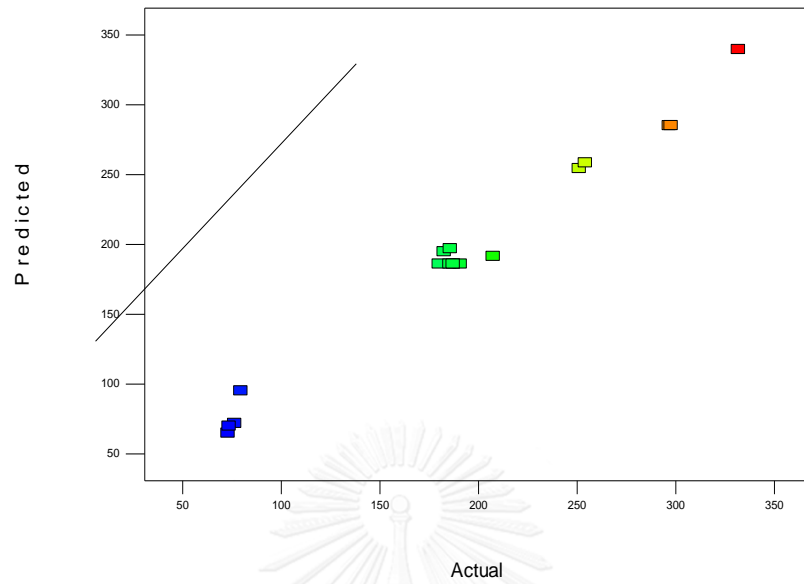
Final equation in terms of actual factors (Quadratic):

$$\text{Breakthrough time} = 615.57 - 30.46A + 41.76B - 107.56C - 0.29AB + 0.07AC + 0.20BC + 0.32A^2 - 0.45B^2 + 40.31C^2 \quad (5-7)$$

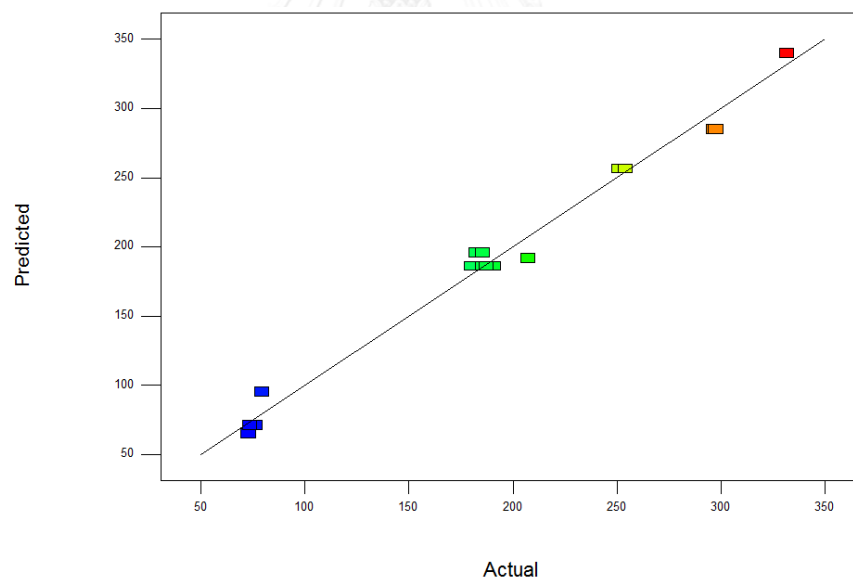
After dropping out the insignificant parameters equation (5-7) can be written as;

$$\text{Breakthrough time} = 186.09 - 44.60A + 92.75B - 29.46AB + 31.81A^2 - 45.03B^2 + 22.67C^2 \text{ based on code} \quad (5-8)$$

The parity plot of Equation 5-7 and 5.8 is shown in Figure 5.7.



(a)



(b)

Figure 5.7 Parity plot of quadratic model (a) all factors and b) exclude insignificant factors.

5.2.2 Linear regression model

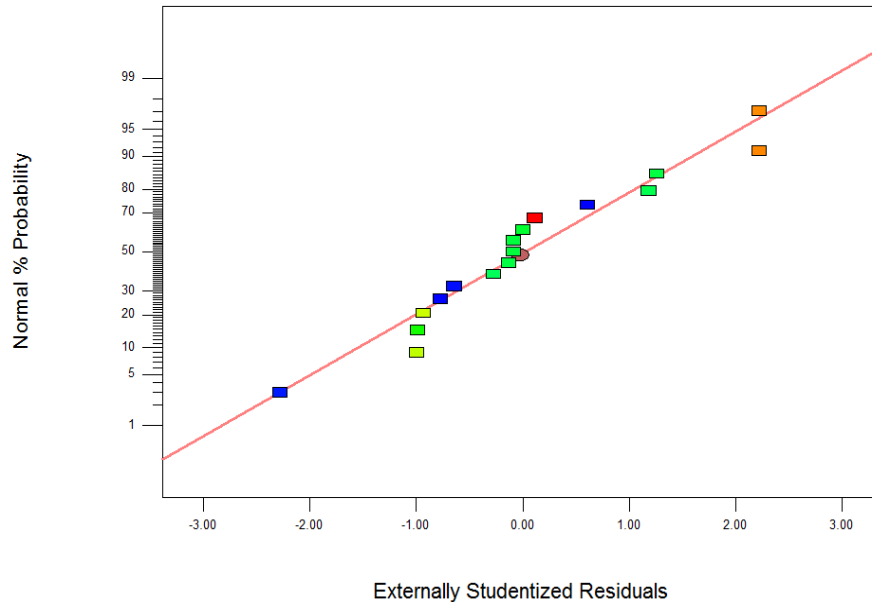


Figure 5.8 Normal probability plot of residuals (response is breakthrough point of HCl adsorption).

Like the study in quadratic model, the significance level of 95% was used throughout the analysis of variance. By testing the following assumptions, the main and interaction effects on the breakthrough time obtained from the adsorption of HCl in a column were specified.

- (iii) H_0 : all parameters did not affect the breakthrough time.
- (iv) H_1 : at least one of parameters affected the breakthrough time.

The effect of parameters on breakthrough time could be specified by p-value. As understood, an effect could be counted for significant effect only if the p-value is less than 0.05. In the other word, it could not be considered significant if the value is greater than 0.05.

The analysis of variance for breakthrough time under linear model is summarized in Table 5.8. p-values of Flow rate (A), Column diameter (B), Particles diameter (C), are not found higher than 0.05. Therefore, all of them are the main effects,

the p-values of A, B, and C were of 4.55×10^{-5} , 0.0058, and 1.16×10^{-5} , respectively. Consequently, the null hypothesis (H_0) was rejected supporting that some main effects were significant. The analysis of variance for breakthrough time for linear model is summarized in Table 5.8.

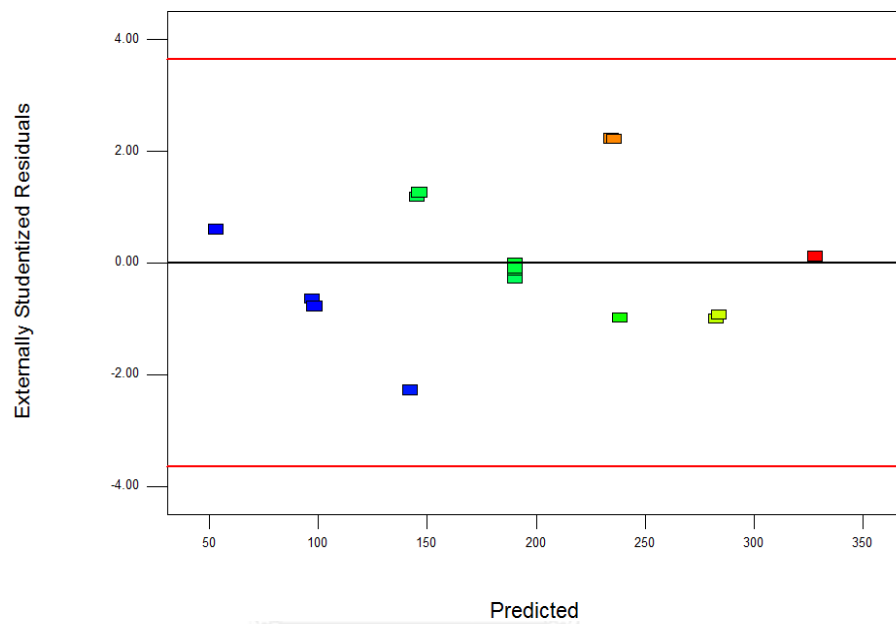


Figure 5.9 Residuals versus predicted plot
(response is breakthrough point of HCl adsorption).

Table 5.5 Variance analysis (Linear regression).

Source	Degree of freedom	Sum of squares	Mean square	F-value	Prob>F (p-value)
Flow rate, (A)	1	15916.85	15916.85	19.29	4.55E-05
Column diameter, (B)	1	68824.21	68824.21	10.87	0.0058
Particles diameter, (C)	1	2.40	2.40	47.00	1.16E-05
Residual	13	19036.22	1464.32	0.002	0.97
Lack of fit	9	18975.23	2108.36		
Pure error	4	60.99	15.25	138.27	0.00023
Correlation total	16	103779.70			

Final Equation in Terms of Actual Factors (Linear regression):

$$\text{Breakthrough time} = 227.15 - 4.46A + 9.27B - 0.73C \quad (5-3)$$

The parity plot of Equation 5-10 is shown in Figure 5.10.

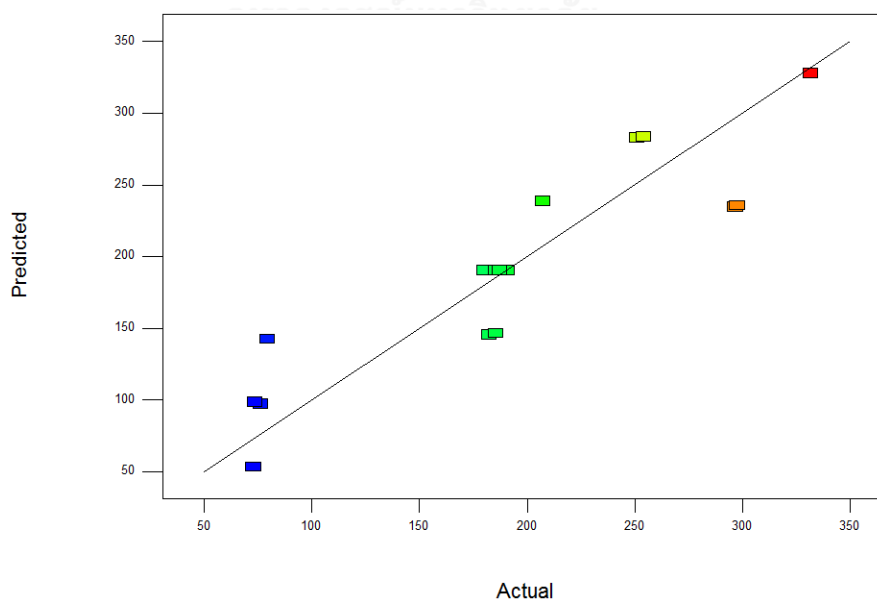


Figure 5.10 Parity plot of linear model.

5.3 Model verification

Two models in quadratic and linear forms have been developed in section 5.2.1 and 5.2.2. It is essential to prove the model for other extra runs. Example is shown in Figure 5.11. It was an experiment under flow rate 50 mL/min, inlet concentration of HCl = 600 ppm, column diameter 1 cm. and particle size 2 mm. It is found that the quadratic model predicts the breakthrough time closer that the linear model. The prediction by a quadratic model is about 3.54% difference from an actual value, while a linear model gives higher difference to 16.0%. Therefore, it's recommended to use quadratic model to predict the breakthrough time.

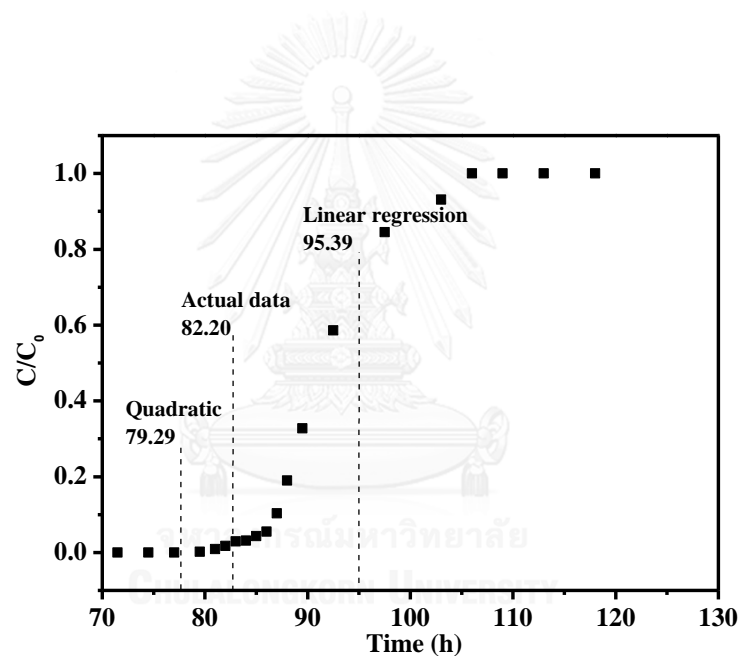


Figure 5.11 A comparison of breakthrough time to the prediction from two models.

Conditions: flow rate 50 mL/min, inlet concentration of HCl = 600 ppm,
column diameter 1 cm. and particle size 2 mm.

CHAPTER 6

CONCLUSIONS AND RECOMMENDATIONS

6.1 Conclusions

1. MCM-41 and silica were not applicable for HCl and VCM captures. Surface area was not a key factor for this case adsorption.
2. Granular activated carbons (GAC) was able to adsorb organic chlorinated hydrocarbons (VCM as a probe), but little adsorb inorganic chlorinated hydrocarbons (HCl as a probe). A modification of GAC with 6N-NaOH showed adsorption capacities for HCl and VCM of 0.0681 g_{HCl}/g and 0.0026 g_{VCM}/g, respectively. The performance was comparable to a benchmark adsorbent.
3. Mesoporous zeolite NaY synthesized by rice husk with the ratio of Si/Al 1.87 (M-NaY-RH-1.87) adsorbed HCl about twice of 6N-NaOH-GAC ($W_b = 0.1437$ g_{HCl}/g), while the adsorption of VCM was almost nil.
4. A combination packing of M-NaY-C-1.87, 6N-GAC and GAC, therefore was tested in a mixed gases contaminated with 600 ppm of HCl and 20 ppm of VCM. The optimal ratio of three adsorbents was 1/1/1, which provide longer adsorbent life span (6.3 months) compared with a commercial one (4 months).
5. Sodium chloride was observed in the spent adsorbent.
6. Spent GAC and Zeolite NaY can be disposed as alternative fuel and alternative material in the cement kilns, respectively. However, due to Chloride (Cl) content in spent adsorbents, they may need to be blended with other fuels or materials prior to process in cement kilns.
7. To reduce the mass diffusion effect, smaller size of particle (0.5 mm) and higher flow rate (60 ml/min) should be applied.
8. Since a guarding of HCl is more essential in the process, a model of breakthrough time has been developed. Three parameters including flow rate, column diameter, and particle diameter, were used. The model, with a correlation coefficient (R^2) = 0.977, can be written as;

$$\text{Breakthrough time} = 615.57 - 30.46A + 41.76B - 107.56C - 0.29AB + 0.07AC \\ + 0.20BC + 0.32A^2 - 0.45B^2 + 40.31C^2$$

where A: flow rate (ml/min)
 B: column diameter (mm)
 C: particle diameter (mm)

9. The quadratic model of adsorption gave reasonably breakthrough time to the actual case, compared with the linear model.

6.2 Recommendations

1. Parameters used in the model involved only flow rate, column diameter, and particle diameter. An amount of adsorbent was not involved in this study. To make the correlation more perfect, particle size diameter should be replaced by the amount of adsorbent.

2. Chloride value in Table 4.4 seems to be high. The values were received from XRF characterization. It was an approximate method. It was just confirmed that chloride was available. The number should be clarified by a simple chemical technique (“Titrimetric analysis base The Fajans Method”).

REFERENCES

- Abello, S., A. Bonilla and J. Pe´rez-Rami´rez (2009). "Mesoporous ZSM-5 zeolite catalysts prepared by desilication with organic hydroxides and comparison with NaOH leaching." Applied Catalysis A: General **364**: 191-198.
- Beck, J. S., J. C. Vartuli, W. J. Roth, M. E. Leonowicz, C. T. Kresge, K. D. Schmitt, C. C. T. W., H. D. Olson, E. W. Sheppard, S. B. McCullen, J. B. Higgins and J. L. Schlenker (1992). "A new family of mesoporous molecular sieves prepared with liquid crystal templates." Journal of the American Chemical Society **114**: 10834-10843.
- Berger, C., R. Gläser, R. A. Rakoczy and J. Weitkamp (2005). "The synthesis of large crystals of zeolite Y re-visited." Microporous and Mesoporous Materials **83**(1-3): 333-344.
- Bouchelta, C., M. S. Medjram, O. Bertrand and J.-P. Bellat (2008). "Preparation and characterization of activated carbon from date stones by physical activation with steam." Journal of Analytical and Applied Pyrolysis **82**(1): 70-77.
- Charles G. Hill, J. (1977). An Introduction to Chemical Engineering Kinetics & Reactor Design. United States of America, John Wiley & Sons, Inc.
- Chatterjee, A., T. Ebina, T. Iwasaki and F. Mizukami (2003). "Chlorofluorocarbons adsorption structures and energetic over faujasite type zeolites a first principle study." Journal of Molecular Structure (Theochem) **630**: 233-242.
- Chumee, J., N. Grisdanurak, S. Neramittagapong and J. Wittayakun (2009). "Characterization of AlMCM-41 synthesized with rice husk silica and utilization as supports for platinum-iron catalysts." Brazilian Journal of Chemical Engineering **26**: 367-373.
- Crittenden, B. and W. J. Thomas (1998). Adsorption technology and design, Biddles Ltd.
- El-Sheikh, A. H., A. P. Newman, H. Al-Daffae, S. Phull, N. Cresswell and S. York (2004). "Deposition of anatase on the surface of activated carbon." Surface and Coatings Technology **187**(2-3): 284-292.
- EPA. (2000). "Hydrochloric Acid (Hydrogen Chloride)." from <http://www.epa.gov/ttnatw01/hlthef/hydrochl.html#ref4>.

- EPA. (2000, 08/07/2000). "Vinyl chloride." 2015, from <http://www.epa.gov/iris/subst/1001.htm>.
- Fogler, H. S. (1999). Elements of Chemical Reaction Engineering. United States of America, Prentice Hall PTR.
- Gani, A. and I. Naruse (2007). "Effect of cellulose and lignin content on pyrolysis and combustion characteristics for several types of biomass." Renewable Energy **32**(4): 649-661.
- García, R., D. P. Serrano and D. Oteroj (2005). "Catalytic cracking of HDPE over hybrid zeolitic-mesoporous." Journal of analytical and Applied Pyrolysis **74**: 379-386.
- Grisdanurak, N. and J. Wittayakun (2004). Catalyst: fundamental and application. Thummasart University.
- Hue, L. e. a. (1976). Process for removing chlorine-containing compounds from hydrocarbon streams. U. S. Patent.
- Kameda, T., U. N., P. K., G. G. and Y. T. (2008). "Removal of hydrogen chloride from gaseous streams using magnesium-aluminum oxide." Chemosphere **73**: 844-847.
- Keller, J. and R. Sraudt (2005). Gas adsorption equilibria: experimental methods and adsorptive isotherms, Springer Science & business Medai Inc.
- Kim, B. J., P. H. and P. S. J. (2008). "Toxic gas removal behaviors of porous carbons in the presence of Ag/Ni Bimetallic clusters." Bulletin of the Korean chemical society **29**: 782-784.
- Lee, M.-T., Z.-Q. Wang and J.-R. Chang (2003). "Activated-Carbon-Supported NaOH for Removal of HCl from Reformer Process Streams." Industrial & Engineering Chemistry Research **42**(24): 6166-6170.
- Lee, M., Z. Wang and J. Chang (2003). "Activated-carbon-supported NaOH for removal of HCl from reformer process streams." Separations: Industrial and engineering chemistry research **42**: 6166-6170.
- Liu, S., X. Cao, L. Li, C. Li, Y. Ji and F. Xiao (2008). "Preformed zeolite precursor route for synthesis of mesoporous X zeolite." Journal of Colloids and Surfaces A: Physicochem. Eng **318**: 269-274.

- McWilliams, e. a. (1988). Guard bed catalyst for organic chloride removal from hydrocarbon feed. U. S. Patent.
- MOI (2005). The Notification of Ministry of Industry Re: Industrial Waste Disposal B.E. 2548. M. o. Industry.
- Namasivayam, C. and D. Kavitha (2006). "IR, XRD and SEM studies on the mechanism of adsorption of dyes and phenols by coir pith carbon from aqueous phase." Microchemical Journal **82**(1): 43-48.
- Park, S. J. and S. Y. Jin (2005). "Effect of nickel Electroplating on HCl removal efficiency of Activated carbon fiber." Journal of Industrial Engineering Chemical **11**: 395-399.
- Petersson, L. and K. Oksman (2006). "Biopolymer based nanocomposites: Comparing layered silicates and microcrystalline cellulose as nanoreinforcement." Composites Science and Technology **66**(13): 2187-2196.
- Rahman, M. J., P. Bozadjiev and Y. Pelovski (1994). "Studies on the effects of some additives on the physicomechanical properties of urea-ammonium sulphate (UAS) pellets." Fertilizer Research **38**: 89-93.
- Rahman, M. M., N. Hasnida and W. B. Wan Nik (2009). "Preparation of Zeolite Y Using Local Raw Material Rice Husk as a Silica Source." Journal of scientific Research **2**: 285-291.
- Rayalu, S., N. K. Labhasetwar and P. Khanna (2000). Process for the synthesis of flyash based zeolite-Y, Google Patents.
- Realpe, R. C. and J. P. Ramírez (2010). "ZSM-5 zeolites prepared by a two-step route comprising sodium aluminate and acid treatments." Journal of Microporous and Mesoporous Materials **128**: 91-100.
- Rodríguez-reinoso, F. (1998). "The role of carbon materials in heterogeneous catalysis." Carbon **36**(3): 159-175.
- Ruthven, D. M. (1984). Principles of adsorption and adsorption process, John Wiley & Sons Inc.
- Sang, S., Z. Liu, P. Tian, Z. Liu, L. Qu and Y. Zhang (2006). "Synthesis of small crystals zeolite NaY." Materials Letters **60**(9-10): 1131-1133.

- Scamehorn, J. F. (1979). "Removal of Vinyl Chloride from Gaseous Streams by Adsorption on Activated Carbon." Industrial & Engineering Chemistry Process Design and Development **18**(2): 210-217.
- SEPA. (2015). "Hydrogen Chloride." 2015, from <http://apps.sepa.org.uk/spria/Pages/SubstanceInformation.aspx?pid=5>.
- Shafeeyan, M. S., W. M. A. W. Daud, A. Houshmand and A. Shamiri (2010). "A review on surface modification of activated carbon for carbon dioxide adsorption." Journal of Analytical and Applied Pyrolysis **89**(2): 143-151.
- The University of Sheffield and WebElements Ltd, U. (2015). "electronegativity."
- Twigg, M. V. and M. S. Spencer (2001). "Deactivation of supported copper metal catalysts for hydrogenation reactions." Applied Catalysis A: General **212**: 161-174.
- Walton, K. S., M. B. Abney and M. D. LeVan (2006). "CO₂ adsorption in Y and X zeolites modified by alkali metal cation exchange." Journal of Microporous and Mesoporous Materials **91**: 78-84.
- Wittayakun, J., P. Khemthong and S. Prayoonpokarach (2008). "Synthesis and characterization of zeolite NaY from rice husk silica." Korean Journal of Chemical Engineering **25**(4): 861-864.
- Yang, R. T., Ed. (2003). Adsorbents: fundamentals and applications. New Jersey, John Wiley and Sons, INC.
- Yangyaim, T. (2010). Mesoporous zeolite NaY for hydrogen chloride adsorption, Chulalongkorn University.
- Yoshida, H., Y. L., H. Nakayama and M. Hirohashi (2009). "Fabrication of TiO₂ film by mechanical coating technique and its photocatalytic activity." Journal of Alloys and Compounds **475**: 383-386.

APPENDIX



จุฬาลงกรณ์มหาวิทยาลัย
CHULALONGKORN UNIVERSITY

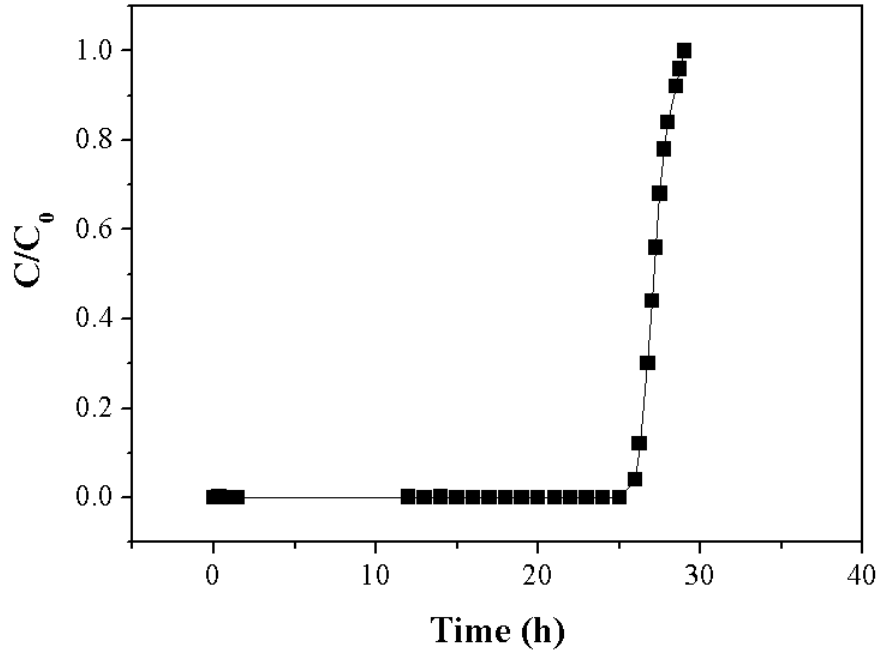


APPENDIX A

Example of HCl Adsorption Calculation

จุฬาลงกรณ์มหาวิทยาลัย
CHULALONGKORN UNIVERSITY

Calculation of HCl adsorption by GAC



Breakthrough curve of GAC for HCl adsorption

At saturated stage of adsorbent

$$W_{Sat} = g \text{ adsorbate} / g \text{ adsorbent}$$

$$W_{Sat} = \frac{F_A \times \text{Area above the graph}}{\text{Mass of adsorbent per unit cross sectional area of bed}} \dots\dots\dots(1)$$

$$F_A = \text{Solute feed rate} \left(\frac{g}{cm^2 h} \right)$$

Where

$$F_A = u_0 c_0 M$$

$$u_0 = \text{Velocity of solute} \left(\frac{cm}{s} \right)$$

$$c_0 = \text{concentration} \left(\frac{mol}{cm^3} \right)$$

$$M = \text{Molecular weight} \left(\frac{g}{mol} \right)$$

F_A is calculated as followed,

$$F_A = \left(\frac{50 \frac{\text{cm}^3}{\text{min}}}{\frac{\pi(1)^2}{4} (\text{cm}^2)} \right) \times \left(\frac{500 \times 10^{-6}}{22,400} \times \frac{273}{303.15} \times \frac{760}{760} \right) \frac{\text{mol}}{\text{cm}^3} \times \left(36.5 \frac{\text{gHCl}}{\text{mol}} \right)$$

$$F_A = 4.671 \times 10^{-5} \frac{\text{gHCl}}{\text{cm}^2 \text{min}} \text{ or } 2.803 \times 10^{-3} \frac{\text{gHCl}}{\text{cm}^2 \text{h}}$$

Area above graph

$$\text{Area above the graph} = \int_0^{29} \left(1 - \frac{C}{C_0} \right) dt$$

$$\text{Area above the graph} = 27.45 \text{ h}$$

Mass of adsorbent

Mass of adsorbent per unit cross sectional area of bed

$$= \text{Bed height (cm)} \times \text{Density} \left(\frac{\text{g}}{\text{cm}^3} \right)$$

$$\text{Mass of adsorbent per unit cross sectional area of bed} = (6 \times 0.4681) \frac{\text{g}_{\text{GAC}}}{\text{cm}^2}$$

$$\text{Mass of adsorbent per unit cross sectional area of bed} = 2.8086 \frac{\text{g}_{\text{GAC}}}{\text{cm}^2}$$

From (1) W_{sat} is calculated as followed,

$$W_{\text{Sat}} = \frac{\left(2.803 \times 10^{-3} \frac{\text{g}_{\text{HCl}}}{\text{cm}^2} \right) \times (27.45 \text{ h})}{2.8086 \frac{\text{g}_{\text{GAC}}}{\text{cm}^2}}$$

$$W_{\text{Sat}} = 0.0274 \frac{\text{g}_{\text{HCl}}}{\text{g}_{\text{GAC}}}$$

At break point condition; $C/C_0 = 0.05$

$$\text{Area above the graph} = \int_0^{26} \left(1 - \frac{C}{C_0} \right) dt$$

$$\text{Area above the graph} = 25.99 \text{ h}$$

$$W_b = \frac{\left(2.803 \times 10^{-3} \frac{g_{HCl}}{cm^2 h}\right) \times (25.99h)}{2.8086 \frac{g_{GAC}}{cm^2}}$$

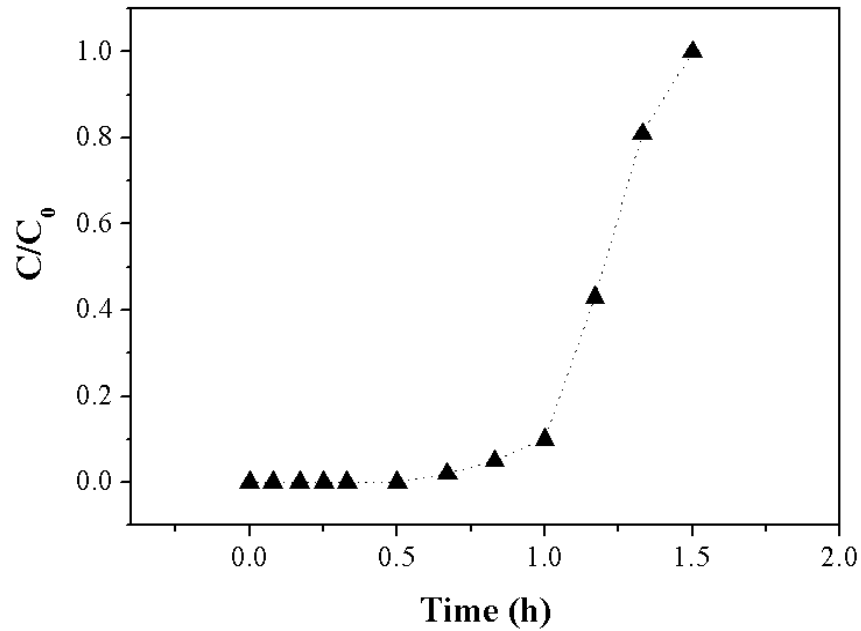
$$W_b = 0.0259 \frac{g_{HCl}}{g_{GAC}}$$

$$Bed\ capacity = \frac{W_b}{W_{Sat}}$$

$$\begin{aligned} Bed\ capacity(max) &= \frac{0.0259 \frac{g_{HCl}}{g_{GAC}}}{0.0274 \frac{g_{HCl}}{g_{GAC}}} \\ &= 0.9453 \end{aligned}$$



Calculation of HCl adsorption by RH-SiO₂



Breakthrough curve of SiO₂ for HCl adsorption

At saturated stage of adsorbent

$$W_{Sat} = g \text{ adsorbate} / g \text{ adsorbent}$$

$$W_{Sat} = \frac{F_A \times \text{Area above the graph}}{\text{Mass of adsorbent per unit cross sectional area of bed}} \dots \dots \dots (1)$$

$$F_A = \text{Solute feed rate} \left(\frac{g}{cm^2 h} \right)$$

Where

$$F_A = u_0 c_0 M$$

$$u_0 = \text{Velocity of solute} \left(\frac{cm}{s} \right)$$

$$c_0 = \text{concentration} \left(\frac{mol}{cm^3} \right)$$

$$M = \text{Molecular weight } \left(\frac{g}{\text{mol}} \right)$$

F_A is calculated as followed,

$$F_A = \left(\frac{50 \frac{\text{cm}^3}{\text{min}}}{\frac{\pi(1)^2}{4} (\text{cm}^2)} \right) \times \left(\frac{580 \times 10^{-6}}{22,400} \times \frac{273}{303.15} \times \frac{760}{760} \right) \frac{\text{mol}}{\text{cm}^3} \times (36.5 \frac{\text{g}_{\text{HCl}}}{\text{mol}})$$

$$F_A = 5.418 \times 10^{-5} \frac{\text{g}_{\text{HCl}}}{\text{cm}^2 \text{min}} \text{ or } 3.251 \times 10^{-3} \frac{\text{g}_{\text{HCl}}}{\text{cm}^2 \text{h}}$$

Area above graph

$$\text{Area above the graph} = \int_0^{1.5} \left(1 - \frac{C}{C_0} \right) dt$$

$$\text{Area above the graph} = 1.09 \text{ h}$$

Mass of adsorbent

Mass of adsorbent per unit cross sectional area of bed

$$= \text{Bed height (cm)} \times \text{Density} \left(\frac{\text{g}}{\text{cm}^3} \right)$$

$$\text{Mass of adsorbent per unit cross sectional area of bed} = (6 \times 0.3977) \frac{\text{g}_{\text{SiO}_2}}{\text{cm}^2}$$

$$\text{Mass of adsorbent per unit cross sectional area of bed} = 2.3862 \frac{\text{g}_{\text{SiO}_2}}{\text{cm}^2}$$

From (1) W_{sat} is calculated as followed,

$$W_{\text{Sat}} = \frac{\left(3.251 \times 10^{-3} \frac{\text{g}_{\text{HCl}}}{\text{cm}^2} \right) \times (1.09 \text{ h})}{2.3862 \frac{\text{g}_{\text{SiO}_2}}{\text{cm}^2}}$$

$$W_{\text{Sat}} = 0.0015 \frac{\text{g}_{\text{HCl}}}{\text{g}_{\text{SiO}_2}}$$

At break point condition; $C/C_0 = 0.05$

$$\text{Area above the graph} = \int_0^1 \left(1 - \frac{C}{C_0}\right) dt$$

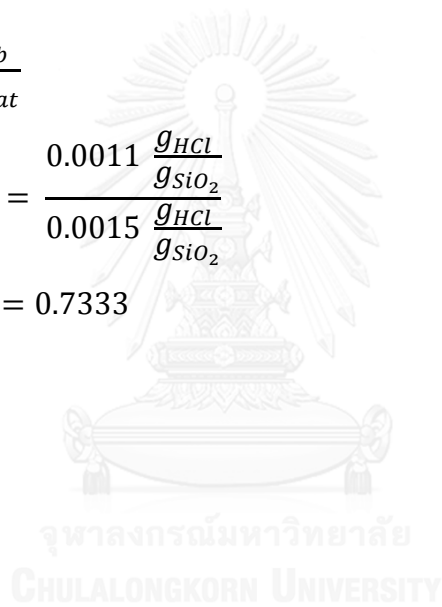
$$\text{Area above the graph} = 0.79 h$$

$$W_b = \frac{\left(3.251 \times 10^{-3} \frac{g_{HCl}}{cm^2 h}\right) \times (0.79 h)}{2.3862 \frac{g_{SiO_2}}{cm^2}}$$

$$W_b = 0.0011 \frac{g_{HCl}}{g_{SiO_2}}$$

$$\text{Bed capacity} = \frac{W_b}{W_{Sat}}$$

$$\begin{aligned} \text{Bed capacity(max)} &= \frac{0.0011 \frac{g_{HCl}}{g_{SiO_2}}}{0.0015 \frac{g_{HCl}}{g_{SiO_2}}} \\ &= 0.7333 \end{aligned}$$

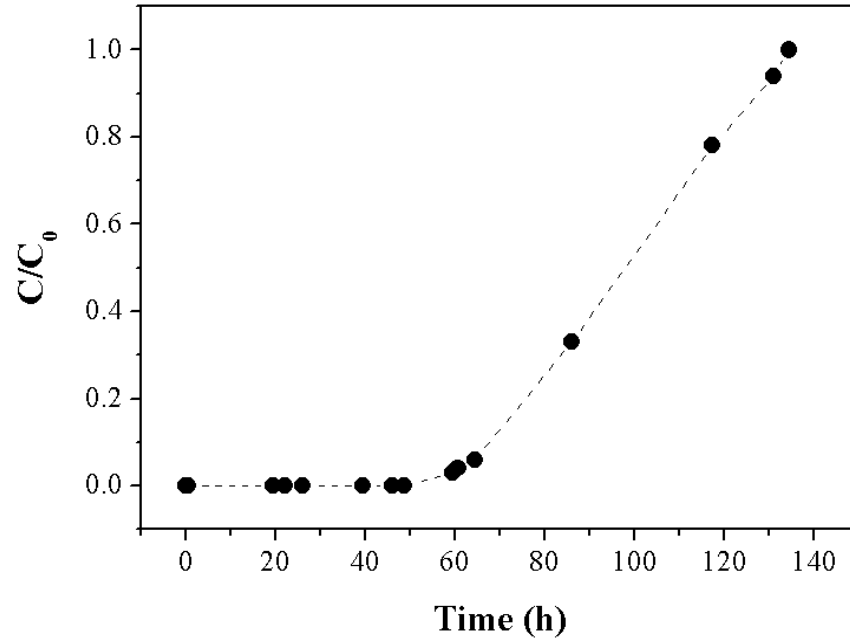


APPENDIX B

Example of Vinyl Chloride Monomer Adsorption Calculation



Calculation of VCM adsorption by 6N-GAC



Breakthrough curve of 6N-GAC for VCM Adsorption

At saturated stage of adsorbent

$$W_{Sat} = g \text{ adsorbate} / g \text{ adsorbent}$$

$$W_{Sat} = \frac{F_A \times \text{Area above the graph}}{\text{Mass of adsorbent per unit cross sectional area of bed}} \dots \dots \dots (1)$$

$$F_A = \text{Solute feed rate} \left(\frac{g}{cm^2 h} \right)$$

Where

$$F_A = u_0 c_0 M$$

$$u_0 = \text{Velocity of solute} \left(\frac{cm}{s} \right)$$

$$c_0 = \text{concentration} \left(\frac{mol}{cm^3} \right)$$

$$M = \text{Molecular weight} \left(\frac{g}{mol} \right)$$

F_A is calculated as followed,

$$F_A = \left(\frac{50 \frac{cm^3}{min}}{\frac{\pi(1)^2}{4} (cm^2)} \right) \times \left(\frac{18 \times 10^{-6}}{22,400} \times \frac{273}{303.15} \times \frac{760}{760} \right) \frac{mol}{cm^3} \times (62.5 \frac{g_{VCM}}{mol})$$

$$F_A = 2.879 \times 10^{-6} \frac{g_{VCM}}{cm^2 min} \text{ or } 1.727 \times 10^{-4} \frac{g_{VCM}}{cm^2 h}$$

Area above graph

$$\text{Area above the graph} = \int_0^{134.3} \left(1 - \frac{C}{C_0}\right) dt$$

$$\text{Area above the graph} = 96.41 h$$

Mass of adsorbent

Mass of adsorbent per unit cross sectional area of bed

$$= \text{Bed height}(cm) \times \text{Density}\left(\frac{g}{cm^3}\right)$$

Mass of adsorbent per unit cross sectional area of bed

$$= (6 \times 0.6831) \frac{g_{6N-GAC}}{cm^2}$$

$$\text{Mass of adsorbent per unit cross sectional area of bed} = 4.0986 \frac{g_{6N-GAC}}{cm^2}$$

From (1) W_{sat} is calculated as followed,

$$W_{Sat} = \frac{\left(1.727 \times 10^{-4} \frac{g_{VCM}}{cm^2 h}\right) \times (96.41 h)}{4.0986 \frac{g_{6N-GAC}}{cm^2}}$$

$$W_{Sat} = 0.0041 \frac{g_{VCM}}{g_{6N-GAC}}$$

At break point condition; $C/C_0 = 0.05$

$$\text{Area above the graph} = \int_0^{63} \left(1 - \frac{C}{C_0}\right) dt$$

$$\text{Area above the graph} = 62.70 \text{ h}$$

$$W_b = \frac{\left(1.727 \times 10^{-4} \frac{g_{VCM}}{cm^2 h}\right) \times (62.70 \text{ h})}{4.0986 \frac{g}{cm^2}}$$

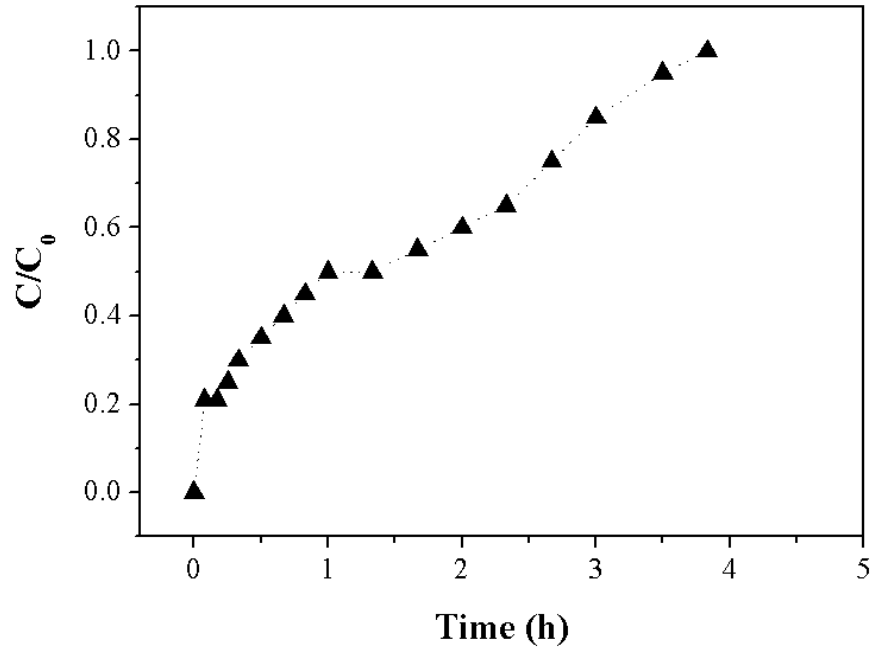
$$W_b = 0.0026 \frac{g_{VCM}}{g_{6N-GAC}}$$

$$\text{Bed capacity} = \frac{W_b}{W_{Sat}}$$

$$\begin{aligned} \text{Bed capacity} &= \frac{0.0026 \frac{g_{VCM}}{g_{6N-GAC}}}{0.0041 \frac{g_{VCM}}{g_{6N-GAC}}} \\ &= 0.6341 \end{aligned}$$



Calculation of VCM adsorption by RH-SiO₂



Breakthrough curve of RH-SiO₂ for VCM adsorption

At saturated stage of adsorbent

$$W_{Sat} = g \text{ adsorbate} / g \text{ adsorbent}$$

$$W_{Sat} = \frac{F_A \times \text{Area above the graph}}{\text{Mass of adsorbent per unit cross sectional area of bed}} \dots \dots \dots (1)$$

$$F_A = \text{Solute feed rate} \left(\frac{g}{cm^2 h} \right)$$

Where

$$F_A = u_0 c_0 M$$

$$u_0 = \text{Velocity of solute} \left(\frac{cm}{s} \right)$$

$$c_0 = \text{concentration} \left(\frac{mol}{cm^3} \right)$$

$$M = \text{Molecular weight} \left(\frac{g}{mol} \right)$$

F_A is calculated as followed,

$$F_A = \left(\frac{50 \frac{\text{cm}^3}{\text{min}}}{\frac{\pi(1)^2}{4} (\text{cm}^2)} \right) \times \left(\frac{20 \times 10^{-6}}{22,400} \times \frac{273}{303.15} \times \frac{760}{760} \right) \frac{\text{mol}}{\text{cm}^3} \times (62.5 \frac{\text{g}_{VCM}}{\text{mol}})$$

$$F_A = 3.199 \times 10^{-6} \frac{\text{g}_{VCM}}{\text{cm}^2 \text{min}} \text{ or } 1.919 \times 10^{-4} \frac{\text{g}_{VCM}}{\text{cm}^2 \text{h}}$$

Area above graph

$$\text{Area above the graph} = \int_0^{3.5} \left(1 - \frac{C}{C_0} \right) dt$$

$$\text{Area above the graph} = 1.58 \text{ h}$$

Mass of adsorbent

Mass of adsorbent per unit cross sectional area of bed

$$= \text{Bed height}(\text{cm}) \times \text{Density} \left(\frac{\text{g}}{\text{cm}^3} \right)$$

Mass of adsorbent per unit cross sectional area of bed

$$= (6 \times 0.3977) \frac{\text{g}_{RH-SiO_2}}{\text{cm}^2}$$

$$\text{Mass of adsorbent per unit cross sectional area of bed} = 2.3862 \frac{\text{g}_{RH-SiO_2}}{\text{cm}^2}$$

From (1) W_{sat} is calculated as followed,

$$W_{\text{Sat}} = \frac{\left(1.919 \times 10^{-4} \frac{\text{g}_{VCM}}{\text{cm}^2} \right) \times (1.58 \text{ h})}{2.3862 \frac{\text{g}_{RH-SiO_2}}{\text{cm}^2}}$$

$$W_{\text{Sat}} = 1.27 \times 10^{-4} \frac{\text{g}_{VCM}}{\text{g}_{RH-SiO_2}}$$

At break point condition; $C/C_0 = 0.05$

$$\text{Area above the graph} = \int_0^{0.02} \left(1 - \frac{C}{C_0} \right) dt$$

Area above the graph = 0.0195 h

$$W_b = \frac{\left(1.92 \times 10^{-4} \frac{g_{VCM}}{cm^2 h}\right) \times (0.0195 h)}{2.3862 \frac{g}{cm^2}}$$

$$W_b = 1.57 \times 10^{-6} \frac{g_{VCM}}{g_{RH-SiO_2}}$$

$$\text{Bed capacity} = \frac{W_b}{W_{Sat}}$$

$$\begin{aligned} \text{Bed capacity(max)} &= \frac{1.57 \times 10^{-6} \frac{g_{VCM}}{g_{RH-SiO_2}}}{1.27 \times 10^{-4} \frac{g_{VCM}}{g_{RH-SiO_2}}} \\ &= 0.0124 \end{aligned}$$



APPENDIX C

Quantity of sodium on granular activated carbon

จุฬาลงกรณ์มหาวิทยาลัย
CHULALONGKORN UNIVERSITY

Calculation of Na adsorption by GAC for 6N-GAC

Tritation Result

V_{NaOH}	=	25 ml
V_{HCl}	=	1.30 ml
C_{HCl}	=	0.1 mol/L
Initial NaOH	=	0.3 mol

Concentration of NaOH after 100 times dilution

$$C_{NaOH}V_{NaOH} = C_{HCl}V_{HCl}$$

$$C_{NaOH} = \frac{C_{HCl}V_{HCl}}{V_{NaOH}}$$

$$C_{NaOH} = \frac{(0.1 \text{ mol/L})(1.30 \text{ ml})}{25 \text{ ml}}$$

$$C_{NaOH} = 0.0052 \text{ mol/L}$$

Amount of remaining NaOH before dilution

$$n_{NaOH} = \frac{CV}{1000} \times 100$$

$$n_{NaOH} = \frac{(0.0052 \text{ mol/L})(25 \text{ ml})}{1000} \times 100$$

$$n_{NaOH} = 0.0130 \text{ mol}$$

Amount of consumed NaOH

$$n_{consumed NaOH} = n_{initial NaOH} - n_{remaining NaOH}$$

$$n_{consumed NaOH} = 0.3 - 0.0130 \text{ mol}$$

$$n_{consumed NaOH} = 0.287 \text{ mol}$$

Molecular weigh of Na = 23 g/mol

$$\text{Amount of Na} = 0.287 \text{ mol} \times 23 \text{ g/mol}$$

$$\text{Amount of Na} = 6.601 \text{ g}$$

Amount of GAC = 5.0023 g

$$\text{Amount of } \frac{g_{Na}}{g_{GAC}} = \frac{6.601 g_{Na}}{5.0023 g_{GAC}}$$

$$\text{Amount of } \frac{g_{Na}}{g_{GAC}} = 1.3196 \frac{g_{Na}}{g_{GAC}}$$



Calculation of Na adsorption by GAC for 12N-GAC

Tritation Result

V_{NaOH}	=	25 mL
V_{HCl}	=	2.75 mL
C_{HCl}	=	0.1 mol/L
Initial NaOH	=	0.6 mol

Concentration of NaOH after 100 times dilution

$$C_{NaOH}V_{NaOH} = C_{HCl}V_{HCl}$$

$$C_{NaOH} = \frac{C_{HCl}V_{HCl}}{V_{NaOH}}$$

$$C_{NaOH} = \frac{(0.1 \text{ mol/L})(2.75 \text{ ml})}{25 \text{ ml}}$$

$$C_{NaOH} = 0.0110 \text{ mol/L}$$

Amount of remaining NaOH before dilution

$$n_{NaOH} = \frac{CV}{1000} \times 100$$

$$n_{NaOH} = \frac{(0.0110 \text{ mol/L})(25 \text{ ml})}{1000} \times 100$$

$$n_{NaOH} = 0.0275 \text{ mol}$$

Amount of consumed NaOH

$$n_{consumed NaOH} = n_{initial NaOH} - n_{remaining NaOH}$$

$$n_{consumed NaOH} = 0.6 - 0.0275 \text{ mol}$$

$$n_{consumed NaOH} = 0.5725 \text{ mol}$$

Molecular weight of Na = 23 g/mol

$$\text{Amount of Na} = 0.5725 \text{ mol} \times 23 \text{ g/mol}$$

$$\text{Amount of Na} = 13.1675 \text{ g}$$

Amount of GAC = 5.0023 g

The amount of Na on GAC

$$\text{Amount of } \frac{g_{Na}}{g_{GAC}} = \frac{13.1675 g_{Na}}{5.0023 g_{GAC}}$$

$$\text{Amount of } \frac{g_{Na}}{g_{GAC}} = 2.6323 \frac{g_{Na}}{g_{GAC}}$$



VITA

Name: Ms. Prapaporn Luekittisup

Nationality: Thai

Education: 1998 M.Sc. in Sanitary Engineering
(Environmental Technology), Mahidol University
1994 B.Sc. in Public Health (Sanitary Science),
Mahidol University

Employment: Department of Industrial Works, Ministry of Industry.

Conference: 14th Asia Pacific Confederation of Chemical
Engineering (APCChE 2012)